

Title: A strong test of the Maximum Entropy Theory of Ecology

Author affiliation: Xiao Xiao^{1,2,3}, Daniel J. McGlinn^{1,2}, and Ethan P. White^{1,2}

¹Department of Biology, Utah State University, 5305 Old Main Hill, Logan, UT 84322-5305;

²Ecology Center, Utah State University, 5205 Old Main Hill, Logan, UT 84322-5205

³Corresponding author; Email: xiao@weecology.org

Summary

The Maximum Entropy Theory of Ecology (METE) is a unified theory of biodiversity that predicts a large number of macroecological patterns using only information on the species richness, total abundance, and total metabolic rate of the community. We conducted a strong test of METE, where four of its major predictions were evaluated simultaneously using data from 60 globally distributed communities including over 300,000 individuals and nearly 2000 species. While METE successfully captured 96% and 93% of the variation in the species abundance distribution and the individual size distribution, it performed poorly when characterizing the size-density relationship and the intraspecific distribution of individual body size. Specifically, METE predicts a negative correlation between individual energy use and species abundance, which is weak in natural communities. By evaluating multiple predictions with large quantities of data, our study not only identifies a mismatch between abundance and body size in METE, but also serves as a general example on the importance of conducting strong tests of ecological theories.

Key index words: biodiversity, body size distributions, macroecology, maximum entropy, species abundance distribution, unified theory

Introduction

In ecology it has long been recognized that general patterns exist across communities that are insensitive to the underlying biological interactions [1]. For instance, almost all ecological communities consist of a few highly abundant species and many rare ones, regardless of the ecological or evolutionary forces shaping the community (the species abundance distribution or SAD; [2,3]). Similarly, the increase of species richness with area (species area relationship or SAR; [4]) has been universally observed to be a smooth monotonically increasing curve. These macroecological patterns provide unified characterizations of ecological systems. Additionally, there are an increasing number of theories that identify links between different macroecological patterns and unite them under a single framework (e.g., [5–7]; see [8] for a review). Such unified theories have the potential to provide fundamental insights into ecological and statistical processes underlying observed patterns [9] and to allow predictions to be made with relatively few inputs [7].

While most existing unified theories are capable of predicting a variety of biodiversity patterns such as the SAD, the SAR, and the decay of similarity with distance [8], the Maximum Entropy Theory of Ecology (METE; [7,10,11]) is unique in that it attempts to capture the distribution of individuals among species (e.g., SAD) and across space (e.g., SAR), and also the allocation of energy (or biomass) among individuals, thus providing a very general characterization of the structure of ecological systems. METE is one of a growing number of theoretical approaches that attempt to synthesize traditionally distinct areas of macroecology dealing with the distribution of individuals and the distribution of energy and biomass [6,12,13].

METE adopts the Maximum Entropy Principle from information theory, which identifies the least biased (most even) probability distribution given a set of constraints [14]. With three state variables (total richness S_0 , total number of individuals N_0 , and total metabolic rate within the community E_0) as inputs, METE makes predictions for the SAD and multiple distributions of energy without tunable parameters. By adding an additional constraint on the area sampled (A_0) it also makes predictions for the SAR, the distance decay of similarity, and the endemics area relationship [7,10,11]. While the spatial and non-spatial components of the theory are both based on identifying the most likely state of the system, their predictions are effectively independent and should therefore be evaluated separately.

Previous studies have evaluated the performance of METE with separate datasets for different patterns and have shown that METE generally provides good characterizations of these patterns across geographical locations and taxonomic groups [7,10,11,15]. However, these tests are relatively weak as they focus on one pattern at a time [16]. As a unified theory with multiple predictions, METE allows stronger tests to be made by testing the ability of the theory to characterize multiple patterns simultaneously [16,17]. In this study, we conduct a strong test of the non-spatial half of METE using data from 60 globally distributed forest communities to simultaneously evaluate four predictions of the theory (Fig. 1) including the SAD (the distribution of individuals among species) and energetic analogs of the individual size distribution (ISD; the distribution of body size among individuals regardless of their species identity) [18,19], the size-density relationship (SDR; the correlation between species abundance and average individual size within species) [20], and the intraspecific individual size distribution (iISD; the distribution of body size among individuals within a species) [21]. This analysis provides insight into the performance of METE, suggests future directions for making

connections between abundance distributions and size related macroecological patterns, and demonstrates the importance of conducting strong multi-patterns tests in the evaluation of ecological theories.

Methods

1. Predicted patterns of METE

METE assumes that allocation of individuals and energy consumption within a community is constrained by three state variables: species richness (S_0), total number of individuals (N_0), and total metabolic rate summed over all individuals in the community (E_0) [7,10,11]. Define $R(n, \varepsilon)$ as the joint probability that a species randomly picked from the community has abundance n and an individual randomly picked from such a species has metabolic rate between $(\varepsilon, \varepsilon + \Delta\varepsilon)$, two constraints are then established on the ratio between the state variables:

$$\sum_{n=1}^{N_0} \int_{\varepsilon=1}^{E_0} d\varepsilon \cdot nR(n, \varepsilon) = \frac{N_0}{S_0} \quad (1)$$

which represents the average abundance per species, and

$$\sum_{n=1}^{N_0} \int_{\varepsilon=1}^{E_0} d\varepsilon \cdot n\varepsilon R(n, \varepsilon) = \frac{E_0}{S_0} \quad (2)$$

which represents the average total metabolic rate per species. Note that the lower limit of individual metabolic rate is set to be 1, and all measures of metabolic rate are rescaled accordingly.

By maximizing information entropy $I = -\sum_{n=1}^{N_0} \int_{\varepsilon=1}^{E_0} d\varepsilon \cdot R(n, \varepsilon) \log(R(n, \varepsilon))$ with respect to the constraints and the normalization condition $\sum_{n=1}^{N_0} \int_{\varepsilon=1}^{E_0} d\varepsilon \cdot R(n, \varepsilon) = 1$, $R(n, \varepsilon)$ can be obtained as

$$R(n, \varepsilon) = \frac{1}{Z} e^{-\lambda_1 n} e^{-\lambda_2 n \varepsilon} \quad (3)$$

where the normalization constant Z is given by

$$Z = \sum_{n=1}^{N_0} \int_{\varepsilon=1}^{E_0} d\varepsilon \cdot e^{-\lambda_1 n} e^{-\lambda_2 n \varepsilon} \quad (4)$$

With reasonable approximations, the Lagrange multipliers λ_1 and λ_2 are given by

$$\sum_{n=1}^{N_0} e^{-(\lambda_1 + \lambda_2) \cdot n} / \sum_{n=1}^{N_0} \frac{e^{-(\lambda_1 + \lambda_2)n}}{n} \approx \frac{N_0}{S_0} \quad (5)$$

$$\lambda_2 \approx \frac{S_0}{E_0 - N_0} \quad (6)$$

We investigated four major ecological patterns that METE predicts - SAD, ISD, SDR, and iISD. Here, body size is used as a surrogate for metabolic rate (see [3. Analysis](#)). All four patterns can be derived from the joint distribution $R(n, \varepsilon)$ under the framework of METE. The SAD is obtained by integrating energy out of $R(n, \varepsilon)$, i.e.,

$$\Phi(n) \approx \frac{1}{cn} e^{-(\lambda_1 + \lambda_2)n} \quad (7)$$

which is Fisher's log-series distribution upper truncated at N_0 , with C being the proper normalization constant. Similarly, the Individual-level Energy Distribution (which is the energetic equivalent of the ISD) is obtained by summing across n :

$$\Psi(\varepsilon) = \frac{S_0}{N_0 Z} \cdot \frac{e^{-\gamma}}{(1 - e^{-\gamma})^2} \cdot (1 - (N_0 + 1)e^{-\gamma N_0} + N_0 e^{-\gamma(N_0 + 1)}) \quad (8)$$

where $\gamma = \lambda_1 + \lambda_2 \cdot \varepsilon$. Conditioned on abundance n , the Species-level Energy Distribution (which is the energetic equivalent of the iISD) is given by

$$\Theta(\varepsilon|n) = \frac{n\lambda_2 e^{-\lambda_2 n \varepsilon}}{e^{-\lambda_2 n} - e^{-\lambda_2 n E_0}} \quad (9)$$

This is an exponential distribution with its parameter equal to $\lambda_2 n$; in other words, METE predicts that the parameter of the iISD for each species within a community is proportional to its abundance. The expected value of the iISD $\Theta(\varepsilon|n)$ then gives the Average Species Energy Distribution (which is the energetic equivalent of the SDR), i.e., the expected average metabolic rate (size) for individuals within a species with abundance n :

$$\bar{\varepsilon}(n) = \frac{1}{n\lambda_2(e^{-\lambda_2 n} - e^{-\lambda_2 n E_0})} \cdot [e^{-\lambda_2 n}(\lambda_2 n + 1) - e^{-\lambda_2 n E_0}(\lambda_2 n E_0 + 1)] \quad (10)$$

See **Appendix A** for detailed derivation and comparison with [7].

2. Data

METE predicts the iISD to be an exponential distribution (Eqn 9; also see Fig. 1d) where the smallest size class is the most abundant, regardless of species identity or abundance.

However, most animal species exhibit interior modes of adult body size (e.g., [21,22]; but see [7]) and large variation in minimum (and maximum) body size among species associated with these modal values [21]. In other words, the body sizes of conspecifics are clustered around some intermediate value, while individuals that are much larger or smaller are rare.

Consequently, assembling all individuals across species in such communities often yields multimodal ISD [23], as opposed to monotonically decreasing predicted by METE (Eqn 8; also

see Fig. 1b). As such animal communities are expected a priori to violate two of the predictions of METE. Therefore, to ensure that the performance of METE was not trivially rejected because of the life history trait of determinate growth, in our analysis we focused exclusively on trees, which are known to have iISDs [24] and ISDs [18,19] that are well characterized by monotonically declining distributions and which arguably have the greatest prevalence of high quality individual level size data among indeterminately growing taxonomic groups.

We compiled forest plot data from previous publications, publicly available databases, and data obtained through personal communication (Table 1). All plots have been fully surveyed with size measurement for all individuals above plot-specific minimum thresholds. For those plots where surveys have been conducted multiple times, we adopted data from the most recent one unless otherwise specified (see Table 1). Individuals that were dead, not identified to species/morphospecies, and/or missing size measurements were excluded. Individuals with size measurements below or equal to the designated minimum thresholds were excluded as well, because it is unclear whether these size classes were thoroughly surveyed or not. Specifically, the smallest size class is generally under-represented as a result of sampling scheme; e.g., if the minimal diameter in a survey is 10cm, then the 10cm size class usually includes individuals with diameters ranging from 10cm to 10.5cm, while the 11cm size class includes individuals with diameters ranging from 10.5 cm to 11.5cm [19]. Overall our analysis encompassed 60 plots that were at least 1 ha in size and had a richness of at least 14 (Table 1), with 1943 species/morphospecies and 379022 individuals in total.

3. Analyses

The scaling relationship between diameter and metabolic rate can be described with good approximation by metabolic theory as $B \propto D^2 \cdot e^{-E/kT}$, where B is metabolic rate, D is diameter, T is temperature, E is the activation energy, and k is the Boltzmann's constant [25,26]. Assuming that E is constant across species and T is constant within a community, the temperature-dependent term $e^{-E/kT}$ is constant within a community, and can be dropped when the metabolic rate of individuals are rescaled. We thus used $(D/D_{min})^2$ as the surrogate for individual metabolic rate, where D_{min} is the diameter of the smallest individual in the community, which sets the minimal individual metabolic rate to be 1 following METE's assumption (see Eqn 2). Applying alternative models that more accurately capture nonlinearities between diameter, mass and metabolic rate did not have any qualitative effect on our results (**Appendix B**). For individuals with multiple stems, we adopted the pipe model to combine the records, i.e., $D = \sqrt{\sum d_i^2}$, where d_i 's were diameter of individual stems [27]. Since metabolic rate scales as D^2 , the pipe model preserves the total area as well as the total metabolic rate for all stems combined.

We calculated the Lagrange multipliers λ_1 and λ_2 in each community using Eqns 5 & 6, with inputs S_0 , N_0 , and E_0 (i.e., the sum over the rescaled individual metabolic rates). Predictions for the four ecological patterns were obtained from Eqns 7-10 and further transformed to facilitate comparison with observations. For the SAD, we converted the predicted probability distribution (Eqn 7) to a rank-abundance distribution (RAD), i.e., abundance at each rank from the most abundant species to the least abundant species [7,10,15], which was compared with the empirical RAD. For the ISD, the scaled individual metabolic rates were grouped into $\log(1.7)$ bins (i.e., 1-1.7, 1.7-2.89, 2.89-4.913, etc.), resulting in 10 to 21 bins for each community. The predicted frequency for each bin, calculated from the cumulative distribution of $\Psi(\varepsilon)$ (Eqn 8), was then compared with the observed frequency. While ISD has been evaluated in previous

studies [7] as rank-size distribution with predicted metabolic rate for individuals at each rank, we adopted binning of predicted and observed frequencies instead to account for the fact that the ISD is a continuous distribution with essentially zero probability for any specific value. Converting the ISD to the rank-size distribution does not qualitatively change our results (**Appendix C**). For the SDR, predicted average metabolic rate was obtained from Eqn 10 for species with abundance n , which was compared to the observed average metabolic rate for that species. For the iISD, we fit an exponential distribution left-truncated at 1 (the minimal rescaled metabolic rate within each community) to species with at least 5 individuals using the method of maximum likelihood, and compared the parameter predicted by METE ($\lambda_2 n$, Eqn 9) to the maximum likelihood estimator. Note that we assumed that all the iISDs can be characterized by the exponential distribution, even though some of them are significantly different (**Appendix D**). Therefore this analysis is favorable to METE, i.e., in some cases METE deviates from the prediction in the general shape of the distribution as well as the specific parameters.

The explanatory power of METE for each pattern was quantified with coefficient of determination R^2 , which was calculated as

$$R^2 = 1 - \frac{\sum_i [\log_{10}(obs_i) - \log_{10}(pred_i)]^2}{\sum_i [\log_{10}(obs_i) - \overline{\log_{10}(obs_i)}}]^2} \quad (11)$$

where obs_i and $pred_i$ were the i th observed value and METE's prediction, respectively. Both observed and predicted values were log-transformed for homoscedasticity. Note that R^2 measures the proportion of variation in the observation explained by the prediction; it is based on the 1:1 line when the observed values are plotted against the predicted values, not the regression line. Thus it is possible for R^2 to be negative, which is an indication that the prediction is worse than taking the average of the observation.

Results

The results for all forest plots combined are summarized in Fig.2, with observations plotted against predictions for each macroecological pattern. METE provides excellent predictions for the SAD ($R^2 = 0.96$) and the ISD ($R^2 = 0.93$). However, the SDR ($R^2 = -2.24$) and the iISD ($R^2 = -0.73$) are not well characterized by the theory.

Further examination of the four macroecological patterns within each community (**Appendix E**, Fig. A4; also see insets in Fig.2) confirms METE's ability to consistently characterize the SAD with R^2 values between 0.60 and 0.99, as well as its inadequacy in characterizing the SDR and the iISD with all R^2 values below zero with a single exception. METE's performance for the ISD exhibits slightly larger variation across communities with R^2 between 0.14 and 0.99; however, in 53 out of 60 communities R^2 values for the ISD are above 0.9, indicating that METE characterizes this pattern well in most cases.

Discussion

Macroecological theory increasingly attempts to make predictions across numerous ecological patterns [8]. The Maximum Entropy Theory of Ecology is one of the most general of these unified theories, making simultaneous predictions for two distinct sets of ecological patterns - the distributions of individuals among species and across space, and distributions related to individual body size and energy use. We show that using only information on the species richness, total abundance, and total energy use of a community that METE captures the

general form of the SAD (allocation of individuals among species) and ISD (allocation of energy/biomass among individuals) within and among 60 forest communities (Fig. 2A, B; Fig. A4).

The SAD and the ISD are among the most well-studied patterns in ecology, and numerous models exist for both patterns. For instance, with metabolic theory and demographic equilibrium models, Muller-Landau *et al.* [19] identified four possible predictions for the ISD under different assumptions of growth and mortality rates. For the SAD more than twenty models have been proposed [2,3], ranging from purely statistical to mechanistic. Our study demonstrates METE's high predictive power for these two patterns, but it does not imply that it is the best model when each pattern is considered independently. Indeed, while METE does generally outperform the most common model of the species abundance distribution [15], model comparisons for the ISD using AIC suggests that the maximum likelihood Weibull distribution (one of the distributions for tree diameter in [19]) almost always outperforms METE (though METE's performance is comparable to that of the other two distributions, the exponential and the Pareto; see **Appendix F**). As a unified theory, however, METE's strength lies in its ability to link together ecological phenomena that were previously considered distinct, and to make predictions based on first principles without fitted parameters. The agreement between METE's predictions and the observed SAD and ISD supports the notion that the majority of variation in these macroecological patterns can be characterized by variation in the state variables S_0 , N_0 , and E_0 alone [7,15,28].

While METE performs well in characterizing the SAD and ISD, it performs poorly when predicting the distribution of energy at the species level (Fig. 2C, D; Fig. A4). These deviations from the predictions imply a mismatch between the predicted metabolic rate of individuals and

their species' abundances. METE predicts a monotonically decreasing relationship between species abundance and average intraspecific metabolic rate, i.e., species with higher abundance are also smaller in size on average and are more likely to contain smaller individuals (Eqns 9, 10, Fig. 1C). Evaluating the total (instead of average) intraspecific metabolic rate, this relationship translates roughly into Damuth's energetic equivalence rule [29], where the total energy consumption within a species does not depend on species identity or abundance [7,10]. While Damuth's rule has been argued to apply at global scales [29,30], our results indicate that it does not hold locally, in concordance with a number of previous studies (e.g., [30,31]). However, it has been suggested that the inverse relationship between abundance and body size predicted by Damuth's rule becomes stronger with increasing body size variation in the assemblage [32,33]. Given that average diameter within species in each forest community spans 1 to 2 orders of magnitude (2 to 4 when converted to metabolic rate), it is possible that METE's predictions for size-abundance relationship and iISD may improve in communities with larger variation in body size.

The consistency of our results across 60 forest communities (as well as confirmative evidence from a concurrent study of a single herbaceous plant community; Newman *et al.* in review) provides strong evidence for METE's mixed performance among the four macroecological patterns. However, several limitations of the study are worth noting. First, we only analyzed a single taxonomic group (trees). This was in part because individual level size data collected in standardized ways is available for a large number of tree communities, and in part based on a prior knowledge that the form of the ISD and the iISD [18,19,24] had a reasonable chance of being well characterized by the theory (see **Methods**). While we know that the SAD predictions of the theory perform well in general [15], further tests are necessary to

determine if the simultaneous good fit of the ISD predictions is supported in other taxonomic groups. There is some evidence that this result holds in invertebrate communities [7]. It is also possible that different groups of indeterminate growers may exhibit better agreement with the iISD and the SDR predictions. Second, we estimated the metabolic rate of individuals based on predictions of metabolic theory rather than direct measurement. While our results were not sensitive to the use of other equations used for estimating metabolic rate (**Appendix B**), it is possible that directly measured metabolic rates could result in different fits to the theory (but see Newman *et al.* in review, which adopts a different method to obtain metabolic rate yet reaches similar conclusions). Finally, a modified version of METE is currently being developed that includes additional constraints, which could yield improved predictions for the SDR and the iISD.

Models and theories can be evaluated at multiple levels which yield different strengths of inference [16,17], progressing from matching theory to empirical observations on a single pattern, to testing against a null hypothesis, to evaluating multiple a priori predictions, to eventually comparing between multiple competing models. With quantitative predictions on various ecological patterns, METE and other unified theories allow for simultaneous examination of multiple predictions, which provides a much stronger test compared to curve-fitting for a single pattern and can often reveal important insight into theories that are otherwise overlooked by single tests (e.g., [34]). As a comprehensive analysis on the performance of METE in predicting diversity and energy distributions in the same datasets, our study demonstrates the importance of moving towards stronger tests in ecology, especially when multiple intercorrelated predictions are available - while previous studies have shown that METE does an impressive job characterizing a single pattern [15], concurrently evaluating all

predictions of the theory identifies a mismatch between species' abundance and individual size that consistently deviates from empirical patterns.

In addition to simultaneously testing multiple predictions, we have also begun to compare competing models to METE (**Appendix F**; [15]). Quantitatively comparing theories that make multiple predictions is challenging and there is no general approach for properly comparing models that make different numbers of predictions. When comparing general theories to single prediction models with tunable parameters it is not surprising that theories such as METE fail to provide the best quantitative fit [35]. However, as Stephen P. Hubbell eloquently stated, 'One of the hallmarks of good theory is to fail in interesting and informative ways.' [5]. METE's failure in predicting species-level energy patterns such as the SDR and the iISD results from its current construction, which forces body size to be negatively correlated with abundance, a pattern that is often weak or absent in local scale empirical data (Fig. 2, Fig. A4). This problem may be remedied by either relaxing the current constraints to remove the association between species level body size and abundance from the theory, or by adding additional constraints to the system so that energetic equivalence among species no longer holds. On the other hand, the success of METE in characterizing the SAD and the ISD supports the state variable approach for studying macroecological patterns, and represents an important step towards the next level of unified theory in macroecology.

Acknowledgements

We thank John Harte, Erica Newman, the rest of the Harte Lab, and members of the Weecology Lab for extensive feedback on this research, general insights into MaxEnt, and for being

incredibly supportive of our efforts to evaluate METE. Nathan G. Swenson provided data for wood density in Luquillo forest plot and gave insightful comments. Robert K. Peet provided data for the North Carolina forest plots. The Serimbu (provided by T. Kohyama), Lahei (provided by T. B. Nishimura), and Shirakami (provided by T. Nakashizuka) datasets were obtained from the PlotNet Forest Database. The ACA Amazon (provided by N. Pitman) and DeWalt Bolivia (provided by S. DeWalt) were obtained from SALVIAS. The BCI forest dynamics research project was made possible by National Science Foundation grants to Stephen P. Hubbell: DEB-0640386, DEB-0425651, DEB-0346488, DEB-0129874, DEB-00753102, DEB-9909347, DEB-9615226, DEB-9615226, DEB-9405933, DEB-9221033, DEB-9100058, DEB-8906869, DEB-8605042, DEB-8206992, DEB-7922197, support from the Center for Tropical Forest Science, the Smithsonian Tropical Research Institute, the John D. and Catherine T. MacArthur Foundation, the Mellon Foundation, the Small World Institute Fund, and numerous private individuals, and through the hard work of over 100 people from 10 countries over the past two decades. The UCSC Forest Ecology Research Plot was made possible by National Science Foundation grants to Gregory S. Gilbert (DEB-0515520 and DEB-084259), by the Pepper-Giberson Chair Fund, the University of California, and the hard work of dozens of UCSC students. These two projects are part of the Center for Tropical Forest Science, a global network of large-scale demographic tree plots. The Luquillo Experimental Forest Long-Term Ecological Research Program was supported by grants BSR-8811902, DEB 9411973, DEB 0080538, DEB 0218039, DEB 0620910 and DEB 0963447 from NSF to the Institute for Tropical Ecosystem Studies, University of Puerto Rico, and to the International Institute of Tropical Forestry USDA Forest Service, as part of the Luquillo Long-Term Ecological Research Program. The U.S. Forest Service (Dept. of Agriculture) and the University of Puerto Rico gave additional support.

This research was supported by a CAREER award from the U.S. National Science Foundation to E. P. White (DEB-0953694).

References

- 1 Brown, J. H. 1995 *Macroecology*. University Of Chicago Press.
- 2 Marquet, P. A., Keymer, J. A. & Cofre, H. 2003 Breaking the stick in space: of niche models, metacommunities and patterns in the relative abundance of species. In *Macroecology: Concepts and Consequences* (eds T. M. Blackburn & K. J. Gaston), pp. 64–86. Blackwell Science Oxford.
- 3 McGill, B. J. et al. 2007 Species abundance distributions: moving beyond single prediction theories to integration within an ecological framework. *Ecology Letters* **10**, 995–1015. (doi:10.1111/j.1461-0248.2007.01094.x)
- 4 Rosenzweig, M. L. 1995 *Species diversity in space and time*. Cambridge University Press.
- 5 Hubbell, S. P. 2001 *The unified neutral theory of biodiversity and biogeography*. Princeton University Press.
- 6 Morlon, H., Chuyong, G., Condit, R., Hubbell, S., Kenfack, D., Thomas, D., Valencia, R. & Green, J. L. 2008 A general framework for the distance-decay of similarity in ecological communities. *Ecology Letters* **11**, 904–917. (doi:10.1111/j.1461-0248.2008.01202.x)
- 7 Harte, J. 2011 *Maximum entropy and ecology: a theory of abundance, distribution, and energetics*. Oxford University Press.
- 8 McGill, B. J. 2010 Towards a unification of unified theories of biodiversity. *Ecology Letters* **13**, 627–642. (doi:10.1111/j.1461-0248.2010.01449.x)
- 9 McGill, B. J. & Nekola, J. C. 2010 Mechanisms in macroecology: AWOL or purloined letter? Towards a pragmatic view of mechanism. *Oikos* **119**, 591–603. (doi:10.1111/j.1600-0706.2009.17771.x)
- 10 Harte, J., Zillio, T., Conlisk, E. & Smith, A. B. 2008 Maximum entropy and the state-variable approach to macroecology. *Ecology* **89**, 2700–2711. (doi:10.1890/07-1369.1)

- 11 Harte, J., Smith, A. B. & Storch, D. 2009 Biodiversity scales from plots to biomes with a universal species-area curve. *Ecology Letters* **12**, 789–97. (doi:10.1111/j.1461-0248.2009.01328.x)
- 12 Dewar, R. C. & Porté A. 2008 Statistical mechanics unifies different ecological patterns. *Journal of Theoretical Biology* **251**, 389–403. (doi:10.1016/j.jtbi.2007.12.007)
- 13 O’Dwyer, J. P., Lake, J. K., Ostling, A., Savage, V. M. & Green, J. L. 2009 An integrative framework for stochastic, size-structured community assembly. *Proceedings of the National Academy of Sciences of the United States of America* **106**, 6170–6175. (doi:10.1073/pnas.0813041106)
- 14 Jaynes, E. T. 2003 *Probability theory: the logic of science*. Cambridge University Press.
- 15 White, E. P., Thibault, K. M. & Xiao, X. 2012 Characterizing species abundance distributions across taxa and ecosystems using a simple maximum entropy model. *Ecology* **93**, 1772–1778.
- 16 McGill, B. 2003 Strong and weak tests of macroecological theory. *Oikos* **102**, 679–685. (doi:10.1034/j.1600-0706.2003.12617.x)
- 17 McGill, B. J., Maurer, B. A. & Weiser, M. D. 2006 Empirical evaluation of neutral theory. *Ecology* **87**, 1411–1423.
- 18 Enquist, B. J. & Niklas, K. J. 2001 Invariant scaling relations across tree-dominated communities. *Nature* **410**, 655–660. (doi:10.1038/35070500)
- 19 Muller-Landau, H. C. et al. 2006 Comparing tropical forest tree size distributions with the predictions of metabolic ecology and equilibrium models. *Ecology Letters* **9**, 589–602. (doi:10.1111/j.1461-0248.2006.00915.x)
- 20 Cotgreave, P. 1993 The relationship between body size and population abundance in animals. *Trends in Ecology & Evolution* **8**, 244–248. (doi:10.1016/0169-5347(93)90199-Y)
- 21 Gouws, E. J., Gaston, K. J. & Chown, S. L. 2011 Intraspecific body size frequency distributions of insects. *PLoS ONE* **6**, e16606. (doi:10.1371/journal.pone.0016606)
- 22 Koons, D. N., Birkhead, R. D., Boback, S. M., Williams, M. I. & Greene, M. P. 2009 The effect of body size on cottonmouth (*Agkistrodon piscivorus*) survival, recapture probability, and behavior in an Alabama swamp. *Herpetological Conservation and Biology* **4**, 221–235.
- 23 Thibault, K. M., White, E. P., Hurlbert, A. H. & Ernest, S. K. M. 2011 Multimodality in the individual size distributions of bird communities. *Global Ecology and Biogeography* **20**, 145–153. (doi:10.1111/j.1466-8238.2010.00576.x)

- 24 Condit, R., Sukumar, R., Hubbell, S. P. & Foster, R. B. 1998 Predicting population trends from size distributions: a direct test in a tropical tree community. *The American Naturalist* **152**, 495–509. (doi:10.1086/286186)
- 25 West, G. B., Brown, J. H. & Enquist, B. J. 1999 A general model for the structure and allometry of plant vascular systems. *Nature* **400**, 664–667. (doi:10.1038/23251)
- 26 Gillooly, J. F., Brown, J. H., West, G. B., Savage, V. M. & Charnov, E. L. 2001 Effects of size and temperature on metabolic rate. *Science* **293**, 2248–2251. (doi:10.1126/science.1061967)
- 27 Ernest, S. K. M., White, E. P. & Brown, J. H. 2009 Changes in a tropical forest support metabolic zero-sum dynamics. *Ecology Letters* **12**, 507–515. (doi:10.1111/j.1461-0248.2009.01305.x)
- 28 Supp, S. R., Xiao, X., Ernest, S. K. M. & White, E. P. 2012 An experimental test of the response of macroecological patterns to altered species interactions. *Ecology* **93**, 2505–2511. (doi:10.1890/12-0370.1)
- 29 Damuth, J. 1981 Population density and body size in mammals. *Nature* **290**, 699–700. (doi:10.1038/290699a0)
- 30 White, E. P., Ernest, S. K. M., Kerkhoff, A. J. & Enquist, B. J. 2007 Relationships between body size and abundance in ecology. *Trends in Ecology & Evolution* **22**, 323–330. (doi:10.1016/j.tree.2007.03.007)
- 31 Brown, J. H. & Maurer, B. A. 1987 Evolution of species assemblages: Effects of energetic constraints and species dynamics on the diversification of the North American avifauna. *The American Naturalist* **130**, 1–17. (doi:10.1086/284694)
- 32 Griffiths, D. 1998 Sampling effort, regression method, and the shape and slope of size-abundance relations. *Journal of Animal Ecology* **67**, 795–804. (doi:10.1046/j.1365-2656.1998.00244.x)
- 33 Hayward, A., Kolasa, J. & Stone, J. R. 2010 The scale-dependence of population density–body mass allometry: Statistical artefact or biological mechanism? *Ecological Complexity* **7**, 115–124. (doi:10.1016/j.ecocom.2009.08.005)
- 34 Adler, P. B. 2004 Neutral models fail to reproduce observed species-area and species-time relationships in Kansas grasslands. *Ecology* **85**, 1265–1272. (doi:10.1890/03-0602)
- 35 White, E. P., Xiao, X., Issac, N. J. B. & Sibly, R. M. 2012 Methodological tools. In *Metabolic Ecology: A Scaling Approach* (eds R. M. Sibly J. H. Brown & A. Kodric-Brown), Wiley, Chichester, UK.

- 36 Kohyama, T., Suzuki, E., Partomihardjo, T. & Yamada, T. 2001 Dynamic steady state of patch-mosaic tree size structure of a mixed dipterocarp forest regulated by local crowding. *Ecological Research* **16**, 85–98. (doi:10.1046/j.1440-1703.2001.00374.x)
- 37 PlotNet 2007 PlotNet Forest Database.
- 38 Baribault, T. W., Kobe, R. K. & Finley, A. O. 2011 Data from: Tropical tree growth is correlated with soil phosphorus, potassium, and calcium, though not for legumes. *Ecological Monographs*. (doi:doi:10.5061/dryad.r9p70)
- 39 Baribault, T. W., Kobe, R. K. & Finley, A. O. 2012 Tropical tree growth is correlated with soil phosphorus, potassium, and calcium, though not for legumes. *Ecological Monographs* **82**, 189–203. (doi:10.1890/11-1013.1)
- 40 Pitman, N. C. A., Cerón, C. E., Reyes, C. I., Thurber, M. & Arellano, J. 2005 Catastrophic natural origin of a species-poor tree community in the world's richest forest. *Journal of Tropical Ecology* **21**, 559–568. (doi:10.1017/S0266467405002713)
- 41 Hubbell, S. P., Foster, R. B., O'Brien, S. T., Harms, K. E., Condit, R., Wechsler, B., Wright, S. J. & Loo de Lao, S. 1999 Light-gap disturbances, recruitment limitation, and tree diversity in a neotropical forest. *Science* **283**, 554–557. (doi:10.1126/science.283.5401.554)
- 42 Condit, R., Aguilar, S., Hernández, A., Pérez, R., Lao, S., Angehr, G., Hubbell, S. P. & Foster, R. B. 2004 Tropical forest dynamics across a rainfall gradient and the impact of an El Niño dry season. *Journal of Tropical Ecology* **20**, 51–72.
- 43 DeWalt, S. J., Bourdy, G., Chávez de Michel, L. R. & Quenevo, C. 1999 Ethnobotany of the Tacana: Quantitative inventories of two permanent plots of Northwestern Bolivia. *Economic Botany* **53**, 237–260. (doi:10.1007/BF02866635)
- 44 Nishimura, T. B. & Suzuki, E. 2001 Allometric differentiation among tropical tree seedlings in heath and peat-swamp forests. *Journal of Tropical Ecology* **17**, 667–681. (doi:10.1017/S0266467401001493)
- 45 Zimmerman, J. K., III, E. M. E., Waide, R. B., Lodge, D. J., Taylor, C. M. & Brokaw, N. V. L. 1994 Responses of tree species to hurricane winds in subtropical wet forest in Puerto Rico: Implications for tropical tree life histories. *The Journal of Ecology* **82**, 911–922. (doi:10.2307/2261454)
- 46 Ramesh, B. R., Swaminath, M. H., Patil, S. V., Pédiissier, R., Venugopal, P. D., Aravajy, S., Elouard, C. & Ramalingam, S. 2010 Forest stand structure and composition in 96 sites along environmental gradients in the central Western Ghats of India. *Ecology* **91**, 3118–3118. (doi:10.1890/10-0133.1)

- 47 Gilbert, G. S. et al. 2010 Beyond the tropics: forest structure in a temperate forest mapped plot. *Journal of Vegetation Science* **21**, 388–405. (doi:10.1111/j.1654-1103.2009.01151.x)
- 48 Nakashizuka, T. et al. 2003 Monitoring beech (*Fagus crenata*) forests of different structure in Shirakami Mountains. *Tohoku Journal of Forest Science* **8**, 67–74.
- 49 Palmer, M. W., Peet, R. K., Reed, R. A., Xi, W. & White, P. S. 2007 A multiscale study of vascular plants in a North Carolina Piedmont forest. *Ecology* **88**, 2674–2674. (doi:10.1890/07-0796.1)
- 50 McDonald, R. I., Peet, R. K. & Urban, D. L. 2002 Environmental correlates of oak decline and red maple increase in the North Carolina piedmont. *Castanea* **67**, 84–95.

Figure Legends

Figure 1. An illustration of the four patterns with data from Barro Colorado Island: A) Rank-abundance distribution; B) Individual size distribution (ISD); C) Size-density relationship (SDR); D) Intraspecific individual size distribution (iISD). Grey dots or bars in each panel represent empirical observations and magenta curve represents METE's prediction. The red curve in the D) represents the MLE exponential distribution, which is then compared to the exponential distribution predicted by METE.

Figure 2. METE's predictions are plotted against empirical observations across 60 communities for A) SAD (each data point is the abundance of a species at a single rank in one community), B) ISD (each data point is the frequency in a single body size bin in my community), C) SDR (each data point is the average metabolic rate within one species in one community), and D) iISD (each data point is the exponential distribution parameter summarizing the shape of the iISD for a single species in one community). The diagonal black line in each panel is the 1:1 line. The points are color-coded to reflect the density of neighbouring points, with warm (red) colors representing higher densities and cold (blue) colors representing lower densities. The inset reflects the distribution of R^2 among 60 communities from negative (left) to 1 (right).

Table 1. Summary of datasets.

Dataset	Description	Area of Individual Plots (ha)	Number of Plots	Survey Year	References
Serimbu	Tropical rainforest	1	2	1995 [*]	[36,37]
La Selva	Tropical wet forest	2.24	5	2009	[38,39]
ACA Amazon Forest Inventories	Tropical moist forest	1	1	2000-2001	[40]
BCI	Tropical moist forest	50	1	2010	[41,42]
DeWalt Bolivia forest plots	Tropical moist forest	1	2	N/A	[43]
Lahei	Tropical moist forest	1	3	1998	[37,44]
Luquillo	Tropical moist forest	16	1	1994-1996 [†]	[45]
Sherman	Tropical moist forest	5.96	1	1999	[42]
Cocoli	Tropical moist forest	4	1	1998	[42]
Western Ghats	Wet evergreen / moist / dry deciduous forests	1	34	1996-1997	[46]
UCSC FERP	Mediterranean mixed evergreen forest	6	1	2007	[47]
Shirakami	Beech forest	1	2	2006	[37,48]
Oosting	Hardwood forest	6.55	1	1989	[49]
North Carolina forest plots	Mixed hardwoods / pine forest	1.3 – 5.65	5	1990 (Plot m12), 1991 (Plot m93), 1992 (Plot m4), 1993 (Plots m13, m14) [‡]	[50]

^{*} One plot has a more recent survey in 1998, however it lacks species ID.

[†] We chose Census 2 because information for multiple stems is not available in Census 3, and the unit of diameter is unclear in Census 4.

[‡] These surveys were chosen to minimize the effect of hurricane disturbance for each plot.

Figure 1.

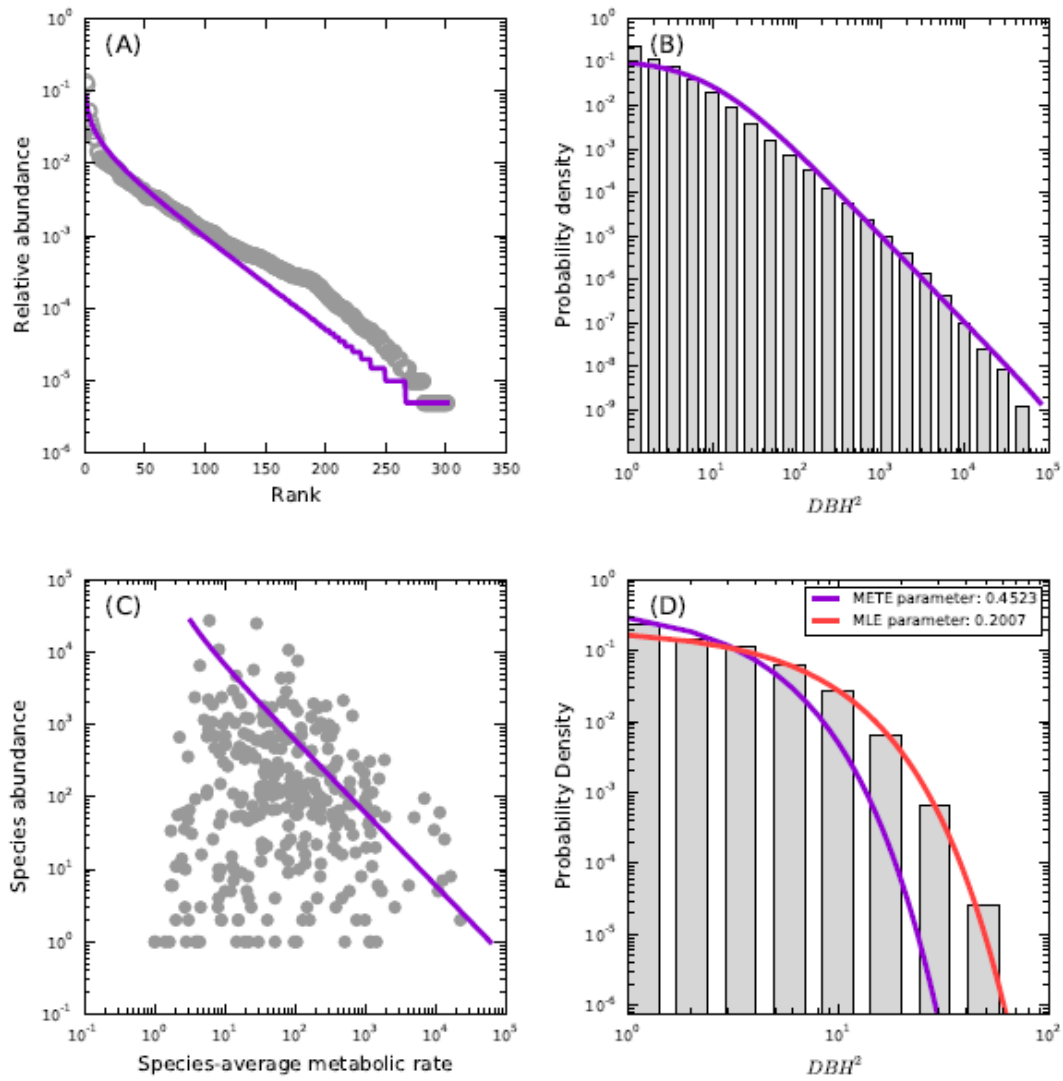
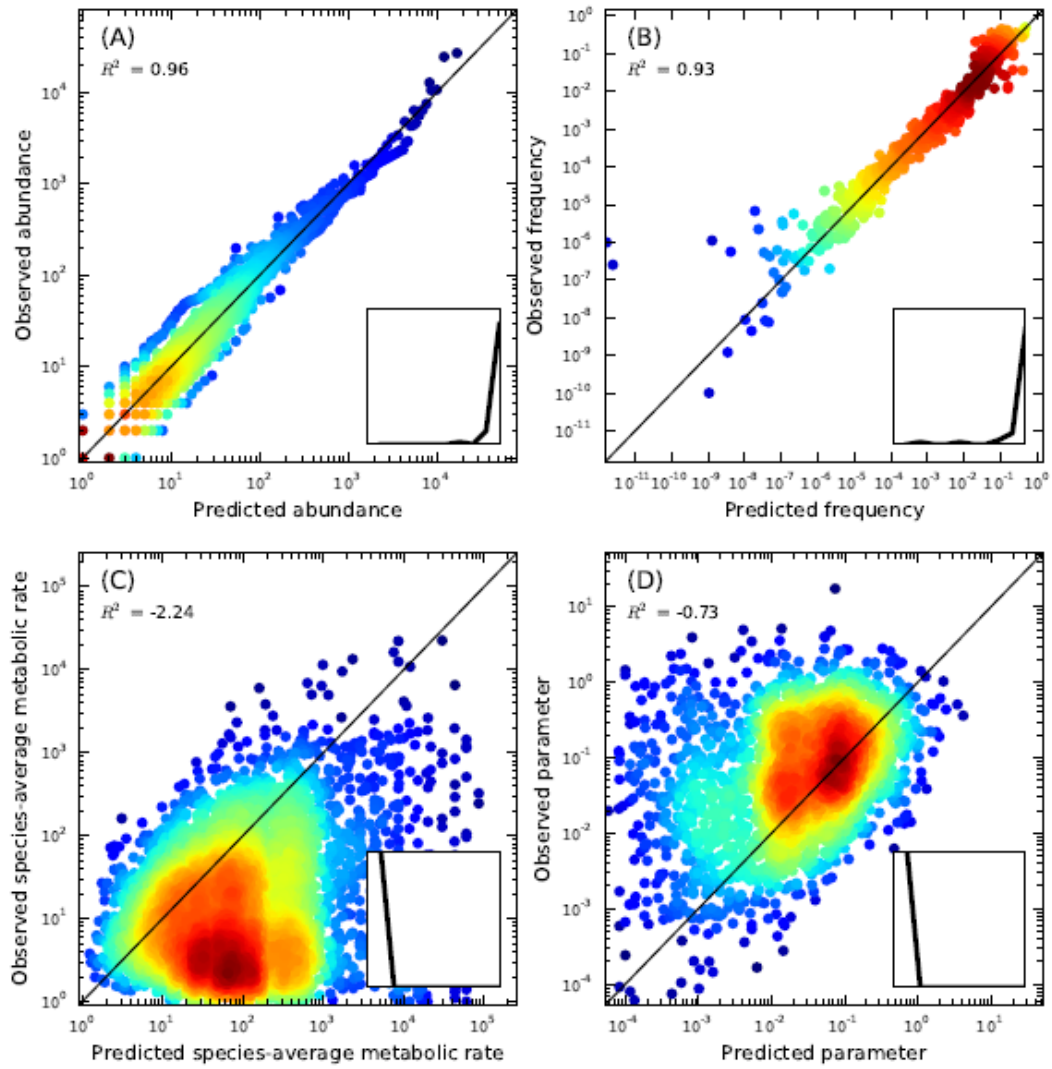


Figure 2.



Appendix A. Derivation for the Equations

The equations we adopted in our analysis (see **Methods: 1. Predicted patterns of METE**) are largely identical to those in Harte (2011), except for a few minor modifications. Below we list equations that are identical (Table A1), and derive those that are slightly different. See Harte (2011) for step-by-step derivations.

Table A1. List of equations in our analysis and the location of their counterparts in Harte (2011).

Equation in this study	Equation in Harte 2011
Eqn 1	Eqn 7.2
Eqn 2	Eqn 7.3
Eqn 3	Eqn 7.13
Eqn 4	Eqn 7.14
Eqn 5	Eqn 7.27
Eqn 6	Eqn 7.26
Eqn 7	N/A
Eqn 8	N/A
Eqn 9	Eqn 7.25
Eqn 10	N/A

Derivation for equations not found in Harte (2011):

1. Species-abundance distribution (SAD; Eqn 7)

From Eqn 7.23 in Harte (2011):

$$\Phi(n) = \int_{\varepsilon=1}^{E_0} d\varepsilon \cdot R(n, \varepsilon) = \frac{e^{-(\lambda_1+\lambda_2)n} - e^{-(\lambda_1+E_0\lambda_2)n}}{\lambda_2 Z n} \quad (\text{Eqn A1})$$

Note that this distribution is properly normalized, i.e., $\sum_{n=1}^{N_0} \Phi(n) = 1$.

Given that E_0 is large, the second term in the numerator, $e^{-(\lambda_1+E_0\lambda_2)n}$, is much smaller than the first term $e^{-(\lambda_1+\lambda_2)n}$. Dropping the second term,

$$\Phi(n) \approx \frac{e^{-(\lambda_1+\lambda_2)n}}{\lambda_2 Z n} \quad (\text{Eqn A2})$$

This approximation leads to the familiar Fisher's log-series distribution, upper-truncated at N_0 . However, the form in Eqn A2 is not properly normalized, which can cause problems when the SAD is converted to the RAD (rank-abundance distribution). To ensure the proper normalization of $\Phi(n)$, we replace the constant term in the Eqn A2, $\lambda_2 Z$, with constant C , where

$$C = \sum_{n=1}^{N_0} \frac{e^{-(\lambda_1+\lambda_2)n}}{n} \quad (\text{Eqn A3})$$

2. The energetic analog of the individual size distribution (ISD; Eqn 8)

From Eqn 7.6 in Harte (2011):

$$\begin{aligned}
 \Psi(\varepsilon) &= \frac{S_0}{N_0} \sum_{n=1}^{N_0} n \cdot R(n, \varepsilon) \\
 &= \frac{S_0}{N_0 Z} \sum_{n=1}^{N_0} n \cdot e^{-\lambda_1 n} e^{-\lambda_2 n \varepsilon} \\
 &= \frac{S_0}{N_0 Z} \sum_{n=1}^{N_0} n \cdot e^{-(\lambda_1 + \lambda_2 \varepsilon)n} \\
 &= \frac{S_0}{N_0 Z} \cdot e^{-(\lambda_1 + \lambda_2 \varepsilon)} \cdot \frac{1 - (N_0 + 1)e^{-N_0(\lambda_1 + \lambda_2 \varepsilon)} + N_0 e^{-(N_0 + 1)(\lambda_1 + \lambda_2 \varepsilon)}}{(1 - e^{-(\lambda_1 + \lambda_2 \varepsilon)})^2} \\
 &= \frac{S_0}{N_0 Z} \cdot \frac{e^{-\gamma}}{(1 - e^{-\gamma})^2} \cdot (1 - (N_0 + 1)e^{-\gamma N_0} + N_0 e^{-\gamma(N_0 + 1)}) \quad (\text{Eqn A4})
 \end{aligned}$$

where $\gamma = \lambda_1 + \lambda_2 \cdot \varepsilon$. Note that Eqn A4 is not identical to Eqn 7.24 in Harte (2011), which contains a minor error (J. Harte, pers. comm.). However, the trivial difference is unlikely to invalidate or significantly change any published results.

3. The energetic analog of the size-density relationship (Eqn 10)

From Eqn 7.25 in Harte (2011):

$$\Theta(\varepsilon|n) = \frac{n\lambda_2 e^{-\lambda_2 n \varepsilon}}{e^{-\lambda_2 n} - e^{-\lambda_2 n E_0}} \quad (\text{Eqn A5})$$

Then

$$\begin{aligned}
 \bar{\varepsilon}(n) &= \int_{\varepsilon=1}^{E_0} d\varepsilon \cdot \varepsilon \cdot \Theta(\varepsilon|n) \\
 &= \int_{\varepsilon=1}^{E_0} d\varepsilon \cdot \varepsilon \cdot \frac{n\lambda_2 e^{-\lambda_2 n \varepsilon}}{e^{-\lambda_2 n} - e^{-\lambda_2 n E_0}} \\
 &= \frac{n\lambda_2}{e^{-\lambda_2 n} - e^{-\lambda_2 n E_0}} \int_{\varepsilon=1}^{E_0} d\varepsilon \cdot \varepsilon \cdot e^{-\lambda_2 n \varepsilon} \\
 &= \frac{1}{n\lambda_2(e^{-\lambda_2 n} - e^{-\lambda_2 n E_0})} \cdot [e^{-\lambda_2 n}(\lambda_2 n + 1) - e^{-\lambda_2 n E_0}(\lambda_2 n E_0 + 1)] \quad (\text{Eqn A6})
 \end{aligned}$$

Appendix B. Alternative Scaling Relationship between Diameter and Metabolic Rate

While we converted diameter (D) to metabolic rate (B) with $B \propto D^2$ in our analyses, alternative relationships between diameter and metabolic rate have been proposed. Specifically, it has been suggested that the aboveground biomass of tropical trees is a function of diameter, wood density, and forest type (Chave et al. 2005), while the relationship between aboveground biomass and metabolic rate is a biphasic, mixed-power function (Mori et al. 2010). Here we demonstrate that adopting this alternative scaling relationship does not quantitatively change our results.

We compiled species-specific wood density (wood specific gravity; WSG) from previous publications (Reyes et al. 1992, Zanne et al. 2009, Chave et al. 2009, Wright et al. 2010, Swenson et al. 2012). Since WSG information is not available for every species, we included only communities of tropical forest where no less than 70% of individuals belonged to species with known WSG to ensure the accuracy of our analysis. This criterion was met by five communities (BCI, Cocoli, Plots 4 and 5 in LaSelva, and Luquillo) out of all 60 that we examined. Individuals in these communities for which WSG information were not available were assigned average WSG value across all species in the WSG compilation.

We obtained metabolic rate of each individual using the alternative scaling relationships specified in Chave et al. 2005 and (Mori et al. 2010). METE was then applied to each community following the steps described in **Methods** in the main text, and its predictions were compared to the observed values for the ISD, the SDR, and the iISD (Fig. A1). Though the patterns differ slightly in shape with metabolic rates obtained from the alternative method, the explanatory power of METE for each pattern does not change qualitatively, i.e., METE characterizes the ISD with high accuracy but is unable to explain much variation in the SDR or the iISD, regardless of the method used to calculate metabolic rate (compare Fig. A1 with corresponding communities in Fig. A4).

Figure A1. METE's predictions are plotted against observed values for A) SAD (which remains unchanged), B) ISD, C) SDR, and D) iISD for each of the five communities individually. Here the metabolic rate was obtained with alternative scaling method, which slightly changes the shape of the ISD, the size-density relationship, and the iISD, without significant impact on the explanatory power of METE. See Pages 38 – 42.

Appendix C. ISD Converted to Rank-Size Distribution

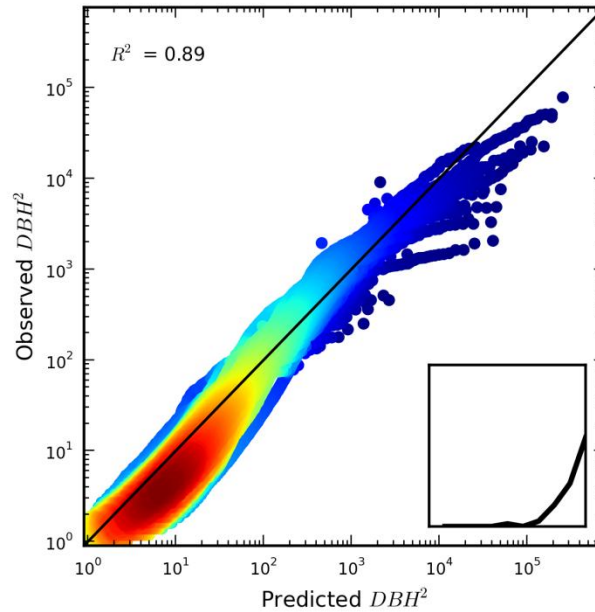


Figure A2. Plot METE's predictions against empirical observations across 60 communities for the ISD, which is converted into rank-size distribution (i.e., each data point is the metabolic rate of an individual at a specific rank in one community). The diagonal black line is the 1:1 line. The points are color-coded to reflect the density of neighbouring points, with warm (red) colors representing higher densities and cold (blue) colors representing lower densities. The inset in the lower right corner shows the distribution of R^2 among individual communities from below zero (left) to 1 (right). Compared with **Fig. 2B**, it is clear that METE has high explanatory power for the ISD regardless of its form ($R^2 = 0.89$ for rank-size distribution vs. $R^2 = 0.93$ for binned frequencies).

Appendix D. Goodness of Fit of the Exponential Distribution to iISDs

METE predicts that the iISD for each species within a community follows an exponential distribution left-truncated at 1, with the parameter of the distribution proportional to the abundance of the species (see Eqn 9 in main text). Deviations of observed iISDs from METE's prediction can result from one of two ways: 1. the observed iISD cannot be characterized by an exponential distribution; 2. the observed iISD can be characterized by an exponential distribution, but with a different parameter value as predicted by METE. Here we focus on the first possibility and evaluate the goodness of fit of the exponential distribution to the iISDs.

In each community, we obtained the maximum likelihood (MLE) parameter of the left-truncated exponential distribution using rescaled individual metabolic rates for every species with an abundance of at least five. For each species, 5,000 independent samples were drawn from a left-truncated exponential distribution with the MLE parameter, where the sample size was equal to the abundance of the species. The two-sample Kolmogorov-Smirnov test was then applied to evaluate if the empirical iISD differ significantly from each sample drawn from the left-truncated exponential distribution. If the proportion of tests (among all 5,000) where the empirical iISD and the randomly generated sample differ in distribution is higher than the significance level (α) of the tests, the empirical iISD for the focal species does not conform to a left-truncated exponential distribution.

Fig. A3 shows a histogram of proportions of Kolmogorov-Smirnov tests that are significant at $\alpha = 0.05$ among species (with abundance ≥ 5) across all 60 communities. Overall the iISDs for more than half of the species are deemed to be significantly different from the left-truncated exponential distribution. Therefore by assuming that all iISDs can be characterized by the left-truncated exponential distribution as predicted by METE, our analysis for iISD (see **Methods**) is biased in favor of METE. The fact that the R^2 for the iISD is below zero even when METE is evaluated with this biased analysis further strengthens our conclusion that METE is unable to meaningfully capture any variation in the iISD.

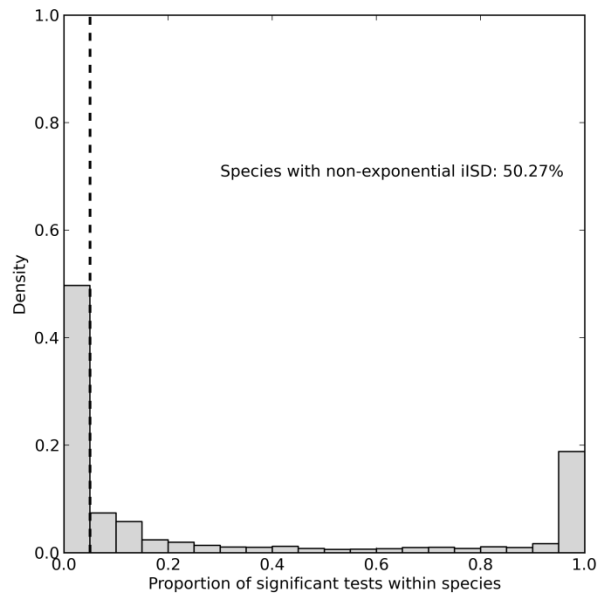


Figure A3. Histogram of the proportion of Kolmogorov-Smirnov tests that are significant for each species. The dashed vertical line represents the significance level of the tests $\alpha = 0.05$. Species for which the proportion of tests (among 5,000) with significant results is higher than 0.05 have iISDs that differ significantly from the left-truncated exponential distribution.

Appendix E. Evaluation of METE within Communities

Figure A4. METE's predictions for A) SAD, B) ISD, C) SDR, and D) iISD are plotted against observed patterns in each of the 60 forest communities. In A), the grey circles represent observed abundance of species in each community at each rank from the most abundant to the least abundant. In B), the grey bars represent the proportion of individuals within each size bin in each community. In C), each grey dot represents one species with a specific abundance and species-average metabolic rate in the community. The magenta curves in subplots A), B), and C) represent the relationships predicted by METE. In D), the parameter of the exponential distribution predicted by METE is plotted against the maximum likelihood parameter, while the diagonal line is the 1:1 line. See Pages 43 – 102.

Appendix F. Model Comparison for ISD

Muller-Landau et al. (2006) proposed four possible distributions (exponential, Pareto, Weibull, and quasi-Weibull) for diameter in old-growth forests, under different assumptions of growth and mortality. Here we compare the fit of three of the four distributions (exponential, Pareto, and Weibull) to the fit of the ISD predicted by METE (Eqn 8) using data from the 60 forest communities. The quasi-Weibull distribution, which has been shown to provide the best fit for the majority of communities (Muller-Landau et al. 2006), is not evaluated due to the difficulty in obtaining its maximum likelihood parameters when it is left-truncated.

All distributions are left-truncated to account for the fact that individuals below the minimal threshold in each community were excluded from the datasets. With the minimal size rescaled as 1 across communities (see **Methods**), the left-truncated exponential distribution takes the form

$$f(D) = \lambda e^{-\lambda(D-1)} \quad (\text{Eqn A7})$$

the left-truncated Pareto distribution takes the form

$$f(D) = \frac{\alpha}{D^{\alpha+1}} \quad (\text{Eqn A8})$$

the left-truncated Weibull distribution takes the form

$$f(D) = \frac{k}{\lambda} \left(\frac{D}{\lambda}\right)^{k-1} e^{-(D/\lambda)^k} / e^{-(1/\lambda)^k} \quad (\text{Eqn A9})$$

where the diameter $D \geq 1$ for all three distributions.

Parameters in Eqns A7, A8 and A9 were obtained with maximum likelihood method (MLE) for each community. While analytical solutions exist for parameters in Eqn A7 and Eqn A8, MLE solutions for parameters in Eqn A9 can only be obtained numerically. The three distributions of D were then transformed into distributions of D^2 (surrogate for metabolic rate; see Methods) to be consistent with METE's prediction (Eqn 8) as:

$$g(D^2) = \frac{1}{2D} f(D) \quad (\text{Eqn A10})$$

where $f(D)$ is the left-truncated exponential, Pareto, or Weibull distribution in Eqns A7, A8 or A9.

The fit of the ISD predicted by METE and the other three distributions was evaluated with Akaike's Information Criterion (AIC; Burnham and Anderson 2002). AIC_c, a second-order variant of AIC which corrects for finite sample size, was computed for each distribution as

$$AIC_c = 2k - 2 \ln(L) + \frac{2k(k+1)}{n-k-1} \quad (\text{Eqn A11})$$

where k is the number of parameters in the corresponding distribution, n is the number of individuals in the community, and L is the likelihood of the distribution across all individuals (Burnham and Anderson 2002). Within a community, the distribution with a lower AIC_c value provides a better fit.

Our results show that overall the Weibull distribution provides the best fit for the ISD, which outperforms the other three distributions (i.e., has the smallest AIC_c value) in 50 out of 60 communities. While METE is exceeded by the Weibull distribution in all except 3 communities, its performance is comparable to that of the other two distributions, with METE outperforming the exponential distribution in 24 communities and the Pareto distribution in 33 (Table A2).

Table A2. The AIC_c value of the four distributions of ISD across communities. The distribution with the best fit (lowest AIC_c value) for each community is in red.

Dataset	Site	AIC_c -exponential	AIC_c -Pareto	AIC_c -Weibull	AIC_c -METE
FERP	FERP	85971.15	82823.11	81893.76	88390.74
ACA	eno-2	3047.892	3123.951	3037.737	3048.544
WesternGhats	BSP104	8447.378	8232.82	8147.375	8597.933
WesternGhats	BSP11	9670.786	9737.739	9565.319	9756.008
WesternGhats	BSP12	8072.348	7580.985	7580.105	8005.097
WesternGhats	BSP16	6505.854	6465.984	6371.536	6473.227
WesternGhats	BSP27	4158.854	4352.934	4154.657	4168.587
WesternGhats	BSP29	5200.085	5601.832	5186.167	5246.872
WesternGhats	BSP30	5228.032	5550.478	5229.22	5272.148
WesternGhats	BSP36	5363.257	4997.568	4994.507	5613.485
WesternGhats	BSP37	6648.723	5882.951	5940.894	6702.201
WesternGhats	BSP42	4862.353	4579.541	4572.774	4912.597
WesternGhats	BSP5	6316.684	5868.932	5879.056	6344.512
WesternGhats	BSP6	8362.132	8224.467	8144.515	8368.706
WesternGhats	BSP65	10730.14	10597.32	10418.12	10323.55
WesternGhats	BSP66	6127.039	6078.716	5969.159	6118.758
WesternGhats	BSP67	5733.979	6116.641	5713.447	5970.901
WesternGhats	BSP69	9639.039	9839.743	9566.506	9677.272
WesternGhats	BSP70	7568.366	7643.62	7475.877	7471.337
WesternGhats	BSP73	13866.8	14638.34	13867.97	14056.6
WesternGhats	BSP74	10384.88	10164.99	10043.66	10178.07
WesternGhats	BSP75	3828.718	4032.776	3830.225	3844.366
WesternGhats	BSP79	10012.15	10192.38	9943.069	10014.63
WesternGhats	BSP80	10351.04	10721.97	10333.53	10392.1
WesternGhats	BSP82	7775.241	8109.038	7766.727	7779.842

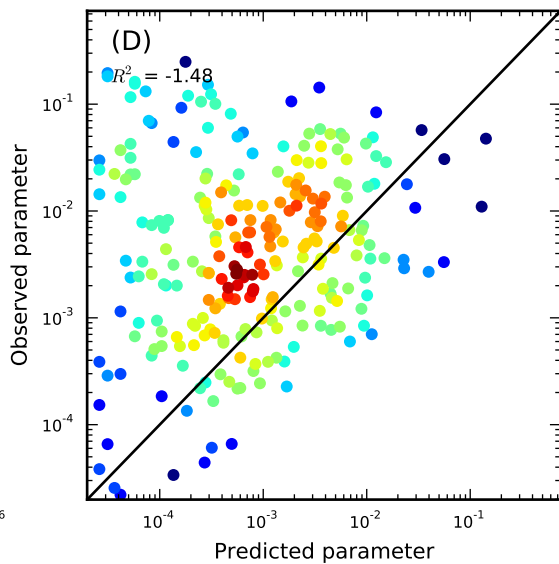
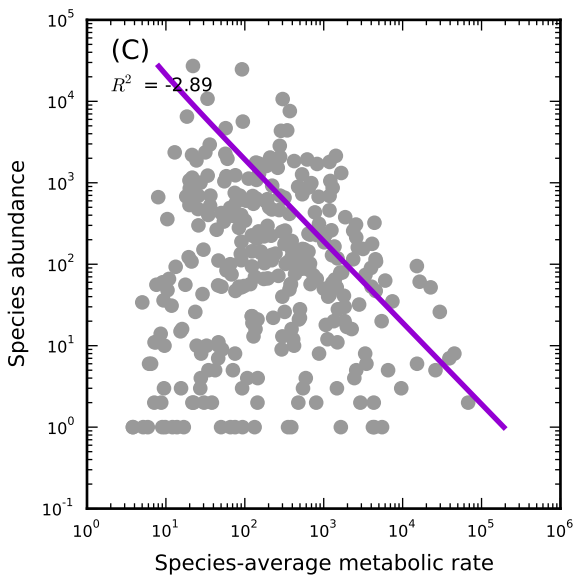
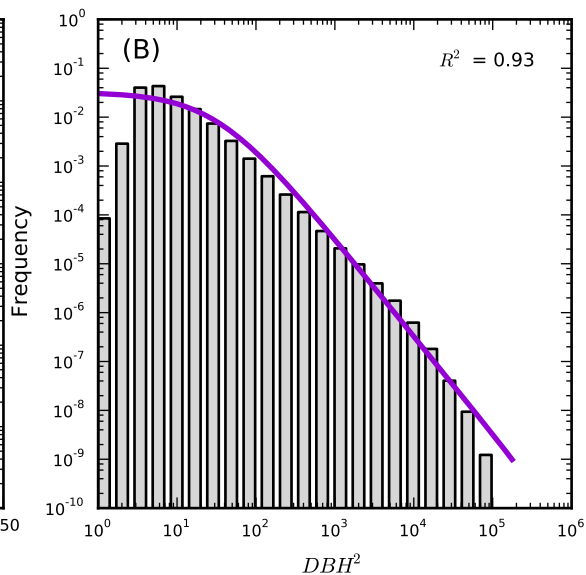
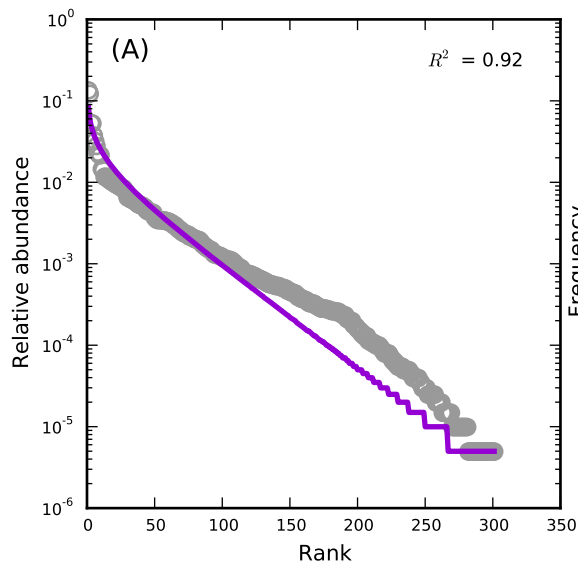
WesternGhats	BSP83	10080.84	10603.67	10082.84	10184.62
WesternGhats	BSP84	9941.77	10676.22	9906.56	10087.81
WesternGhats	BSP85	4090.759	4051.023	3986.417	4092.965
WesternGhats	BSP88	9539.878	10007.25	9532.9	9468.538
WesternGhats	BSP89	7758.469	8040.773	7746.257	7749.632
WesternGhats	BSP90	7802.77	8287.765	7800.707	7891.673
WesternGhats	BSP91	8443.673	9081.623	8392.871	8709.277
WesternGhats	BSP92	5010.321	5156.128	4980.47	5037.136
WesternGhats	BSP94	4995.435	5113.566	4949.09	4997.738
WesternGhats	BSP98	6338.305	6535.699	6312.535	6336.033
WesternGhats	BSP99	8329.191	8461.831	8238.427	8268.363
BCI	bci	1663761	1595835	1580094	1616953
BVSF	BVPlot	2801.075	2851.043	2790.895	2792.688
BVSF	SFPlot	2452.828	2427.723	2409.388	2413.466
Cocoli	cocoli	73752.32	68152.93	67835.59	75938.32
Lahei	heath1	9947.228	9966.227	9841.178	9888.052
Lahei	heath2	9795.598	9650.197	9595.179	9618.001
Lahei	peat	9183.332	9040.189	8961.699	9030.188
LaSelva	1	5518.14	5434.672	5376.494	5555.8
LaSelva	2	5504.011	5548.332	5444.005	5489.366
LaSelva	3	6337.174	6328.63	6237.519	6294.73
LaSelva	4	5445.745	5527.303	5402.815	5409.85
LaSelva	5	4410.166	4318.777	4281.463	4440.427
Luquillo	lfdp	534427.2	515126.9	509926.5	525725.7
NC	12	45716.48	44860.83	44212.08	45592.31
NC	13	36251.18	34948.55	34539.55	36220.19
NC	14	56695.06	52506.98	52273.61	55964.15
NC	4	36203.17	36553.64	35587.05	36447.78
NC	93	34667.37	33277.48	32934.38	34730.18
Oosting	Oosting	74293.18	69837.5	69718.9	74739.21
Serimbu	S-1	7887.232	7471.463	7463.06	7981.97
Serimbu	S-2	8507.118	8123.406	8102.843	8614.922
Shirakami	Akaishizawa	3105.173	3104.759	3057.59	3188.967
Shirakami	Kumagera	3473.692	3680.852	3473.805	3597.692
Sherman	sherman	191735.8	188206	185424	190339.9

References

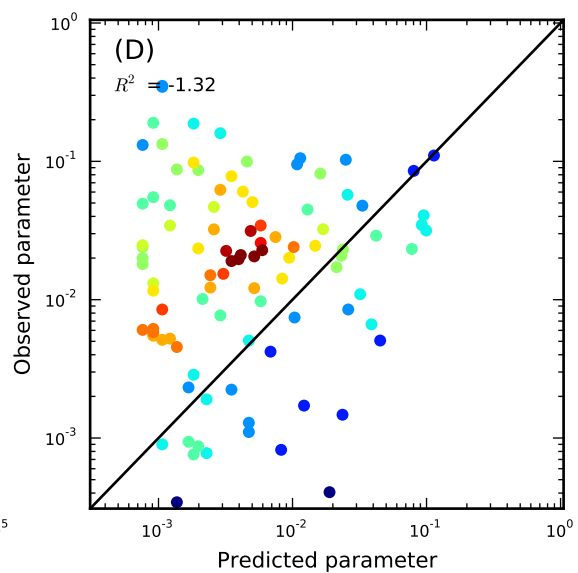
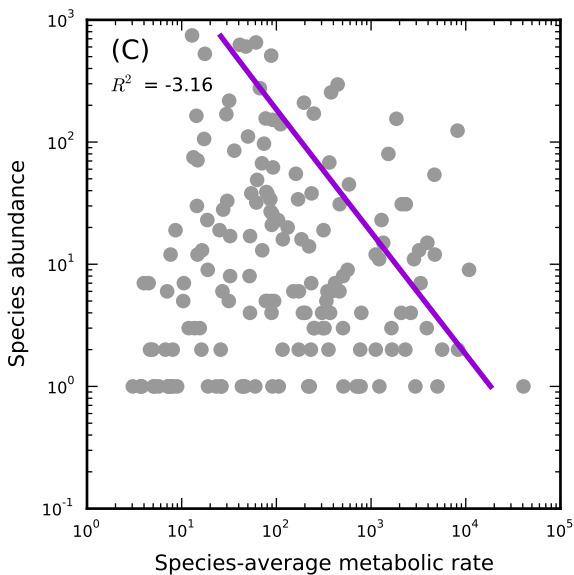
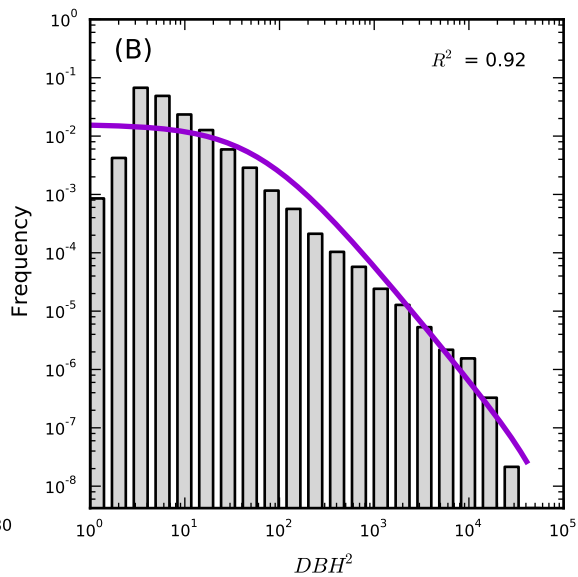
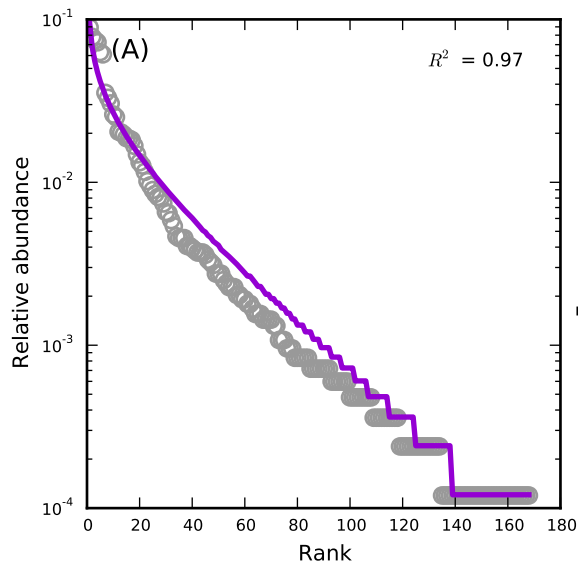
- Burnham, K. P., and D. R. Anderson. 2002. Model selection and multimodel inference: a practical information-theoretic approach. Springer-Verlag, New York, New York, USA.
- Chave, J., C. Andalo, S. Brown, M. a Cairns, J. Q. Chambers, D. Eamus, H. Fölster, F. Fromard, N. Higuchi, T. Kira, J.-P. Lescure, B. W. Nelson, H. Ogawa, H. Puig, B. Ri éra, and T. Yamakura. 2005. Tree allometry and improved estimation of carbon stocks and balance in tropical forests. *Oecologia* 145:87–99.
- Chave, J., D. Coomes, S. Jansen, S. L. Lewis, N. G. Swenson, and A. E. Zanne. 2009. Towards a worldwide wood economics spectrum. *Ecology letters* 12:351–366.
- Harte, J. 2011. Maximum Entropy and Ecology: A Theory of Abundance, Distribution, and Energetics. Oxford University Press.
- Mori, S., K. Yamaji, A. Ishida, S. G. Prokushkin, O. V Masyagina, A. Hagihara, a T. M. R. Hoque, R. Suwa, A. Osawa, T. Nishizono, T. Ueda, M. Kinjo, T. Miyagi, T. Kajimoto, T. Koike, Y. Matsuura, T. Toma, O. a Zyryanova, A. P. Abaimov, Y. Awaya, M. G. Araki, T. Kawasaki, Y. Chiba, and M. Umari. 2010. Mixed-power scaling of whole-plant respiration from seedlings to giant trees. *Proceedings of the National Academy of Sciences of the United States of America* 107:1447–1451.
- Muller-Landau, H. C., R. S. Condit, K. E. Harms, C. O. Marks, S. C. Thomas, S. Bunyavejchewin, G. Chuyong, L. Co, S. Davies, R. Foster, S. Gunatilleke, N. Gunatilleke, T. Hart, S. P. Hubbell, A. Itoh, A. R. Kassim, D. Kenfack, J. V LaFrankie, D. Lagunzad, H. S. Lee, E. Losos, J.-R. Makana, T. Ohkubo, C. Samper, R. Sukumar, I.-F. Sun, M. N. Nur Supardi, S. Tan, D. Thomas, J. Thompson, R. Valencia, M. I. Vallejo, G. V. Muñoz, T. Yamakura, J. K. Zimmerman, H. S. Dattaraja, S. Esufali, P. Hall, F. He, C. Hernandez, S. Kiratiprayoon, H. S. Suresh, C. Wills, and P. Ashton. 2006. Comparing tropical forest tree size distributions with the predictions of metabolic ecology and equilibrium models. *Ecology letters* 9:589–602.
- Reyes, G., S. Brown, J. Chapman, and A. E. Lugo. 1992. Wood Densities of Tropical Tree Species. Gen. Tech. Rep. SO-88. New Orleans, LA: U.S. Dept of Agriculture, Forest Service, Southern Forest Experiment Station.
- Swenson, N. G., J. C. Stegen, S. J. Davies, D. L. Erickson, J. Forero-Montaña, A. H. Hurlbert, W. J. Kress, J. Thompson, M. Uriarte, S. J. Wright, and J. K. Zimmerman. 2012. Temporal turnover in the composition of tropical tree communities: functional determinism and phylogenetic stochasticity. *Ecology* 93:490–499.
- Wright, S. J., K. Kitajima, N. J. B. Kraft, P. B. Reich, I. J. Wright, D. E. Bunker, R. Condit, J. W. Dalling, S. J. Davies, S. D áz, B. M. J. Engelbrecht, K. E. Harms, S. P. Hubbell, C. O. Marks, M. C. Ruiz-Jaen, C. M. Salvador, and A. E. Zanne. 2010. Functional traits and the growth–mortality trade-off in tropical trees. *Ecology* 91:3664–3674.

Zanne, A. E., G. Lopez-Gonzalez, D. A. Coomes, J. Ilic, S. Jansen, S. L. Lewis, R. B. Miller, N. G. Swenson, M. C. Wiemann, and J. Chave. 2009. Data from: Towards a worldwide wood economics spectrum. Dryad Digital Repository.

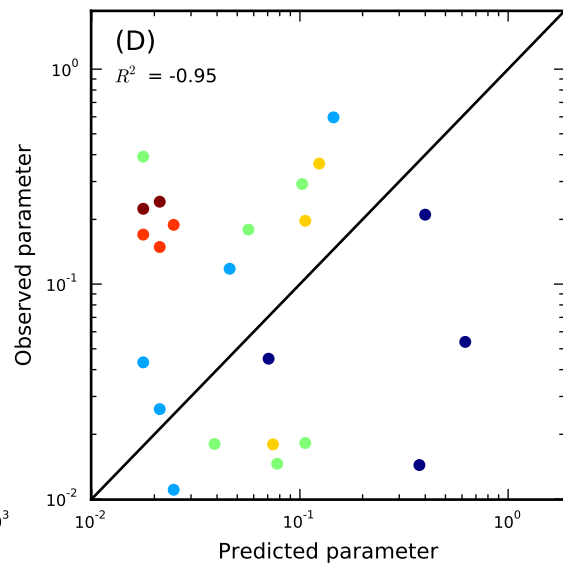
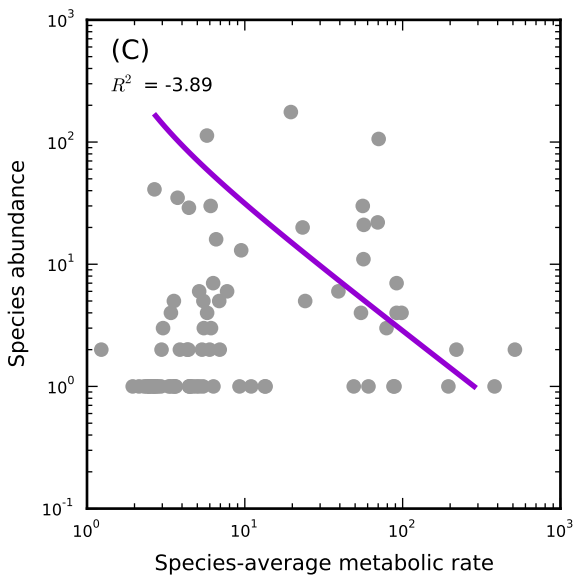
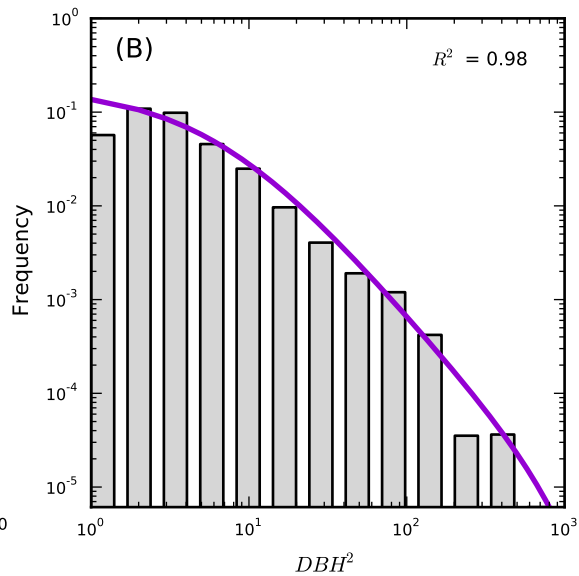
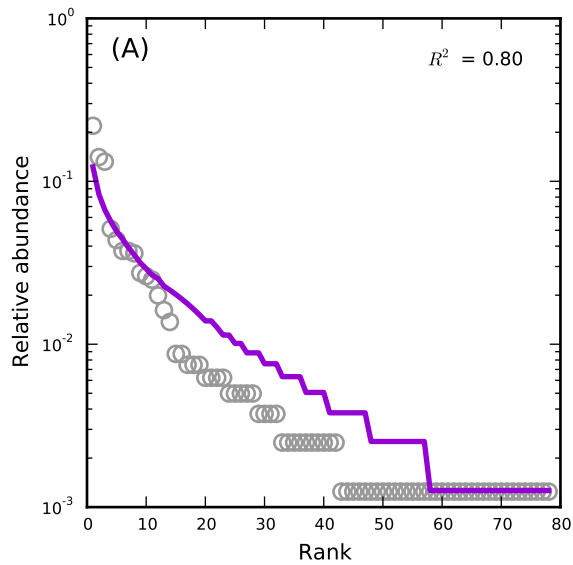
BCI_alt,bci



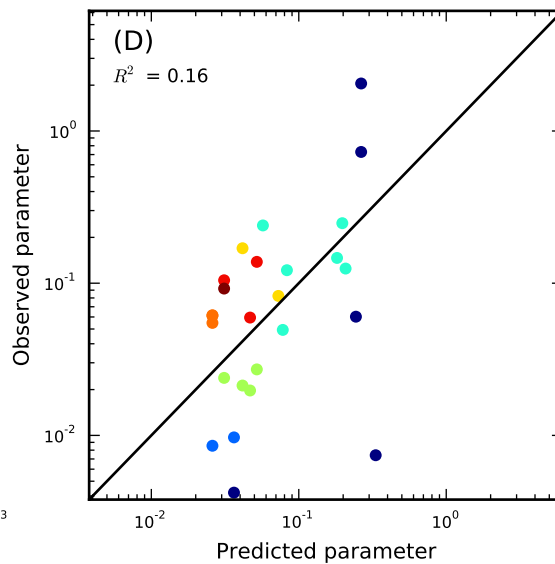
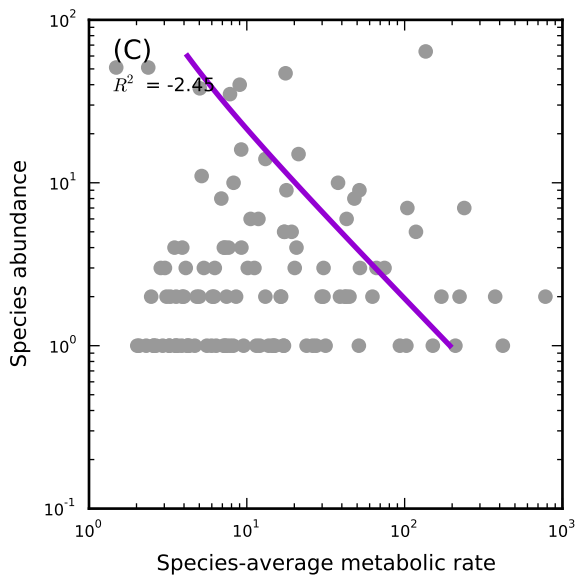
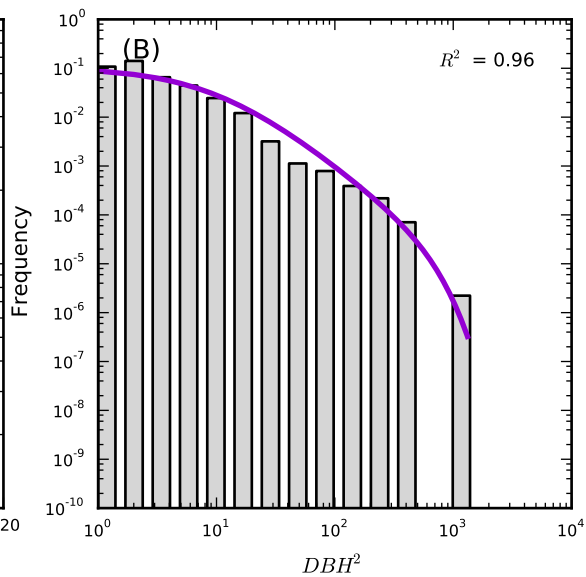
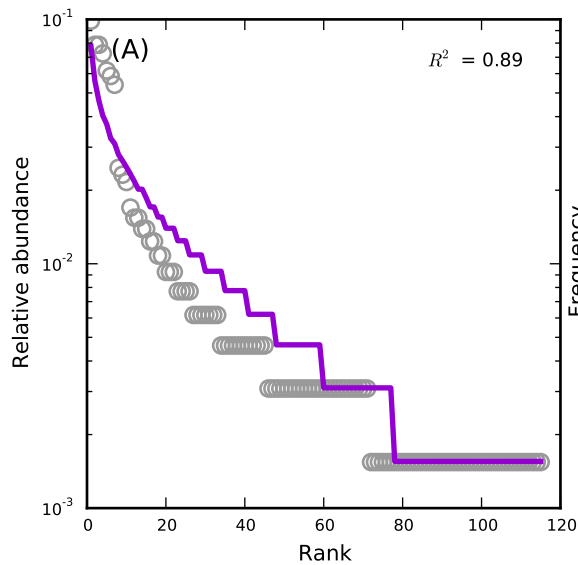
Cocoli_alt,cocoli



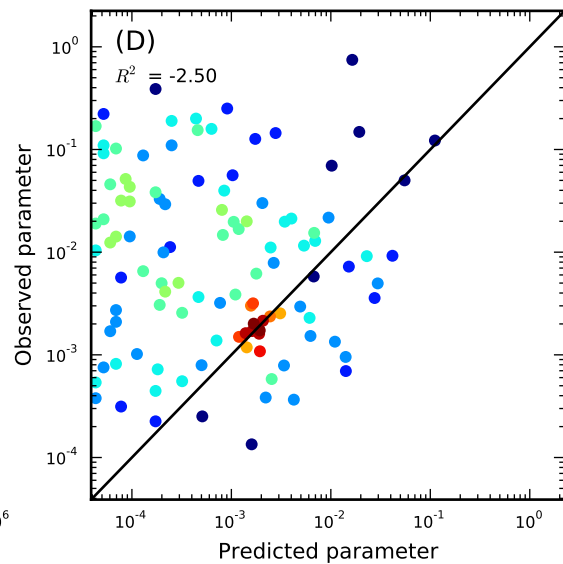
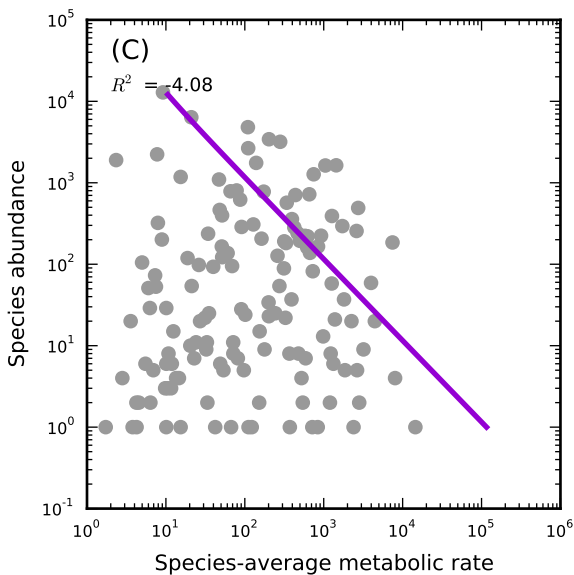
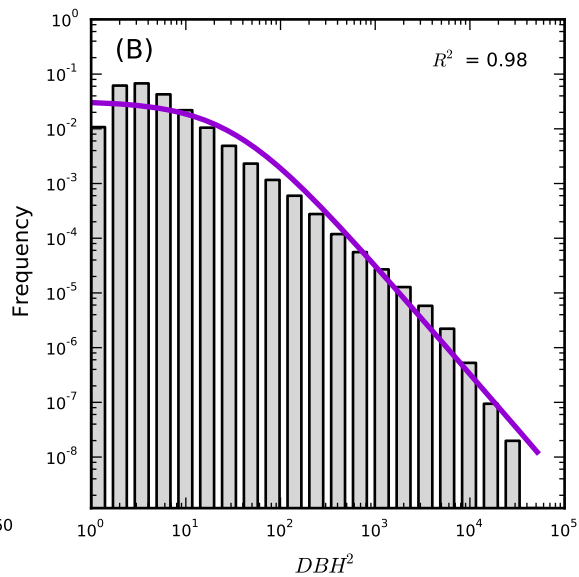
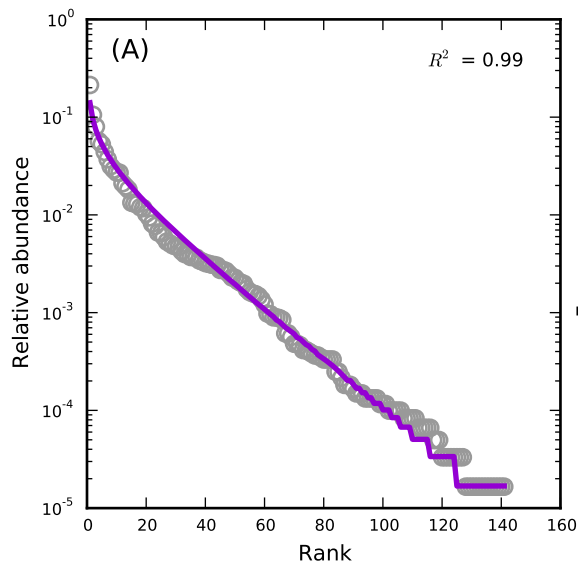
LaSelva_alt,4



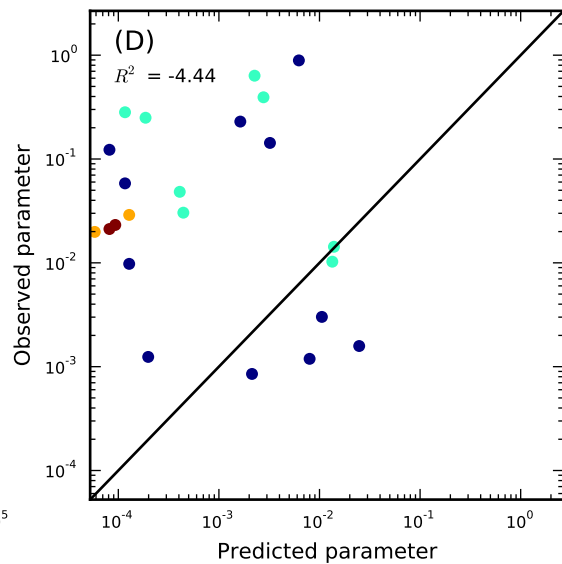
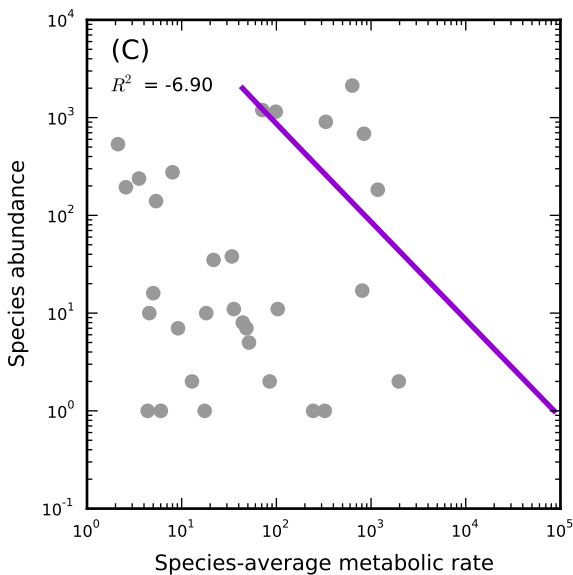
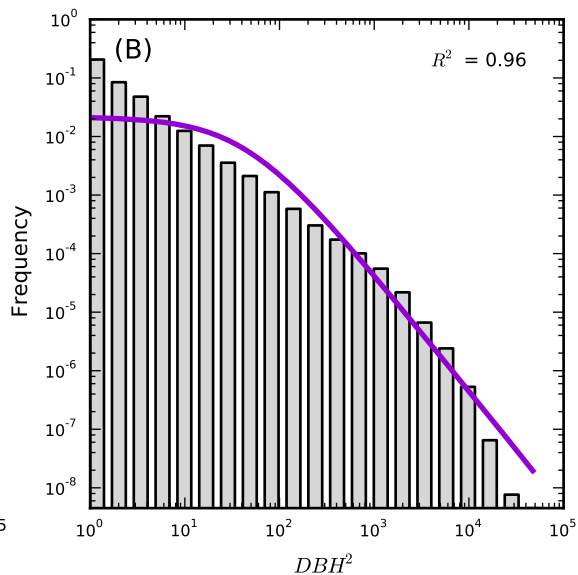
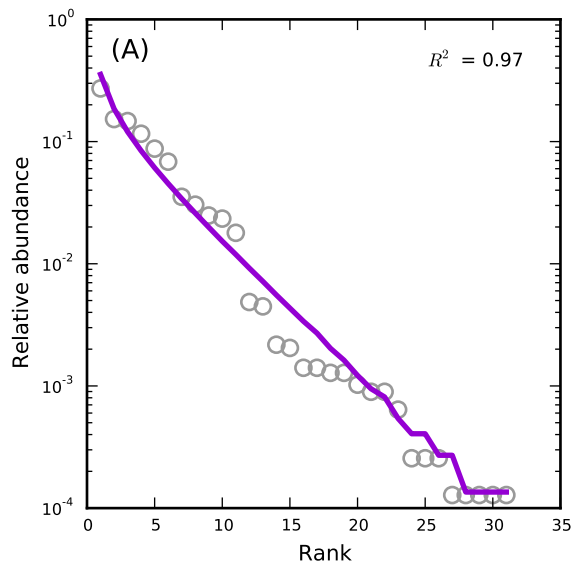
LaSelva_alt,5



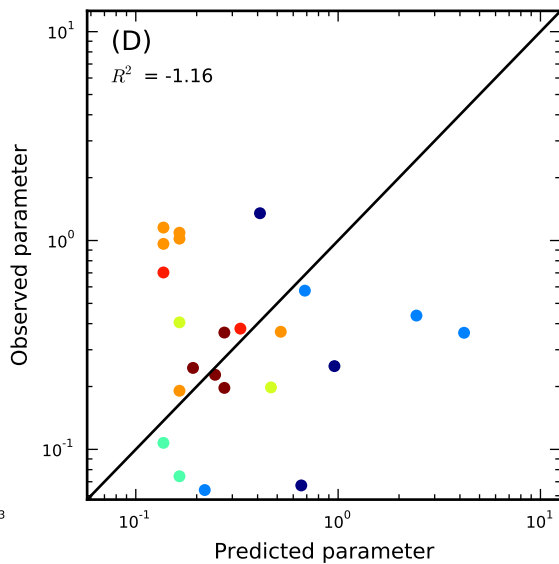
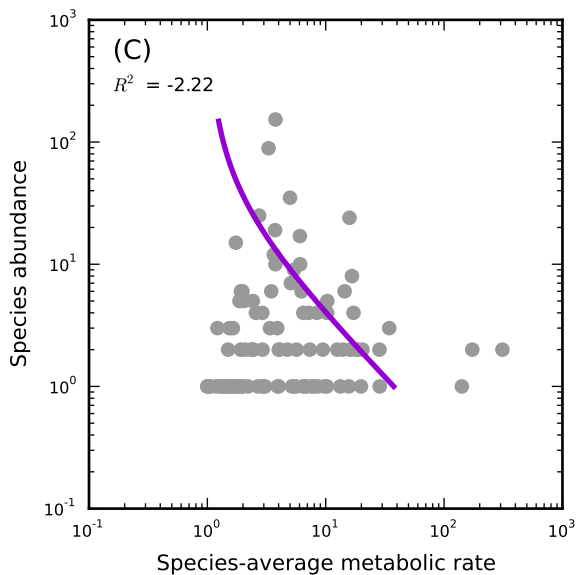
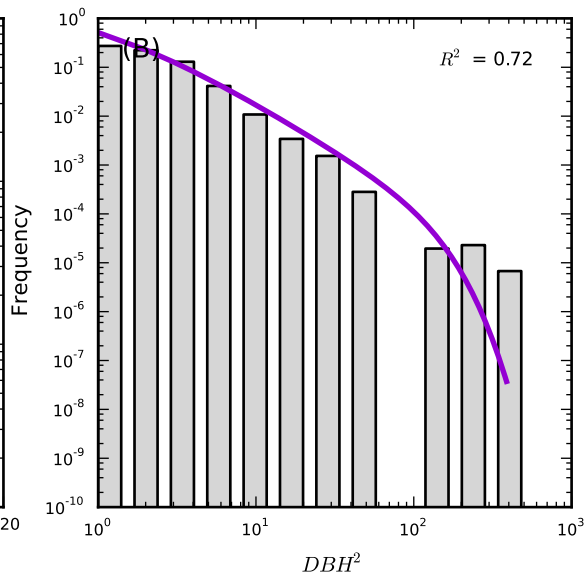
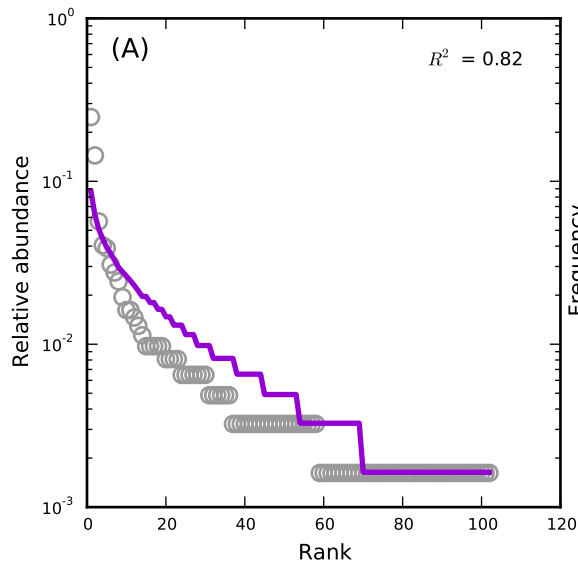
Luquillo_alt,lfdp



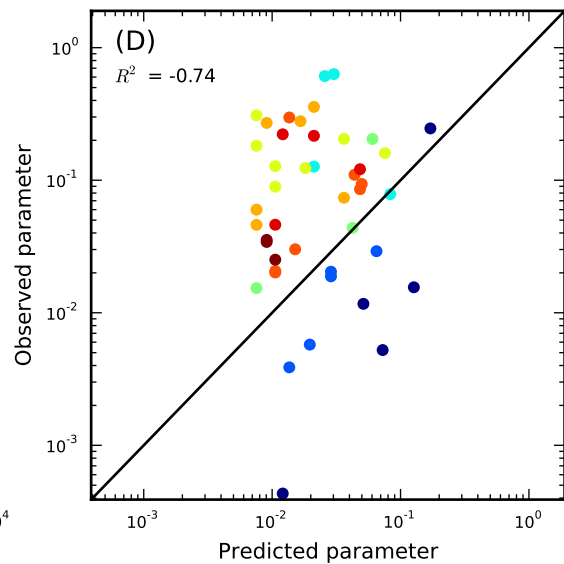
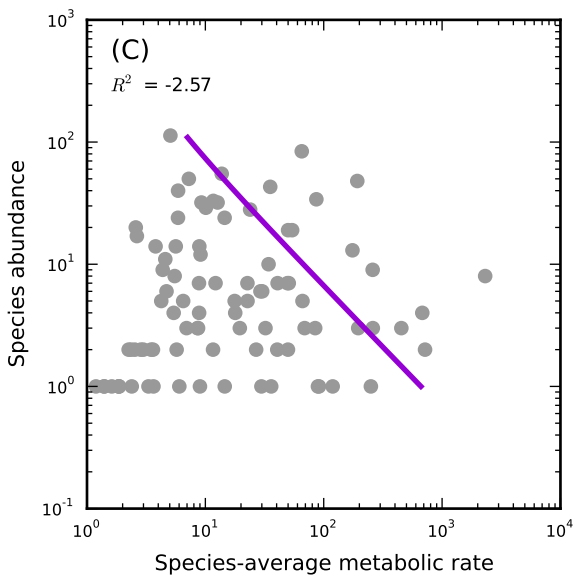
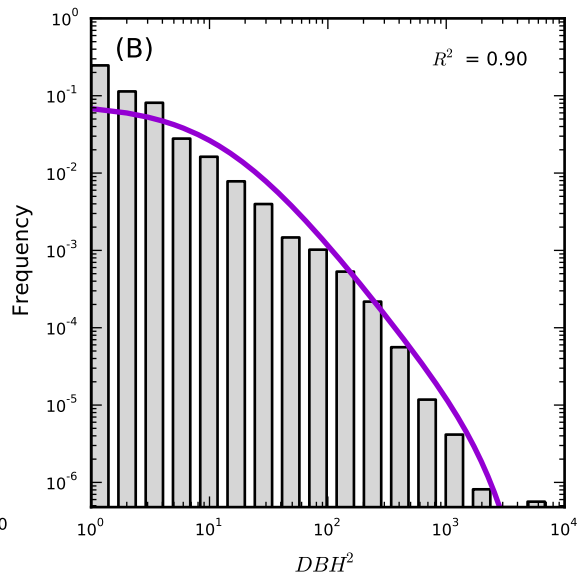
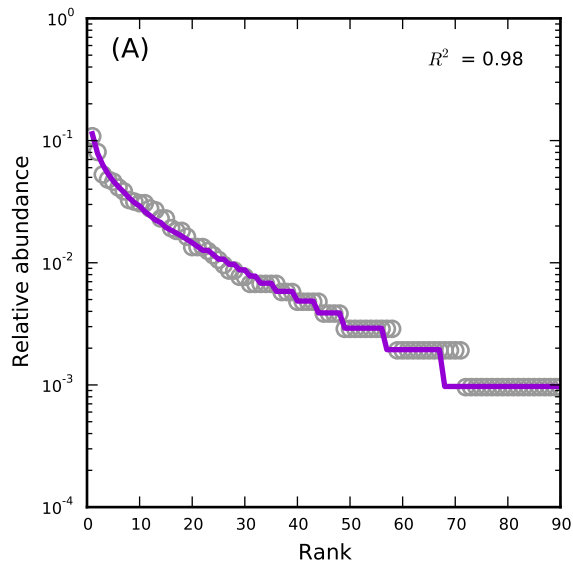
FERP, FERP



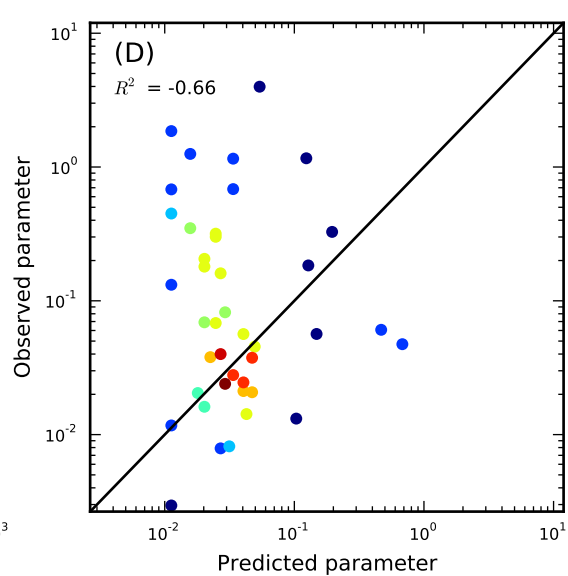
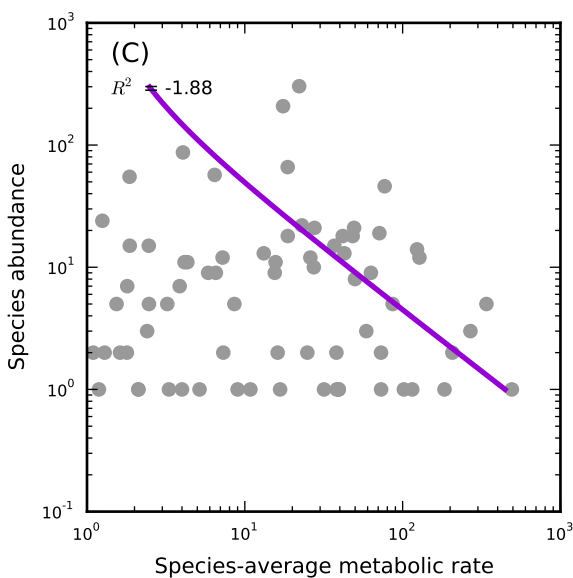
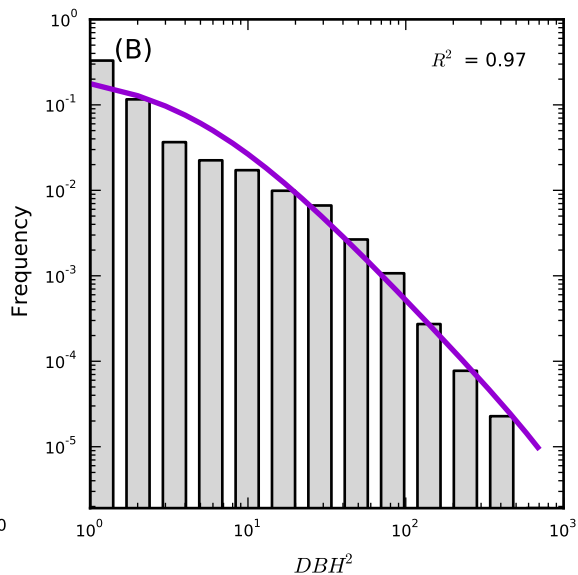
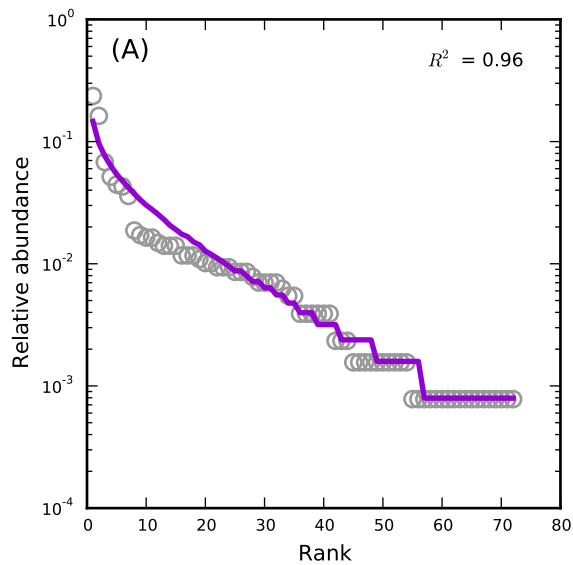
ACA,eno-2



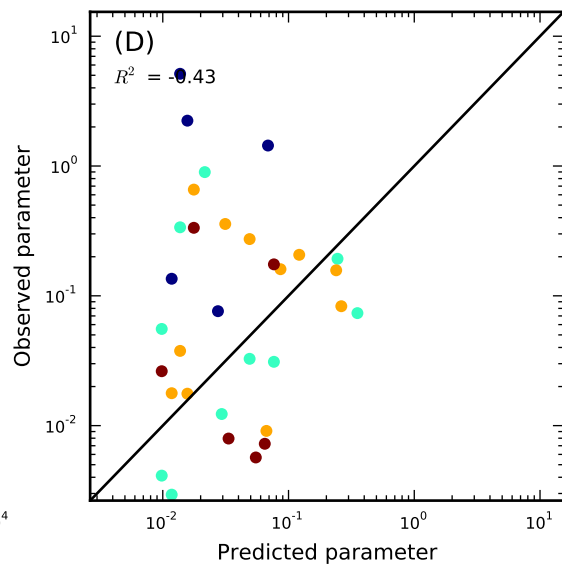
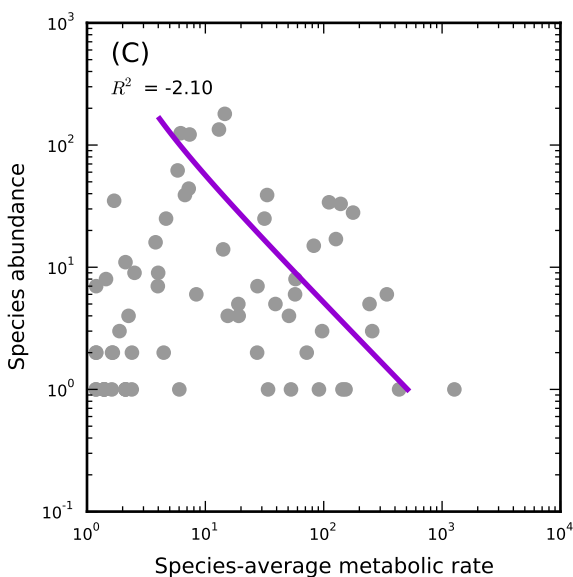
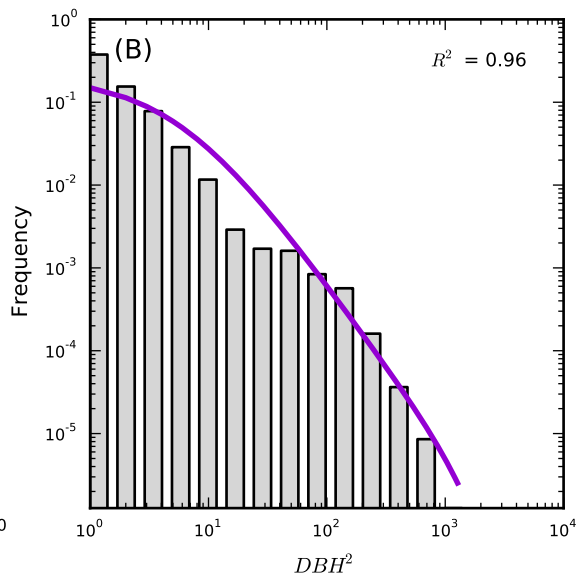
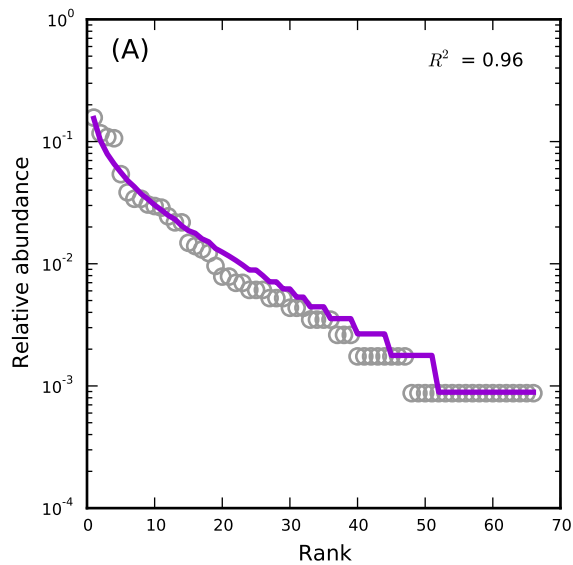
WesternGhats,BSP104



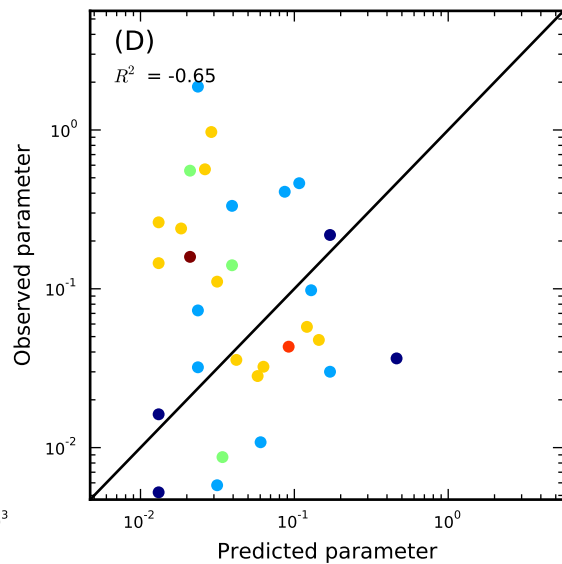
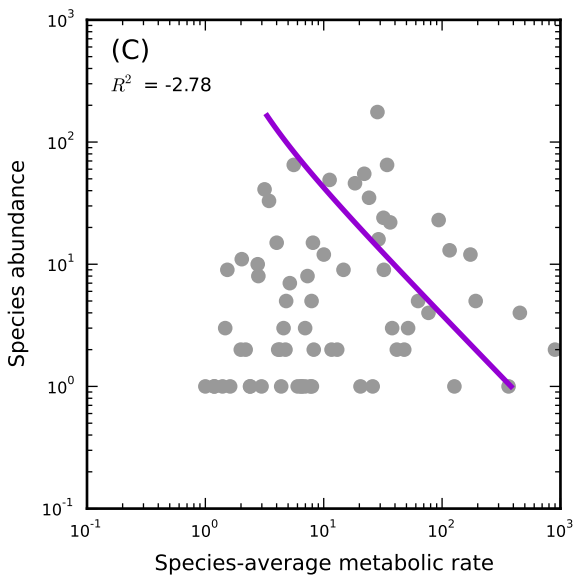
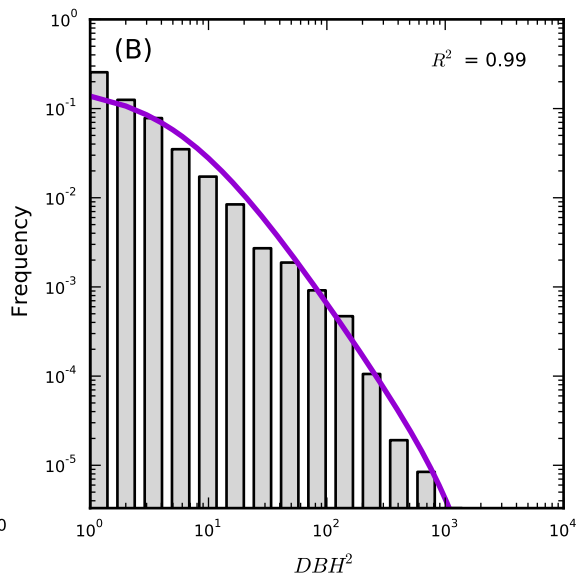
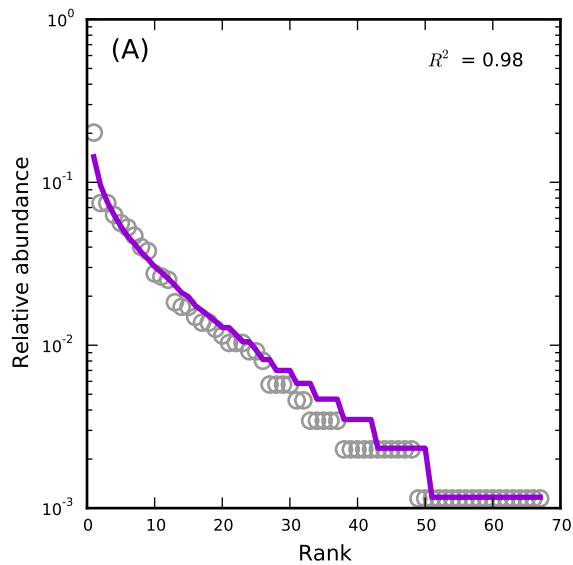
WesternGhats,BSP11



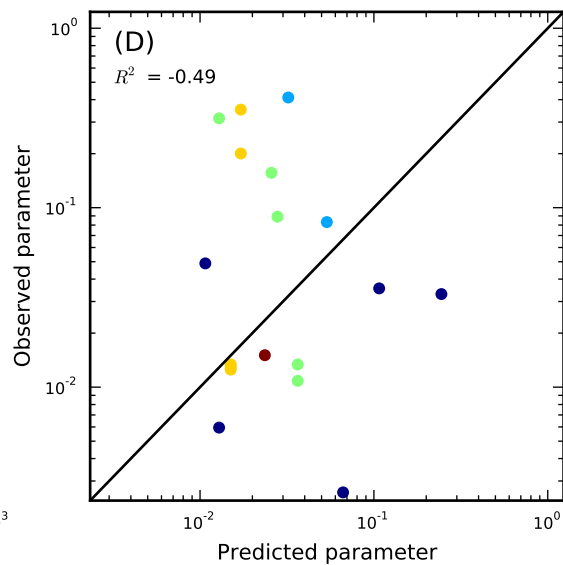
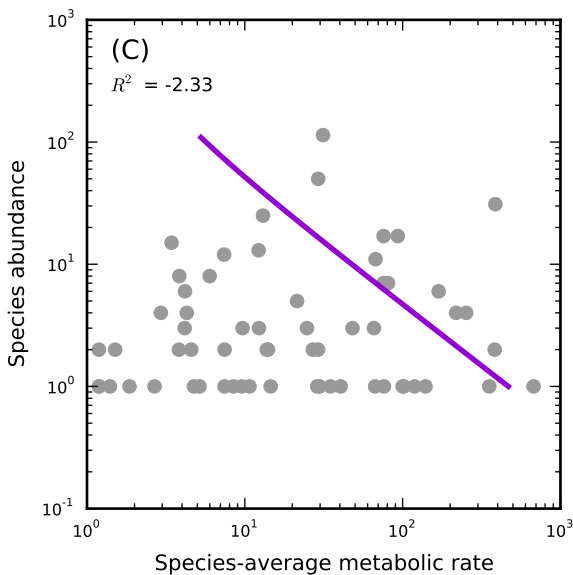
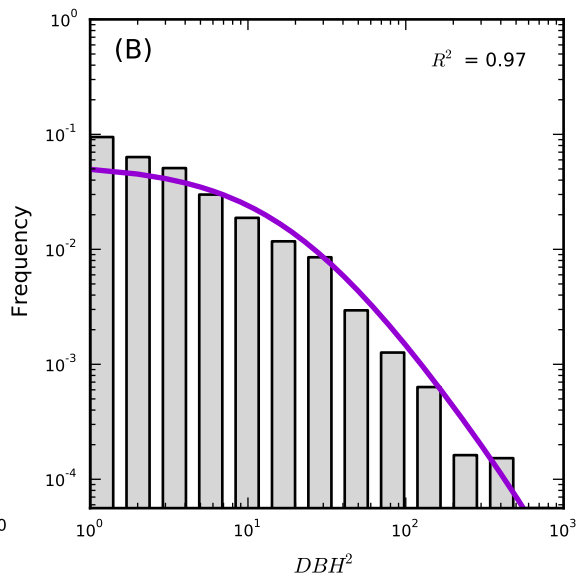
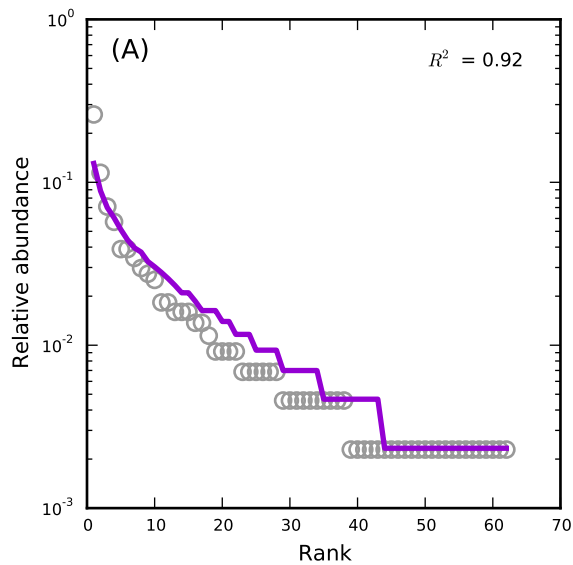
WesternGhats,BSP12



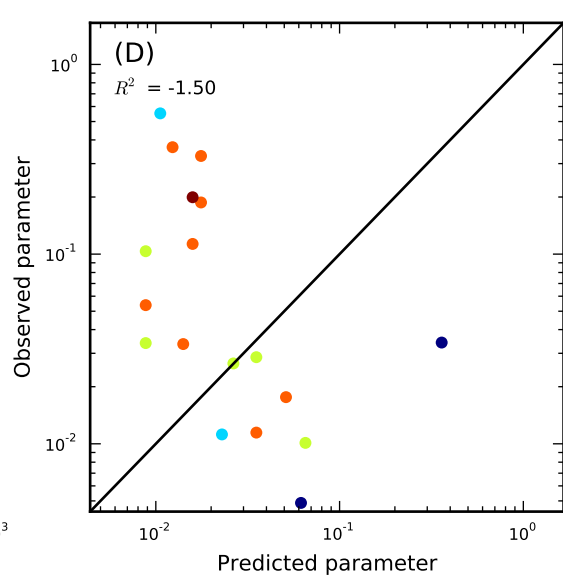
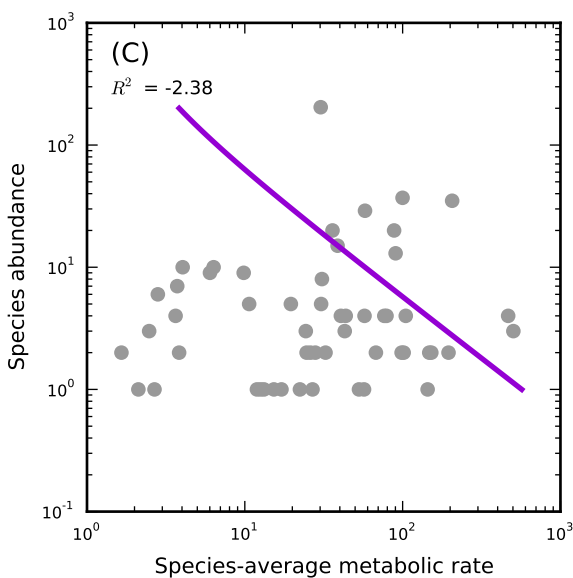
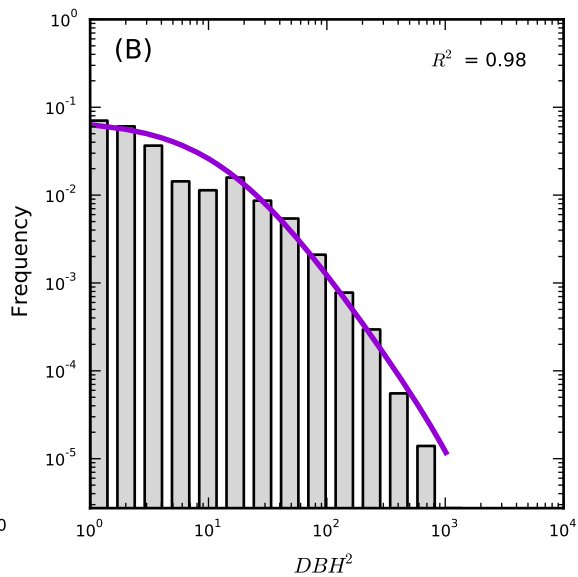
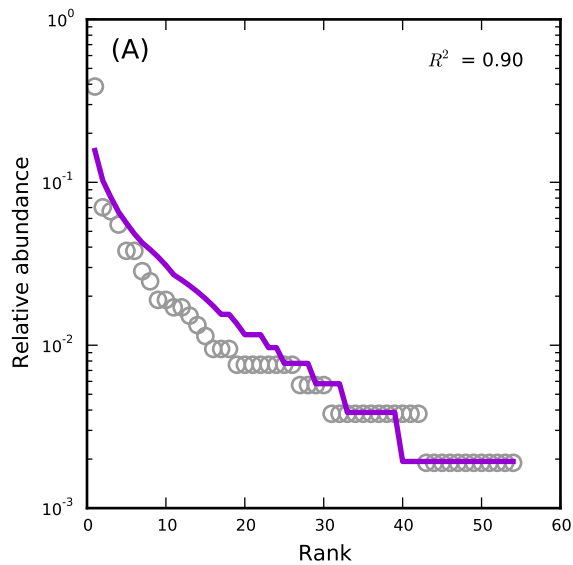
WesternGhats,BSP16



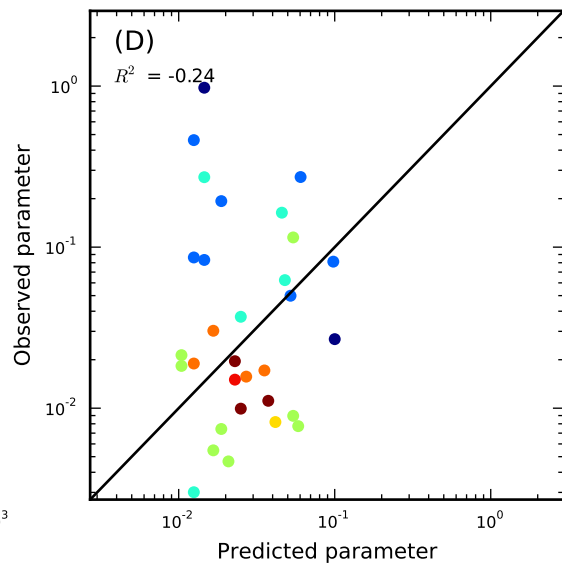
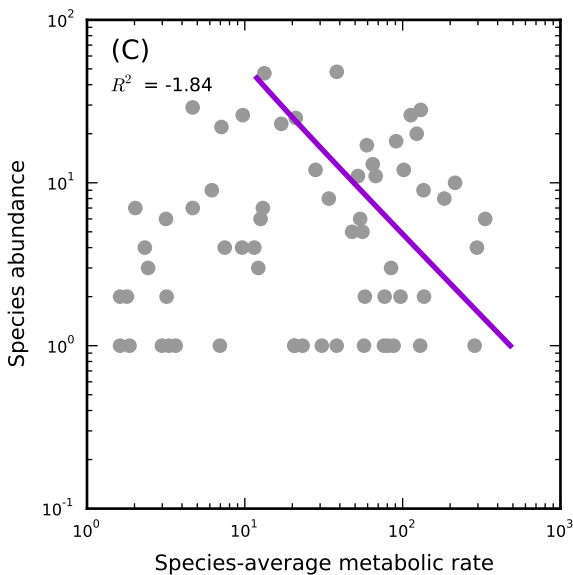
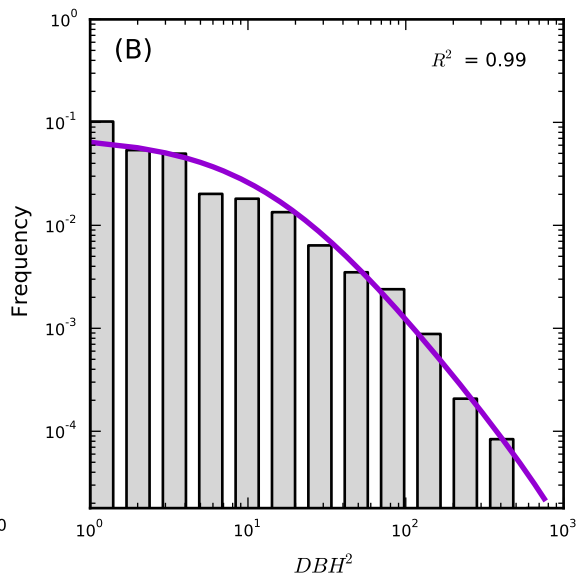
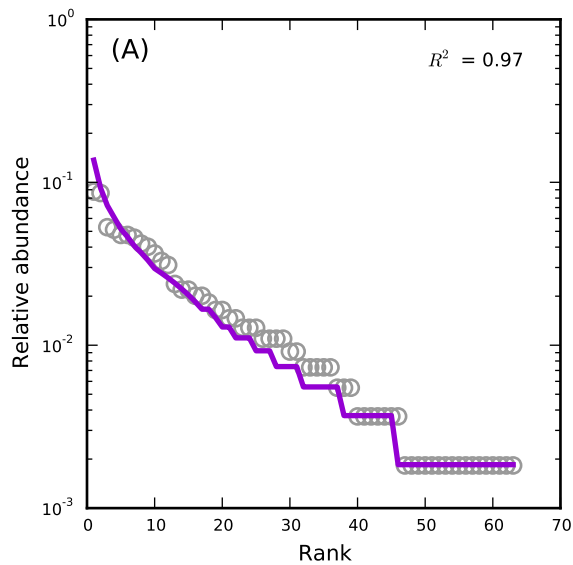
WesternGhats,BSP27



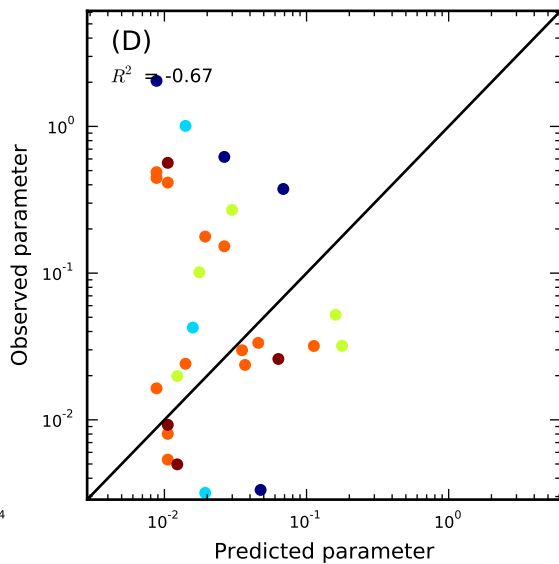
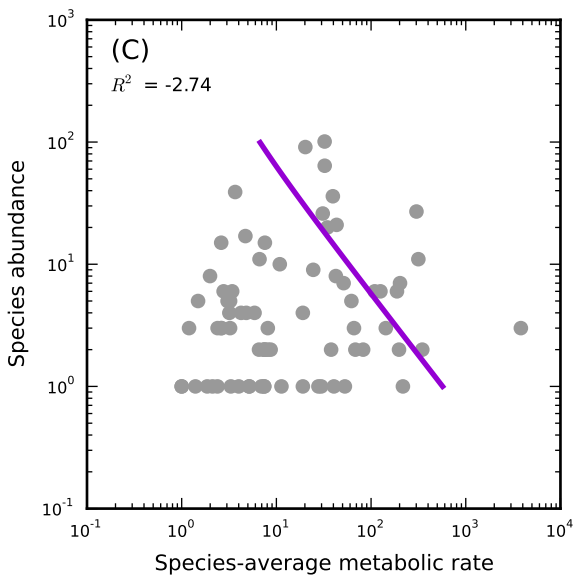
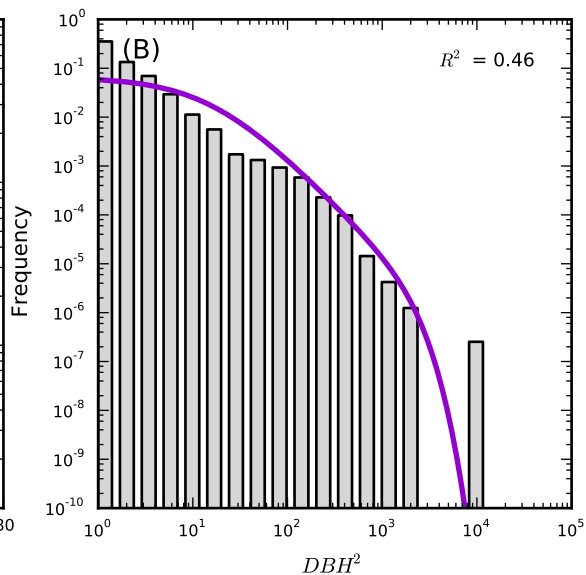
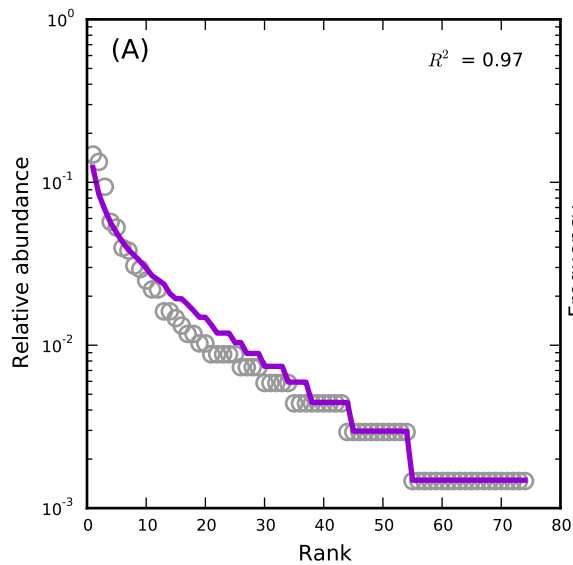
WesternGhats,BSP29



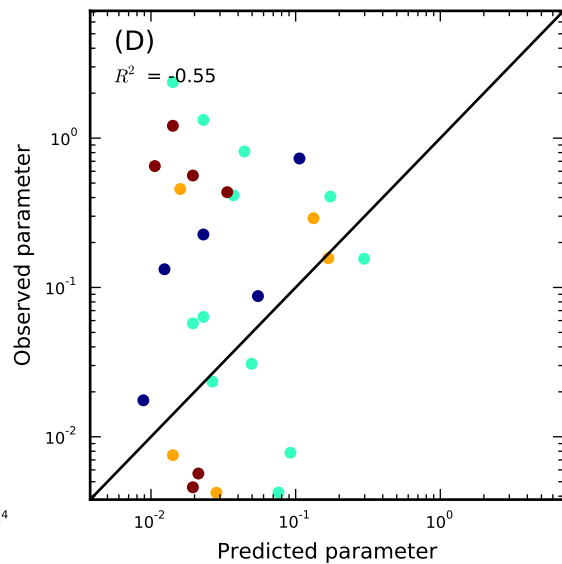
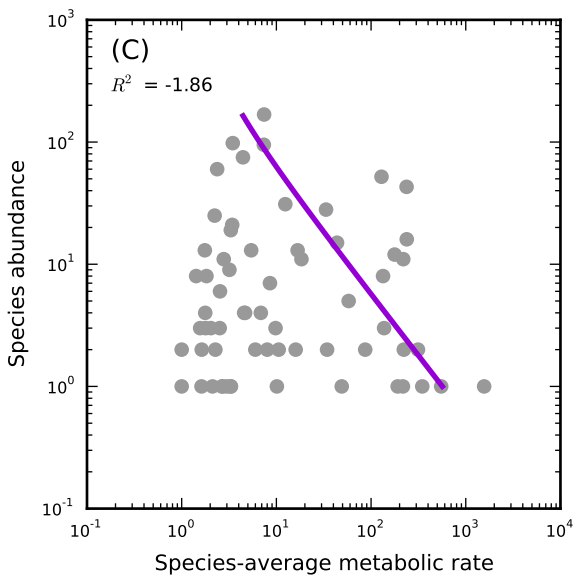
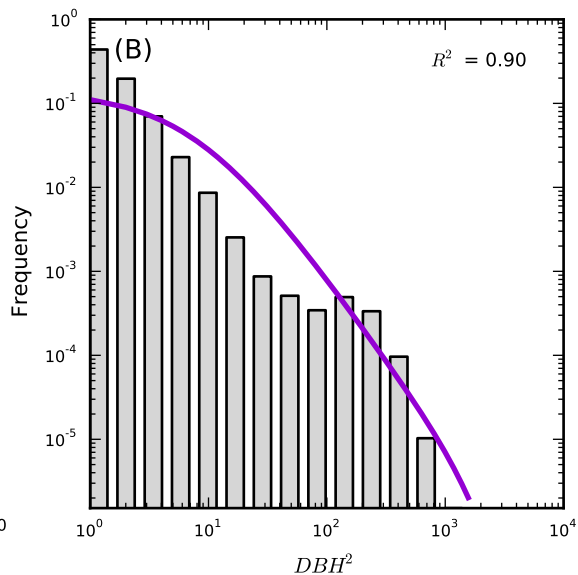
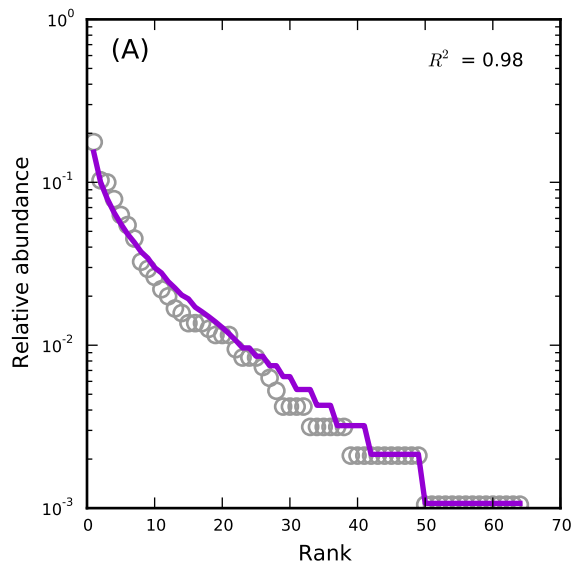
WesternGhats,BSP30



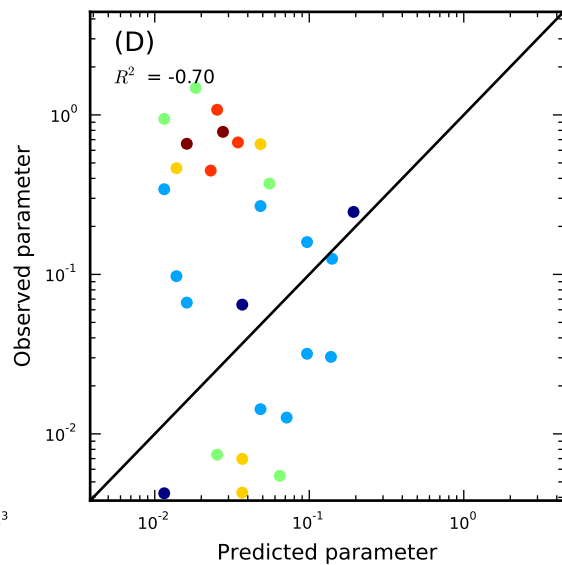
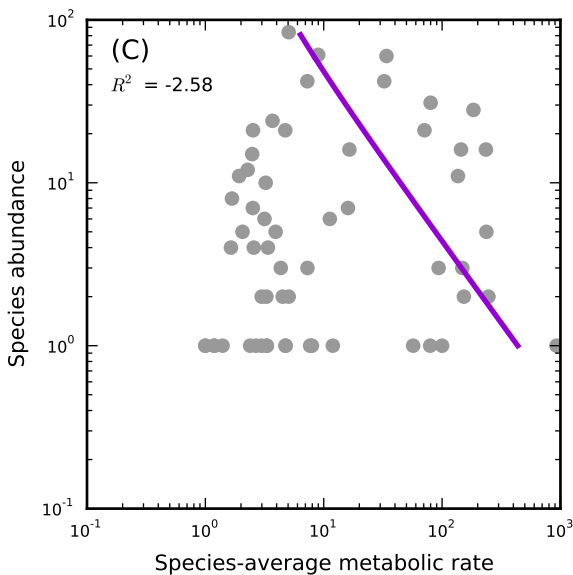
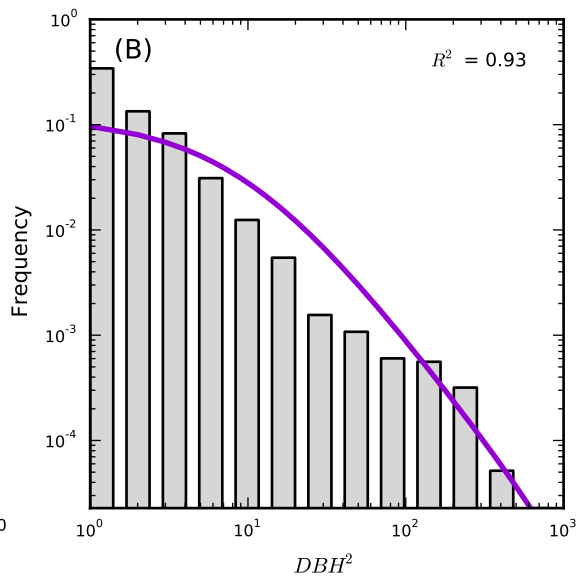
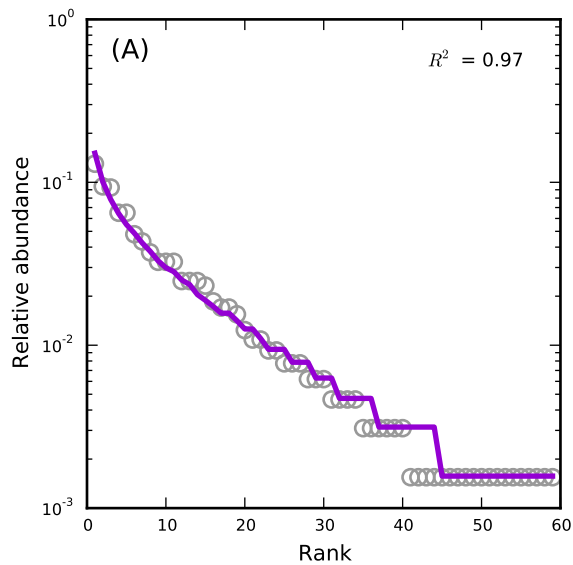
WesternGhats,BSP36



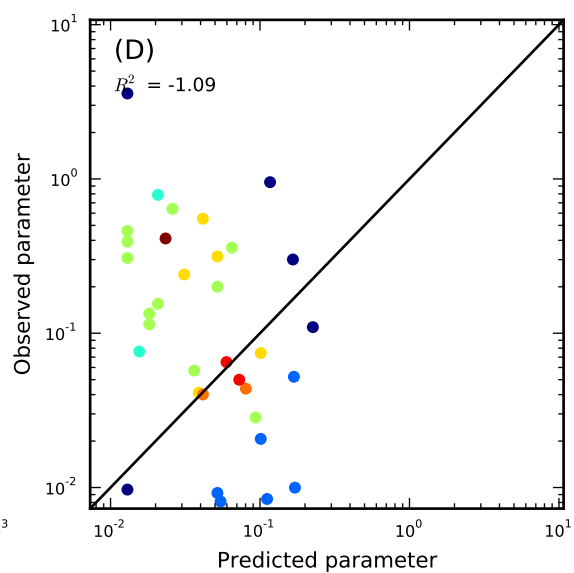
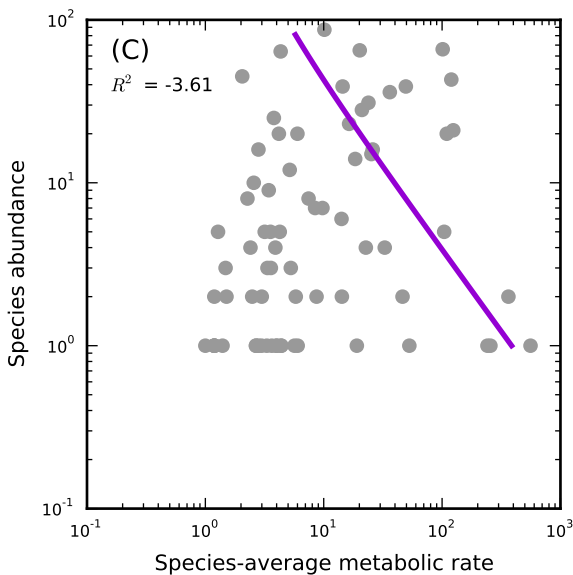
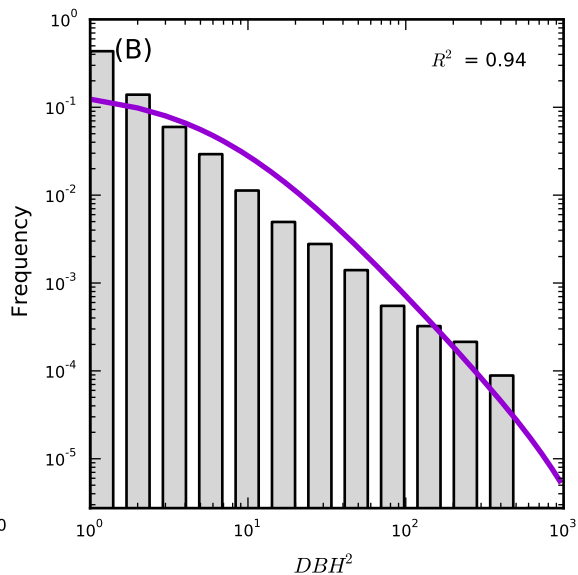
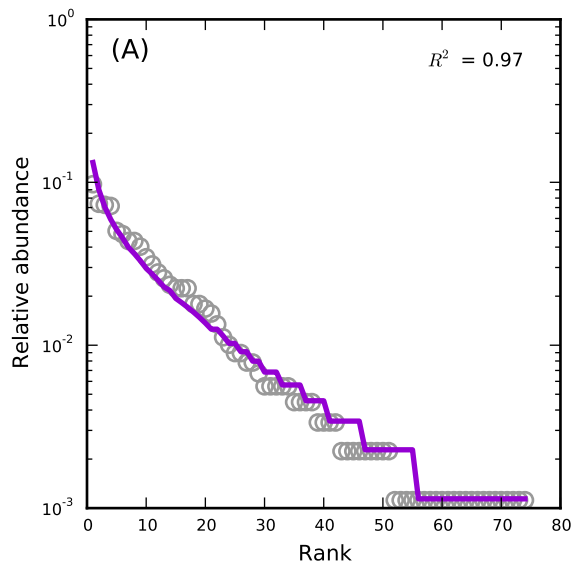
WesternGhats,BSP37



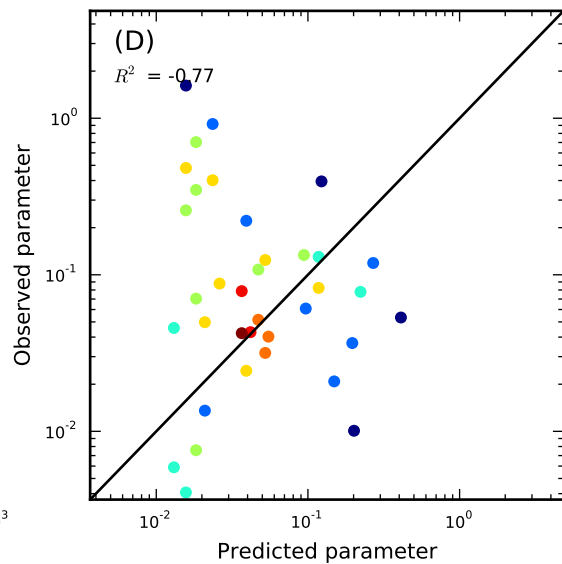
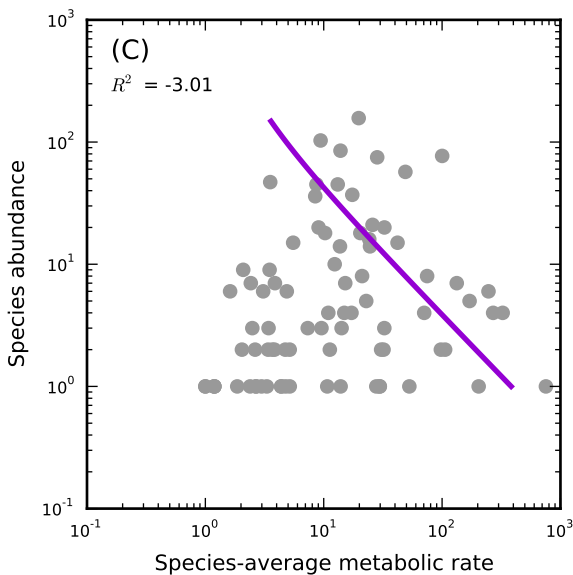
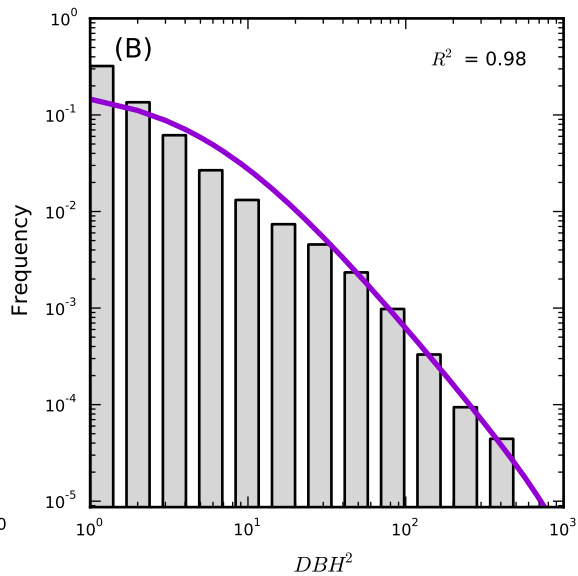
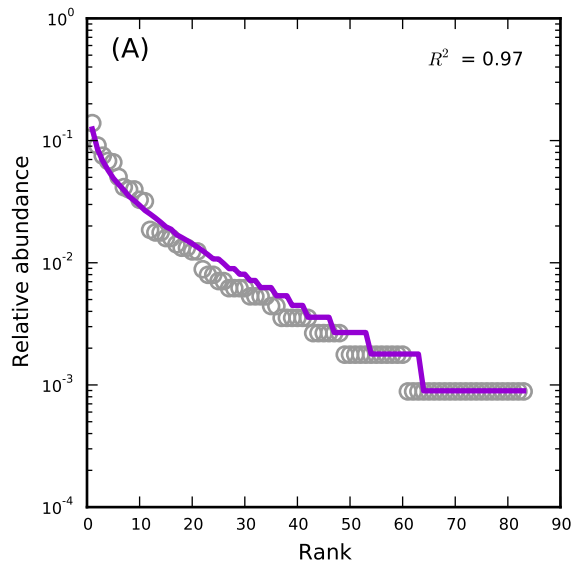
WesternGhats,BSP42



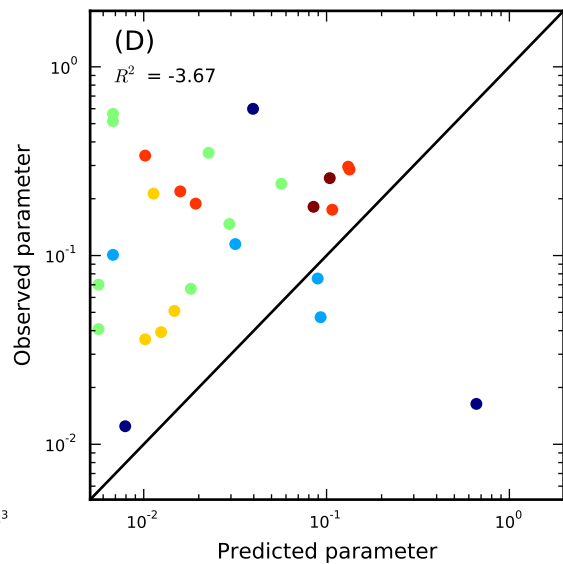
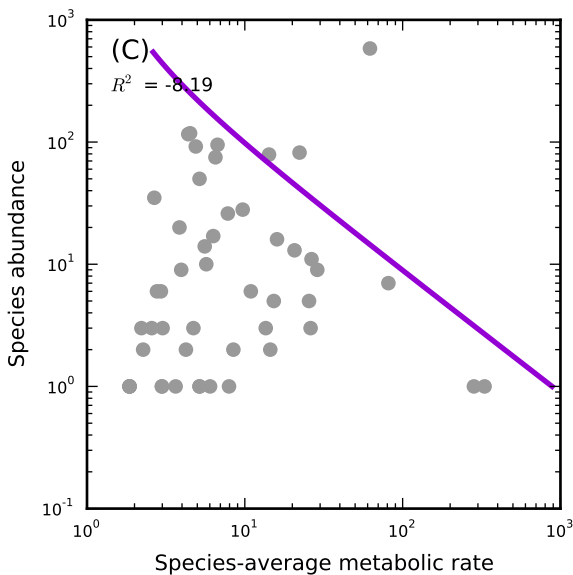
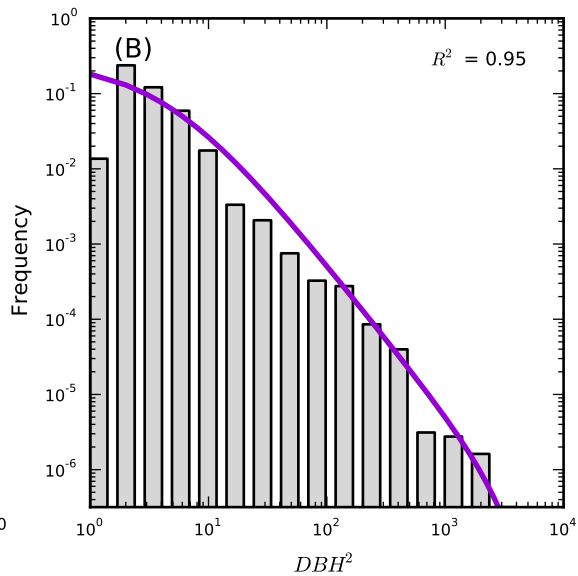
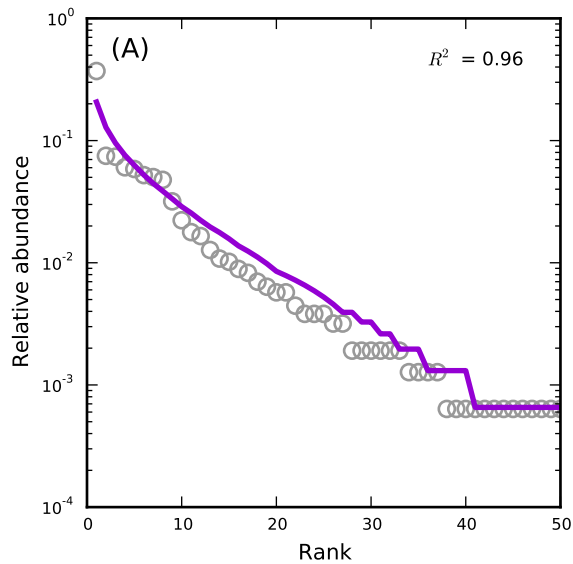
WesternGhats,BSP5



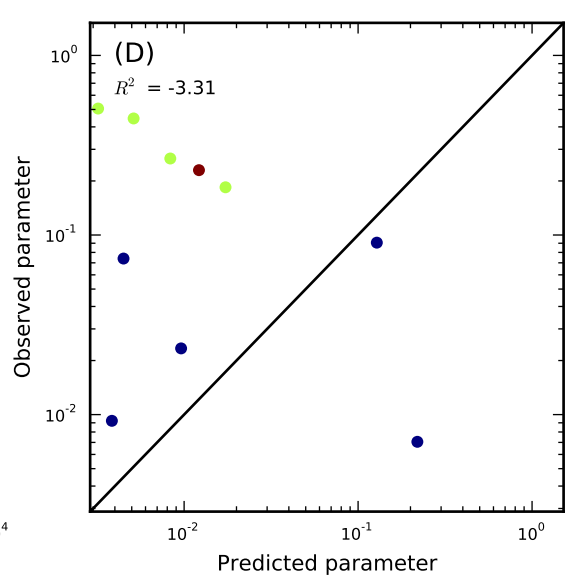
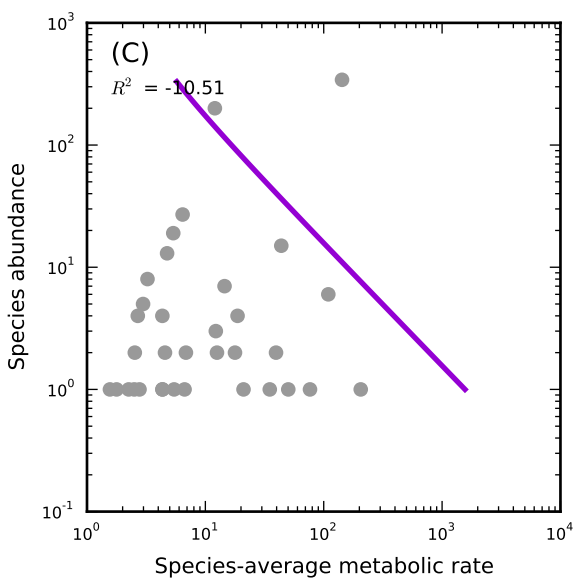
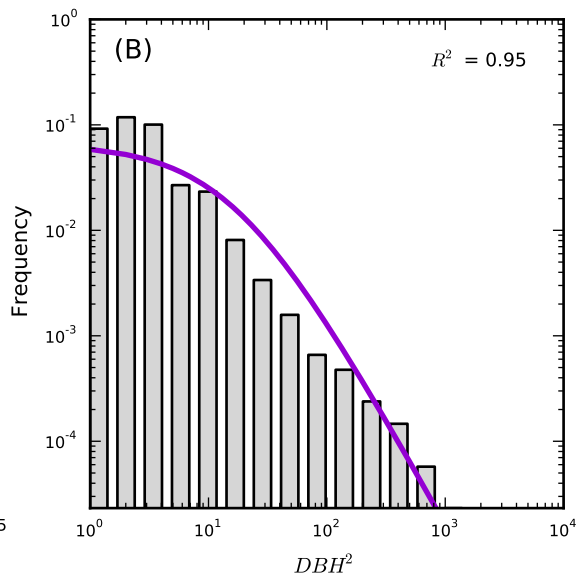
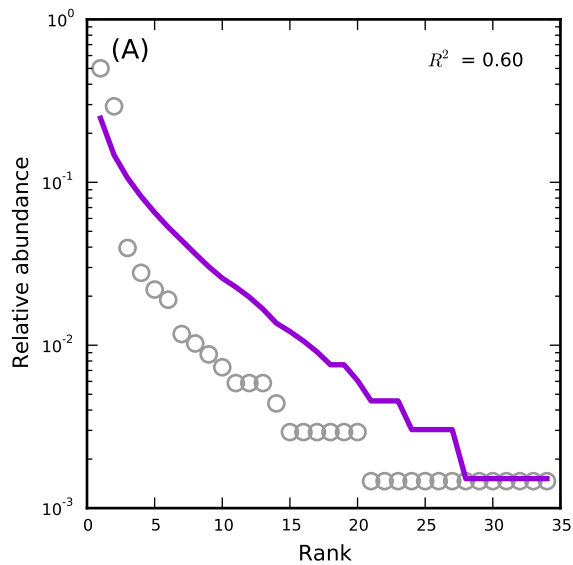
WesternGhats,BSP6



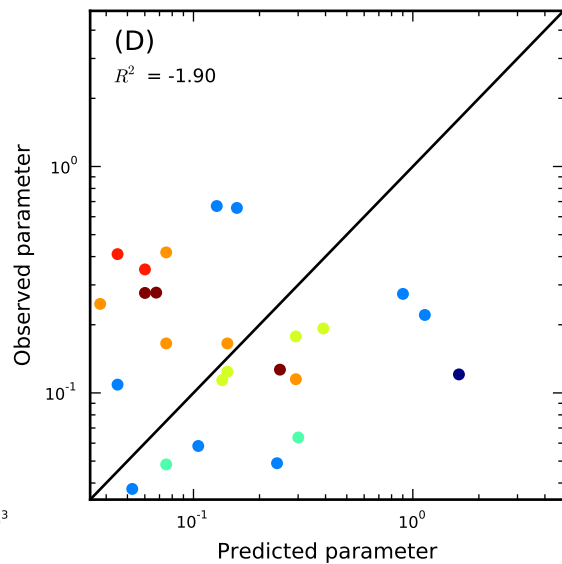
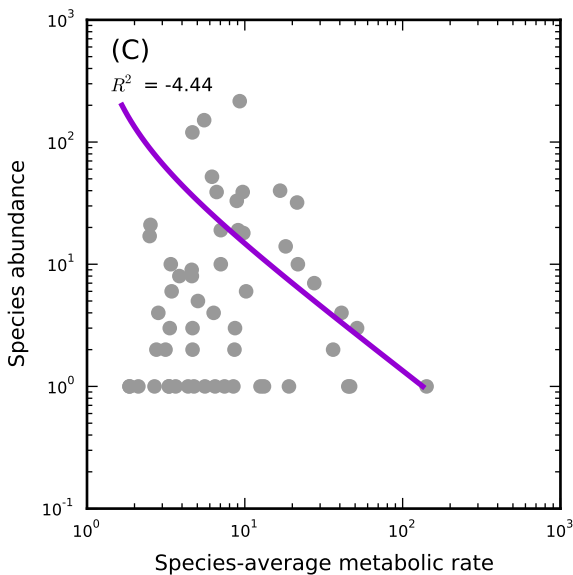
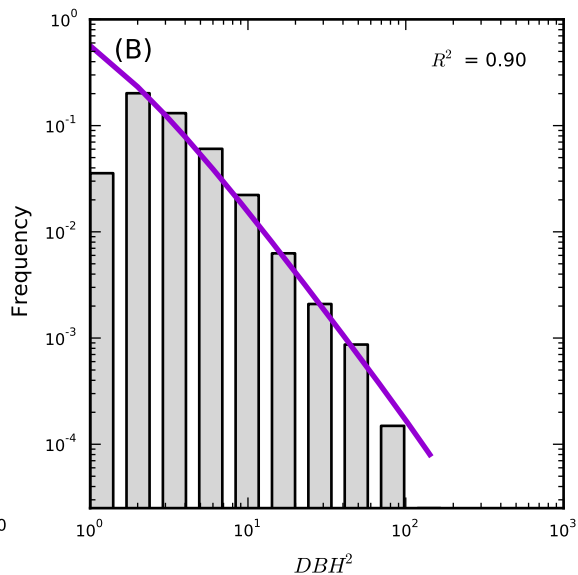
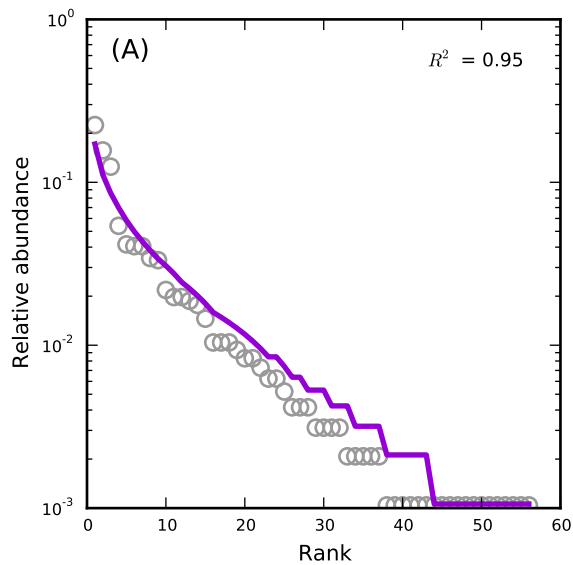
WesternGhats,BSP65



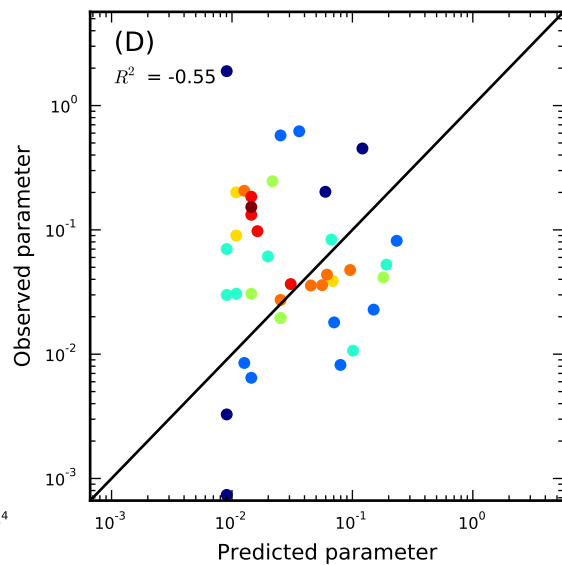
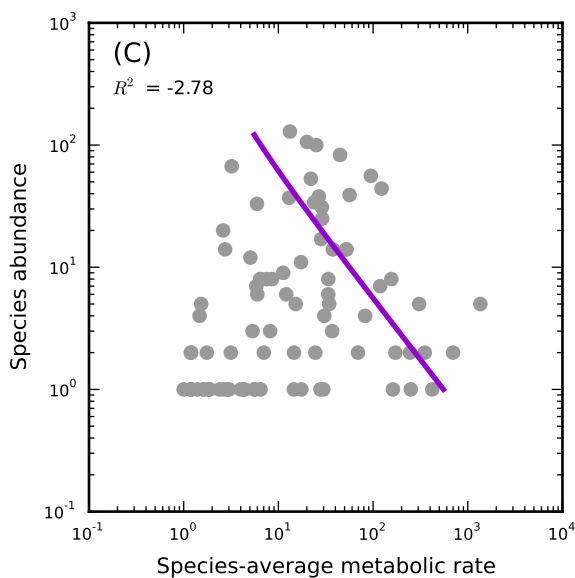
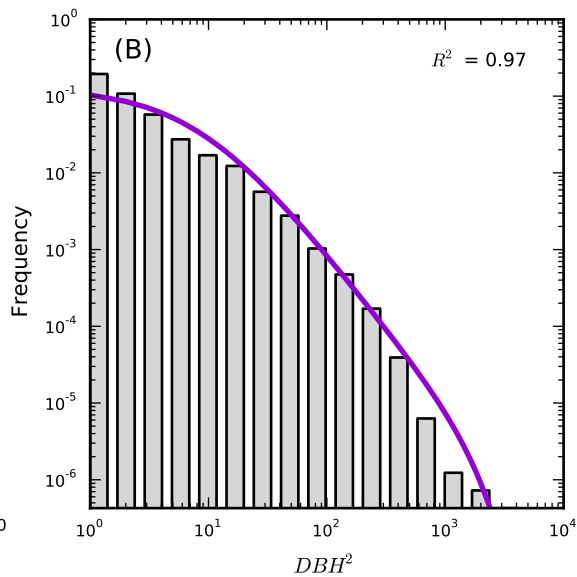
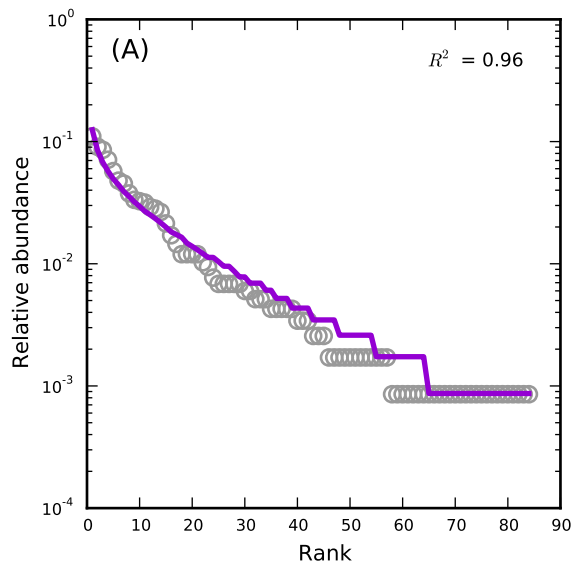
WesternGhats,BSP66



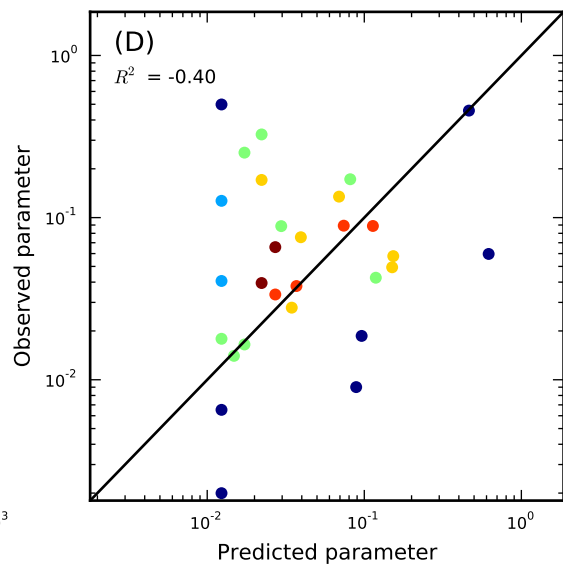
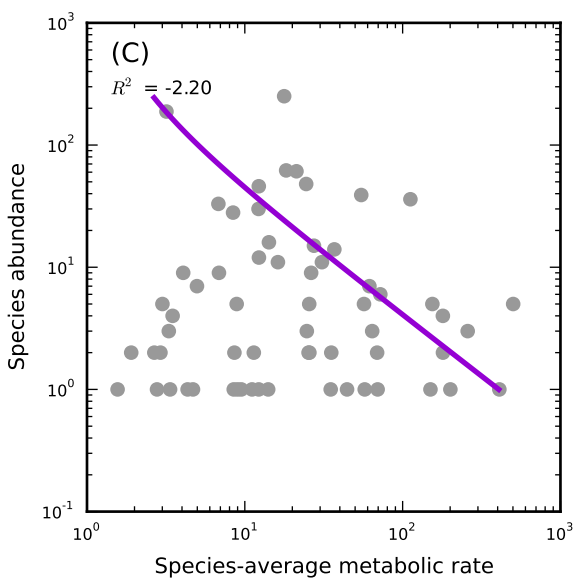
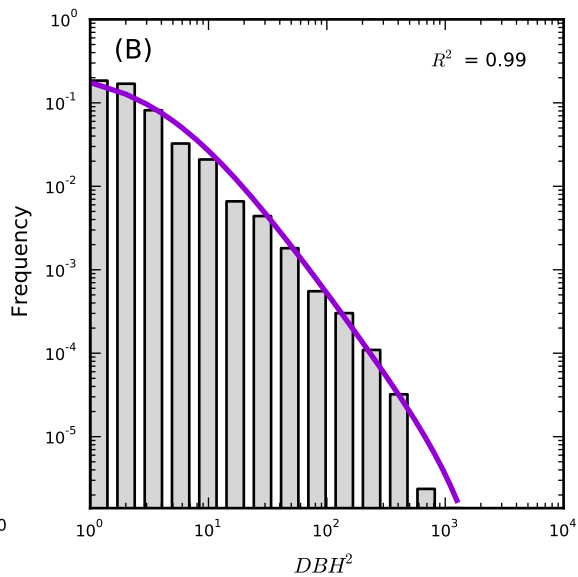
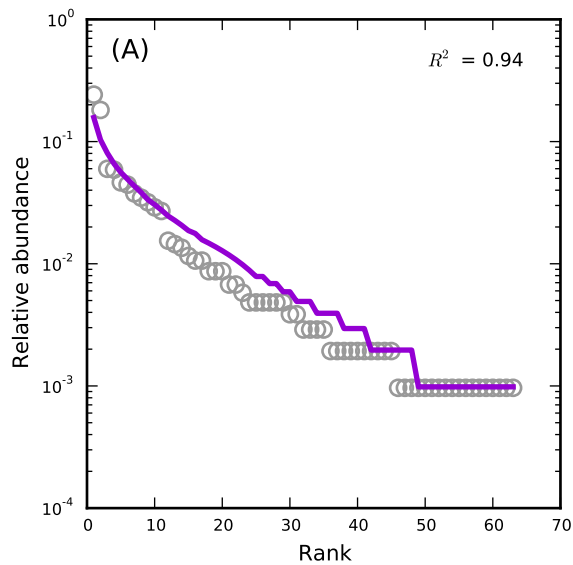
WesternGhats,BSP67



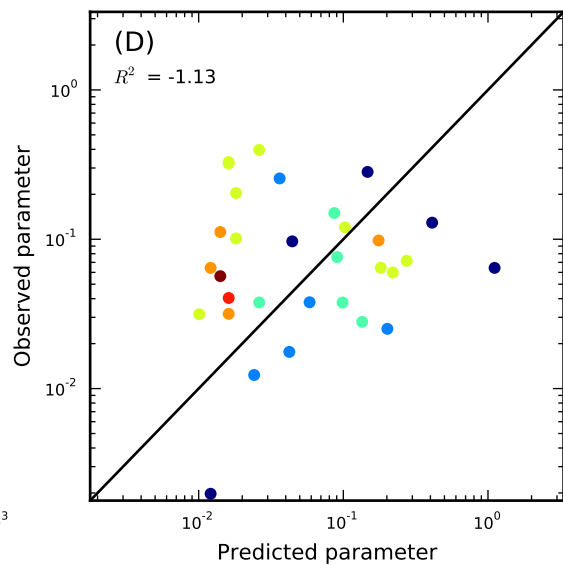
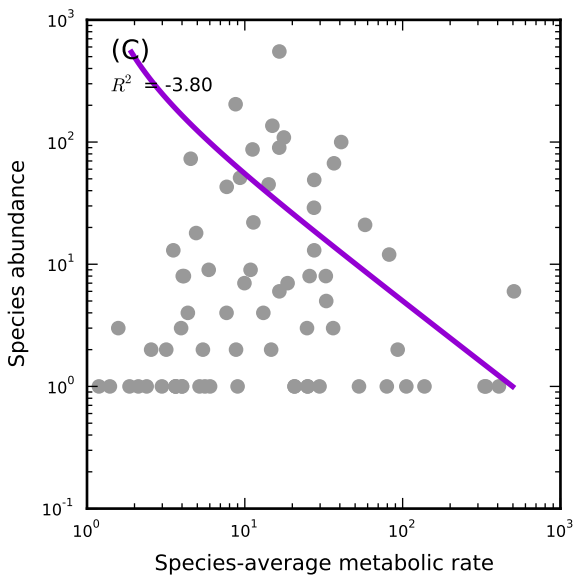
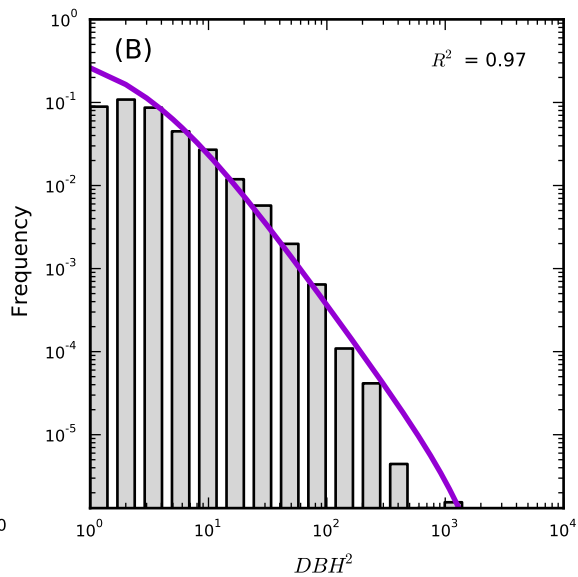
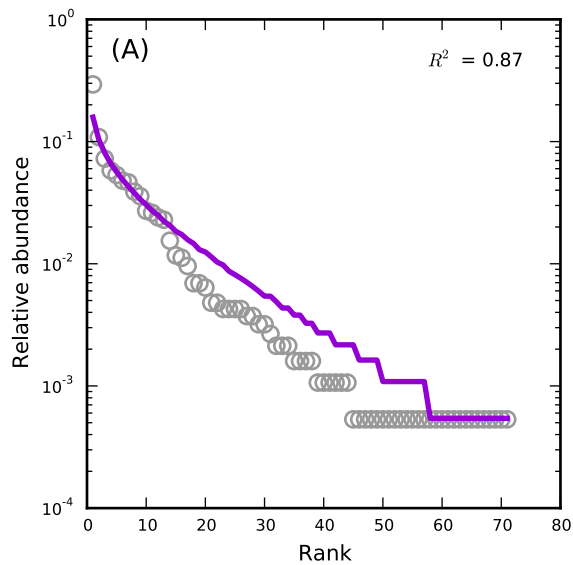
WesternGhats,BSP69



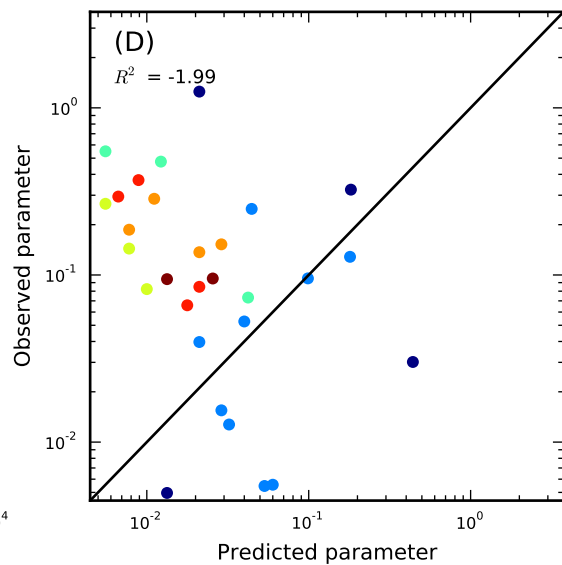
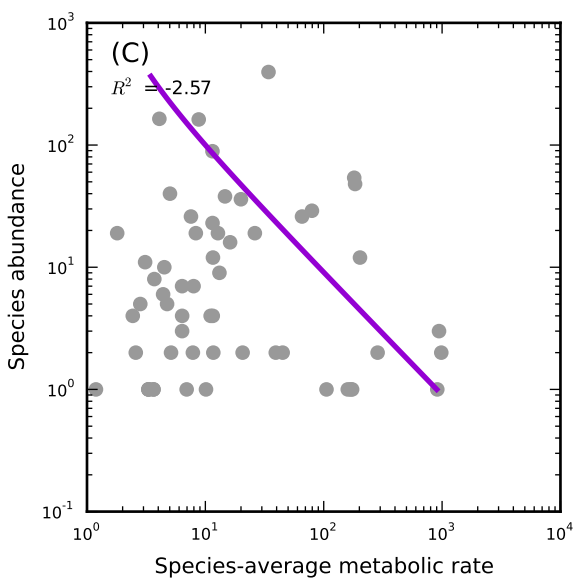
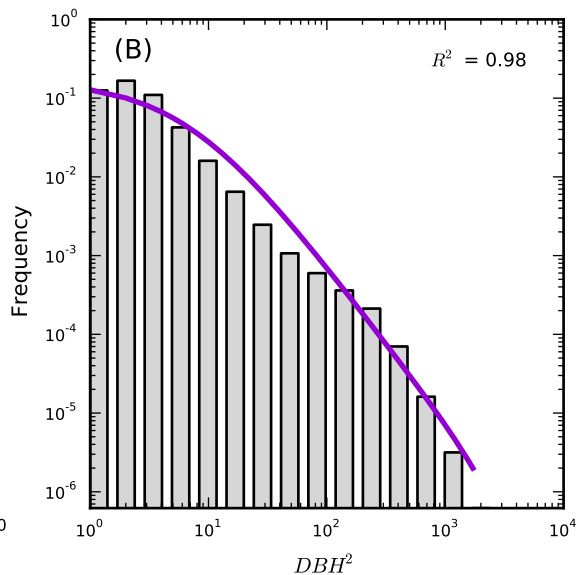
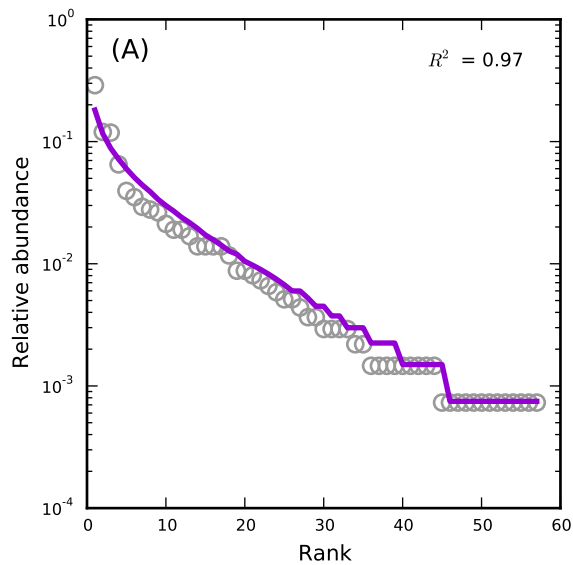
WesternGhats,BSP70



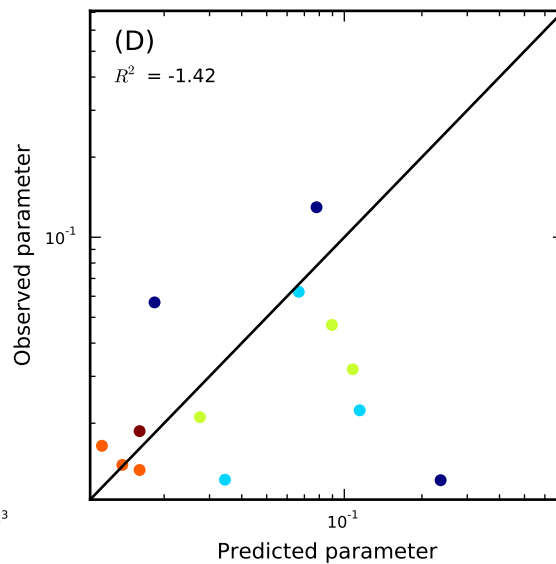
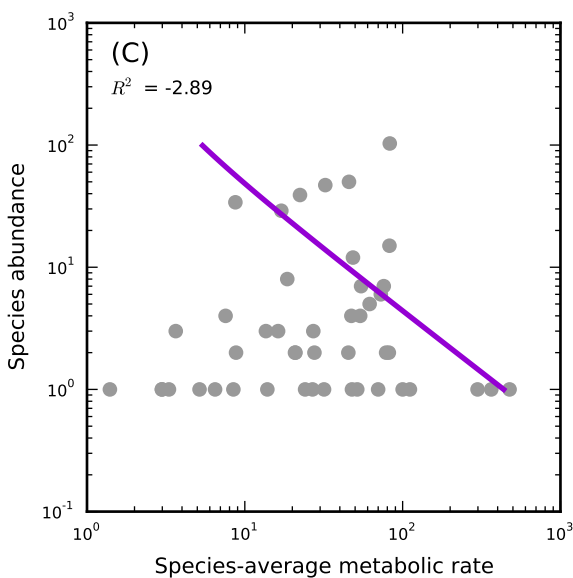
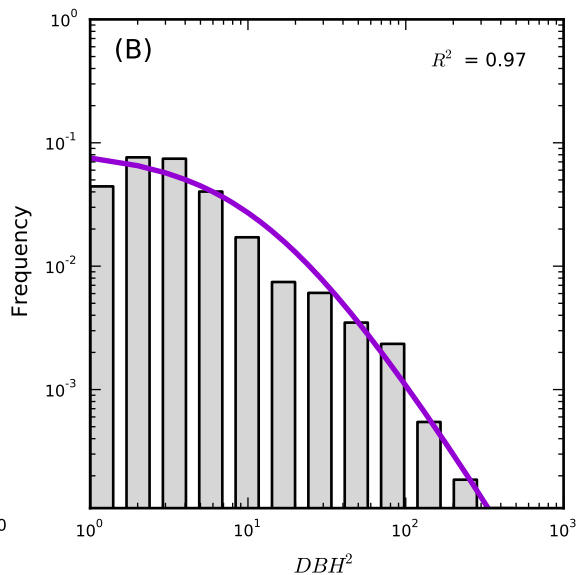
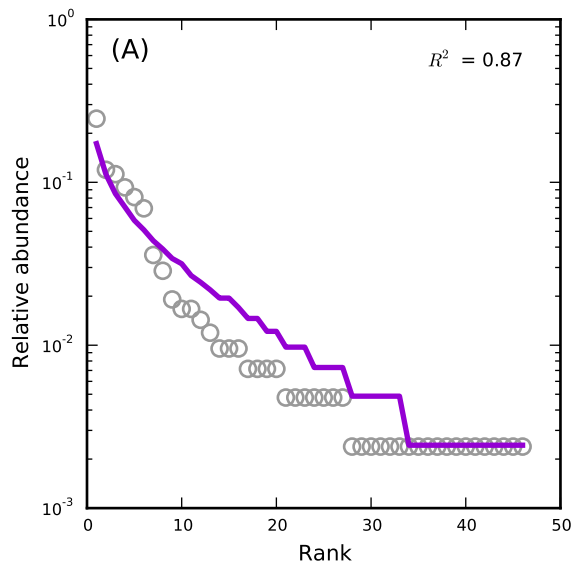
WesternGhats,BSP73



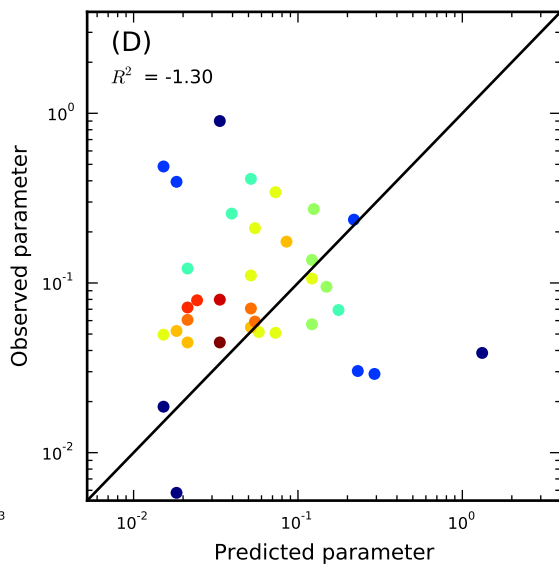
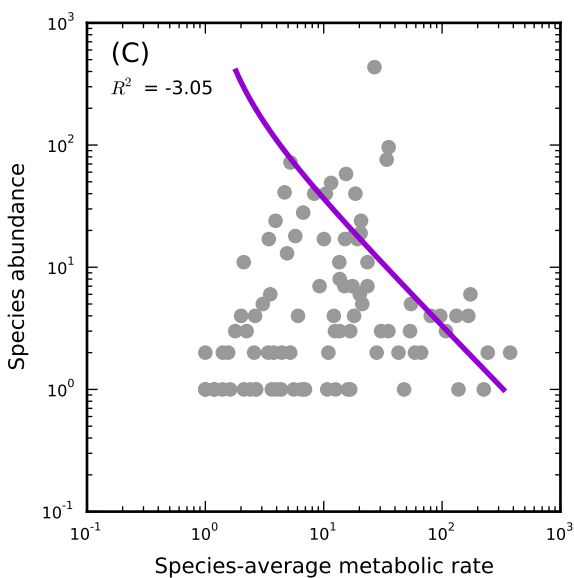
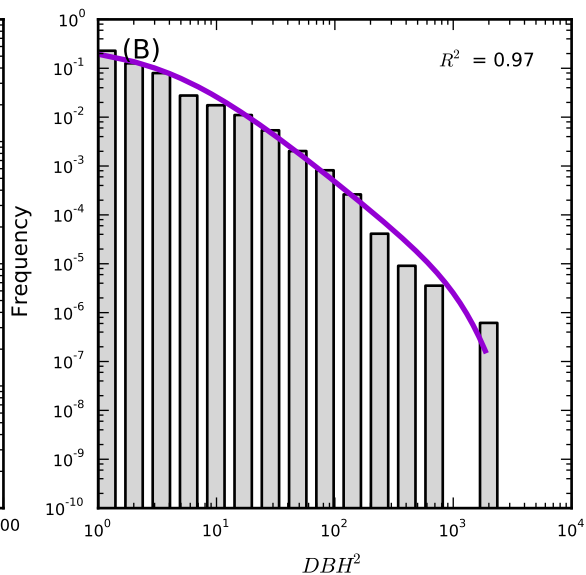
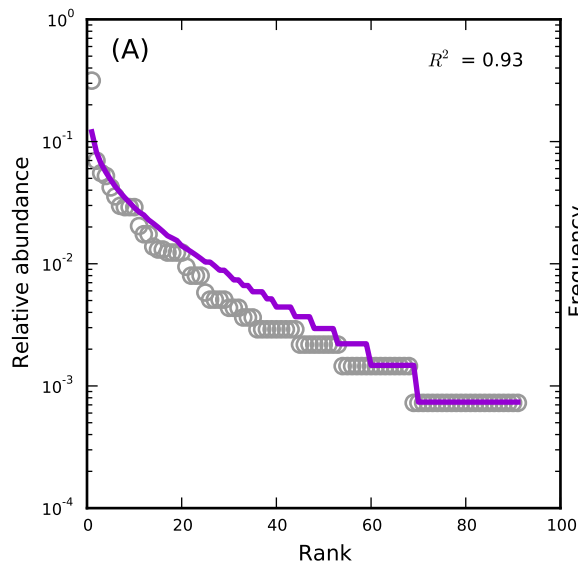
WesternGhats,BSP74



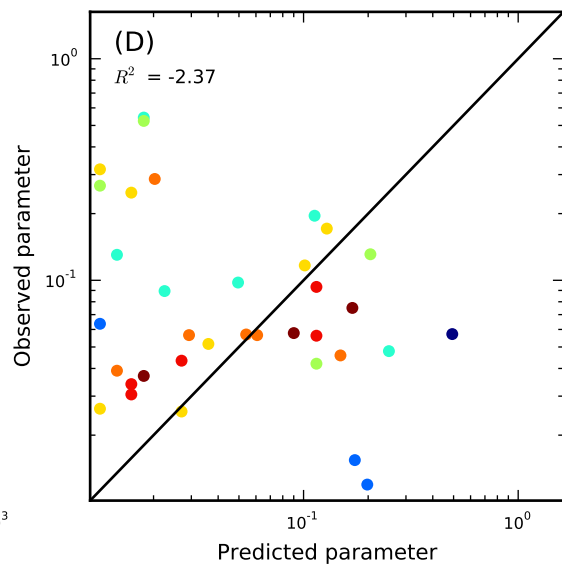
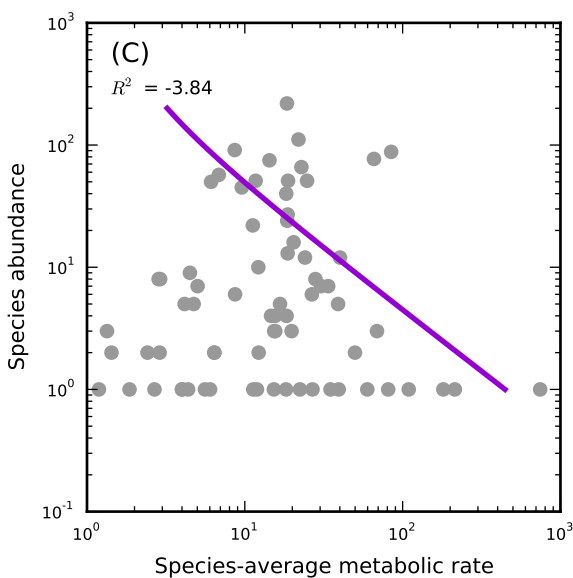
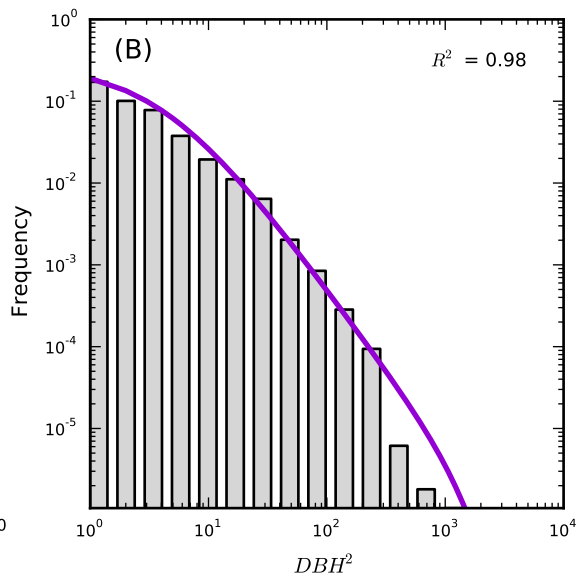
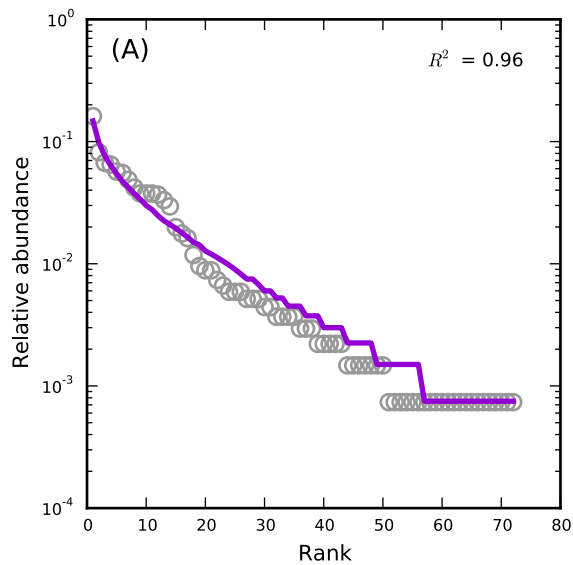
WesternGhats,BSP75



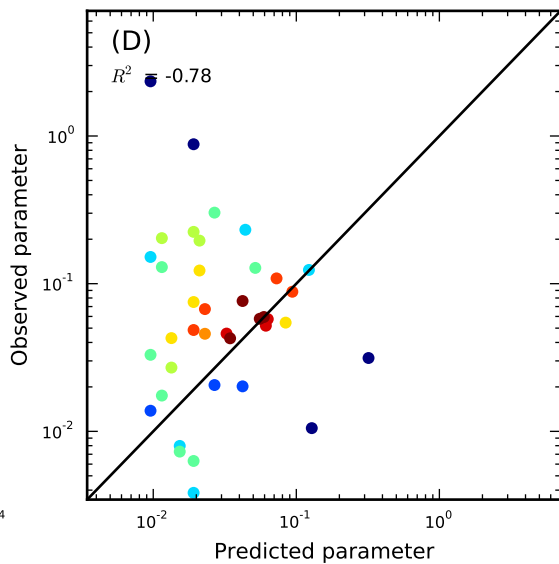
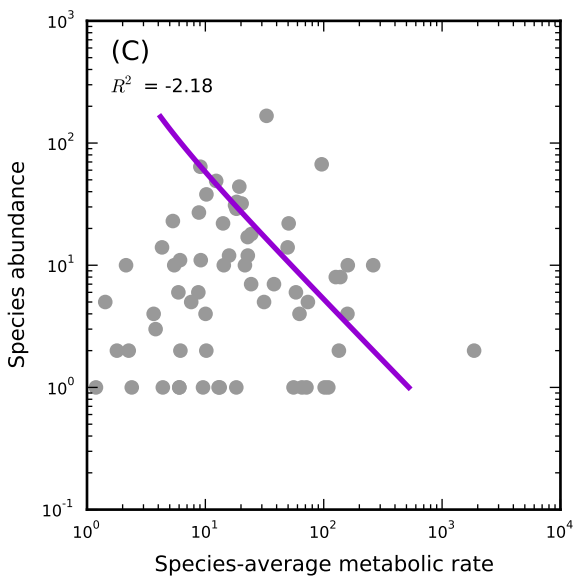
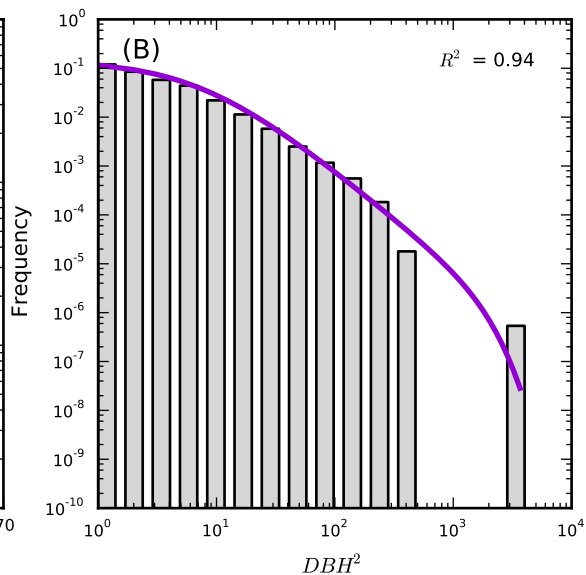
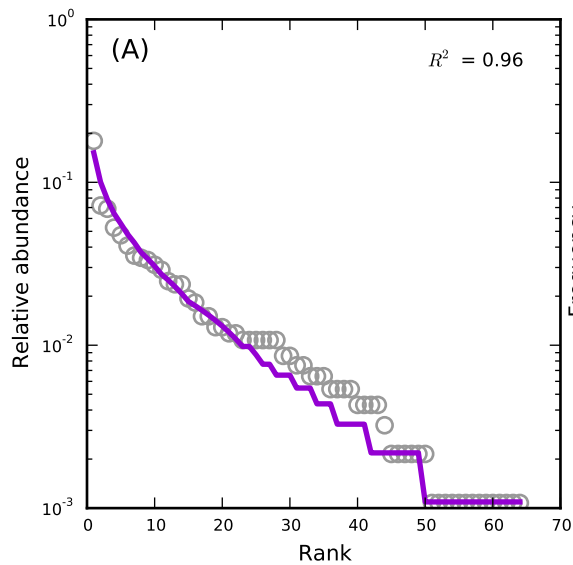
WesternGhats,BSP79



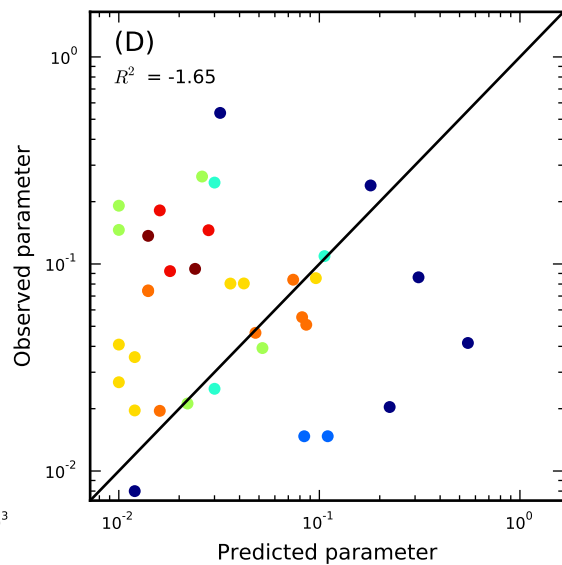
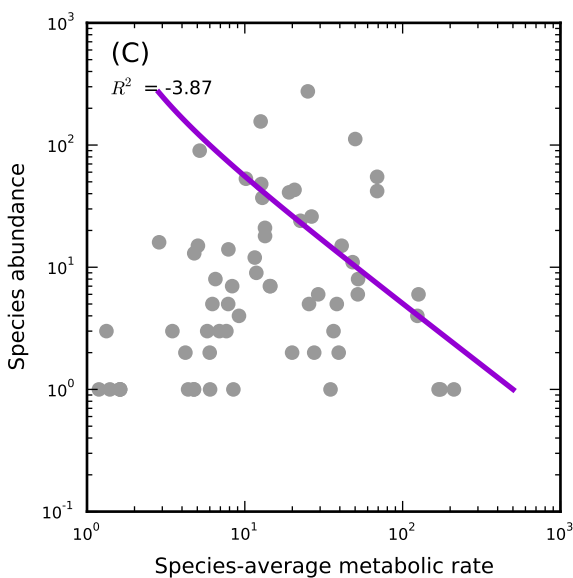
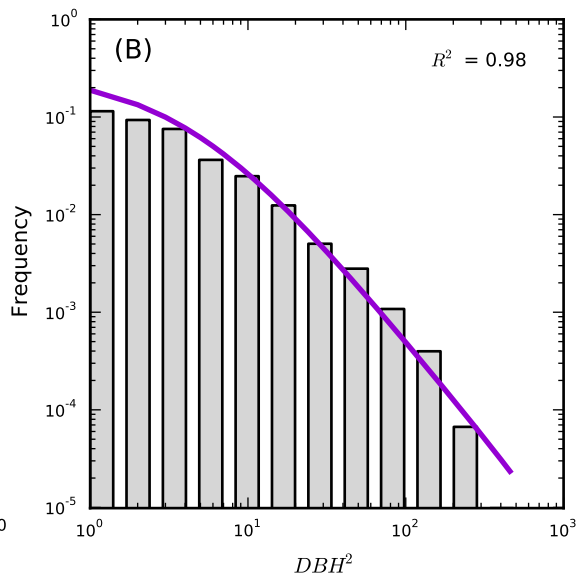
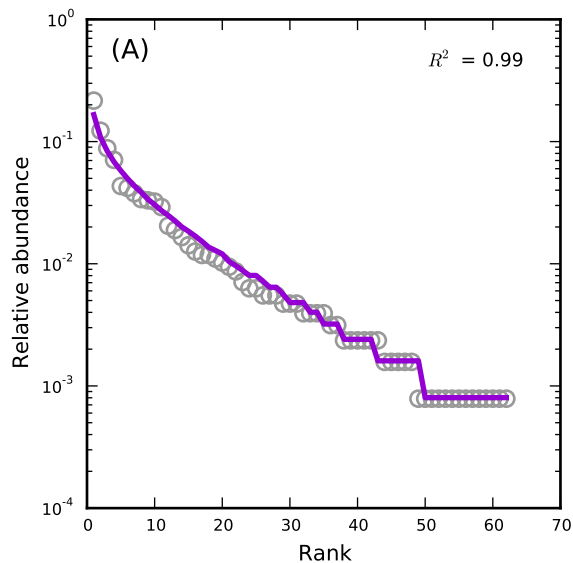
WesternGhats,BSP80



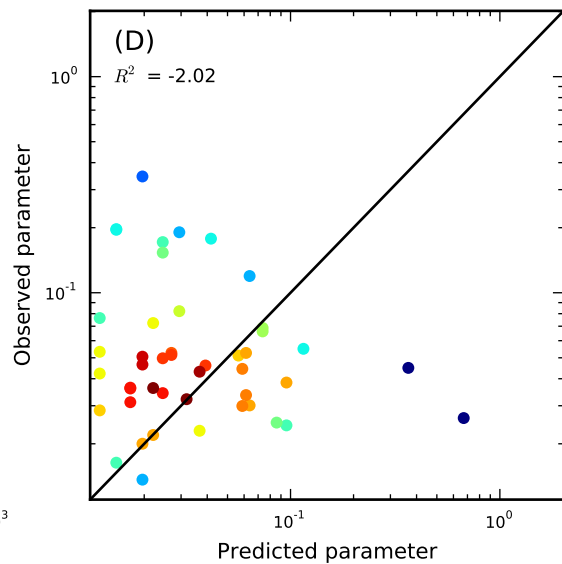
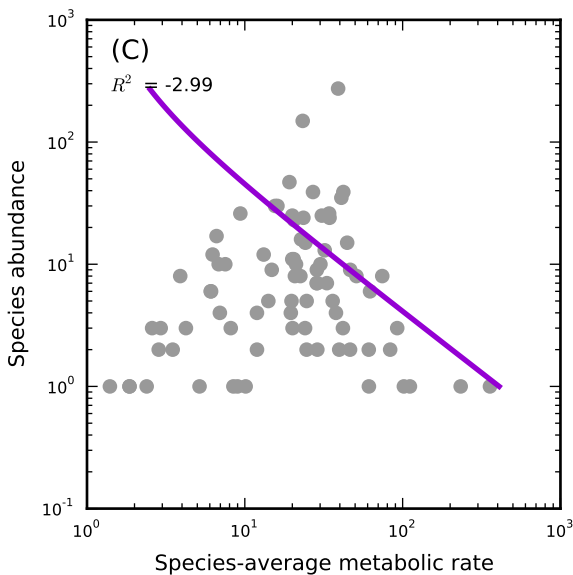
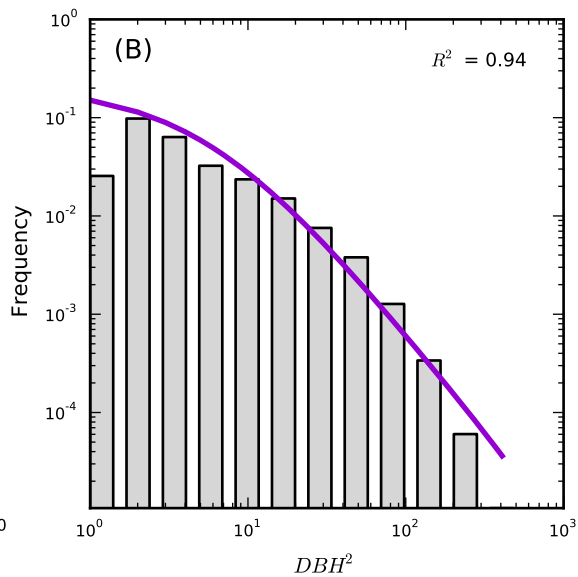
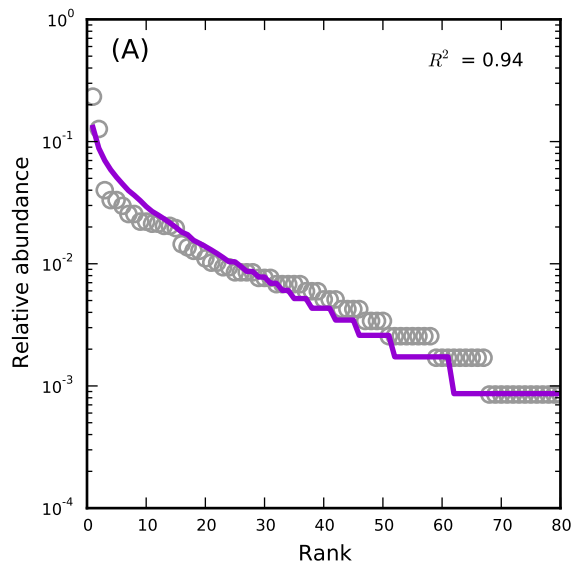
WesternGhats,BSP82



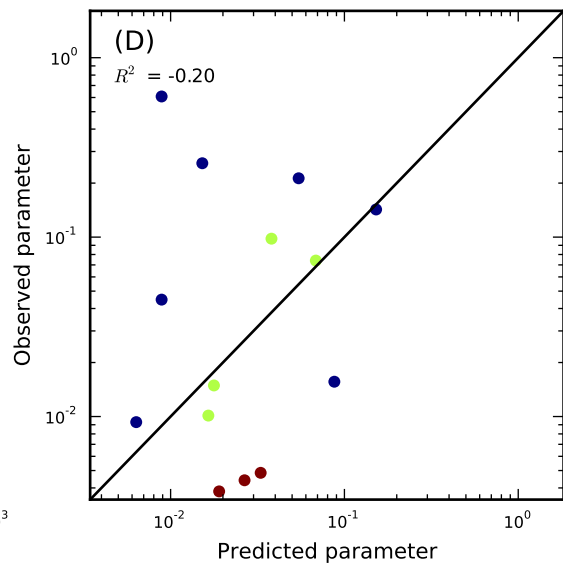
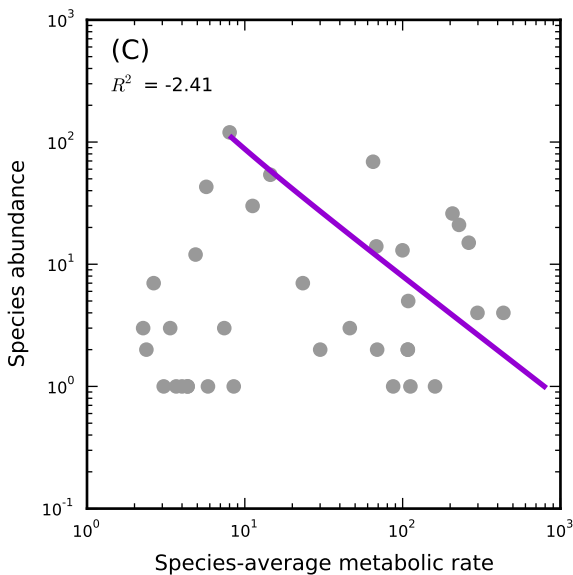
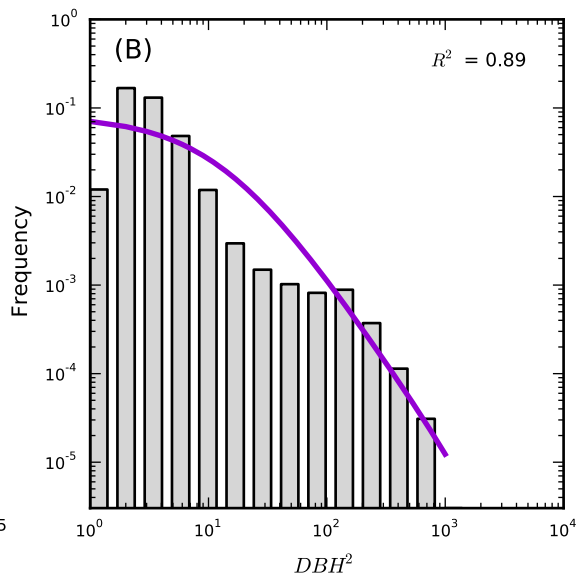
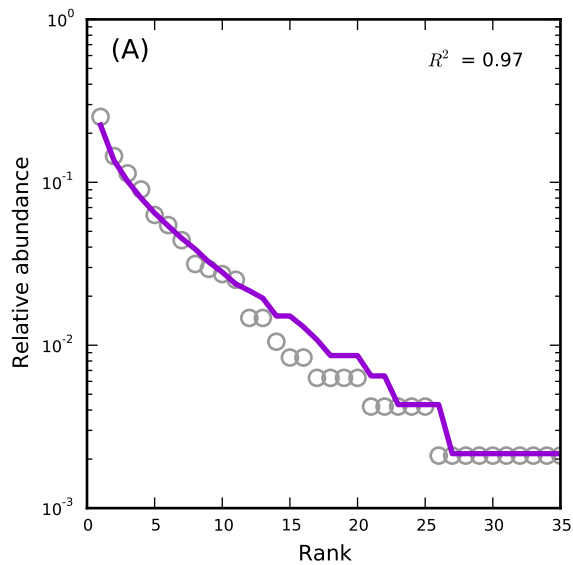
WesternGhats,BSP83



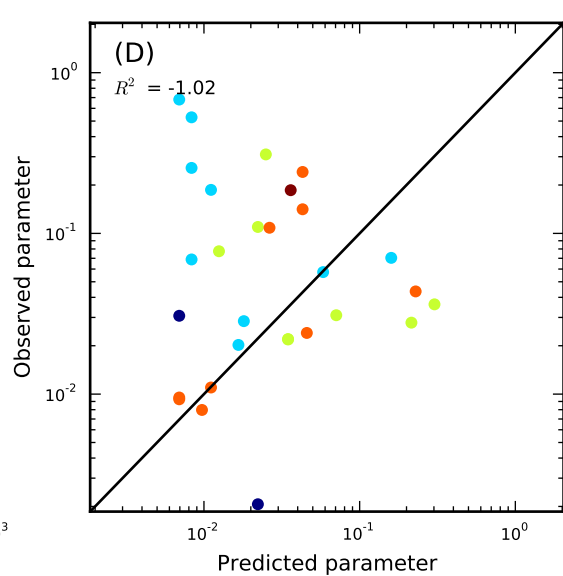
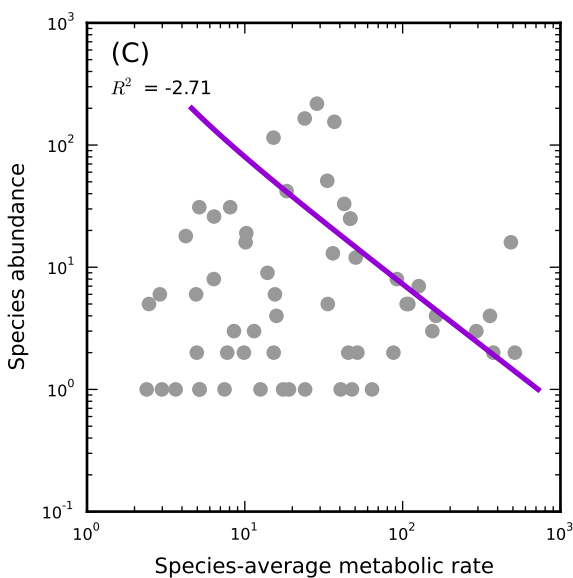
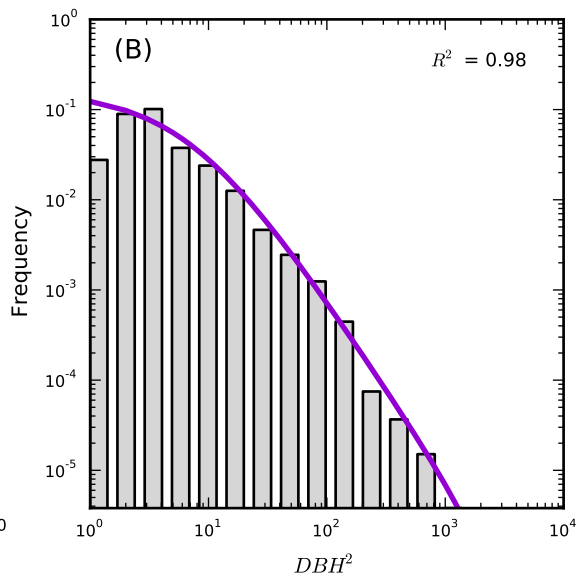
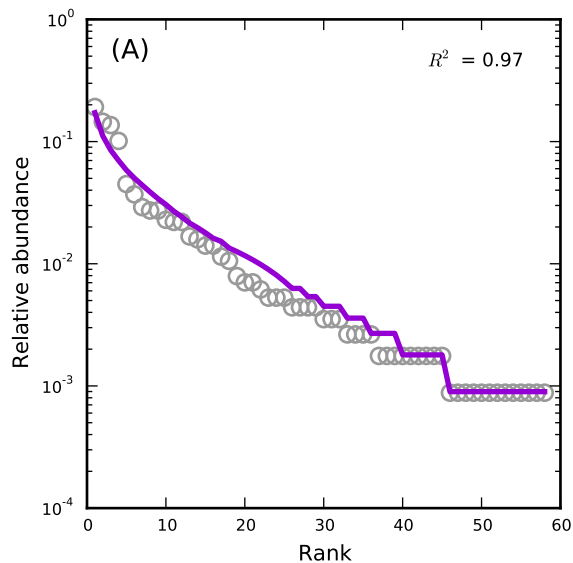
WesternGhats,BSP84



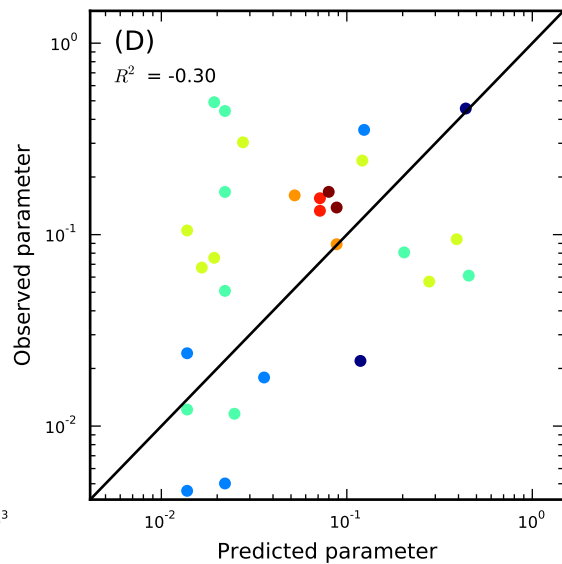
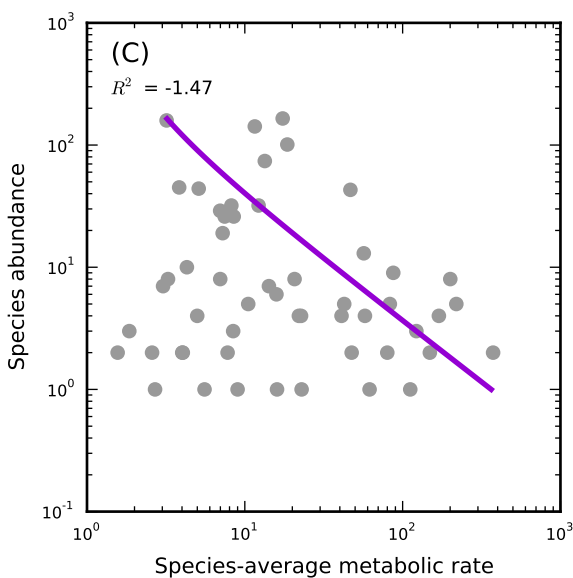
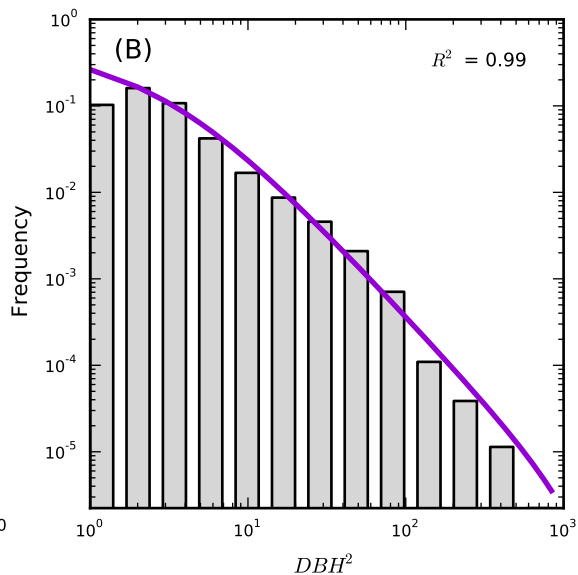
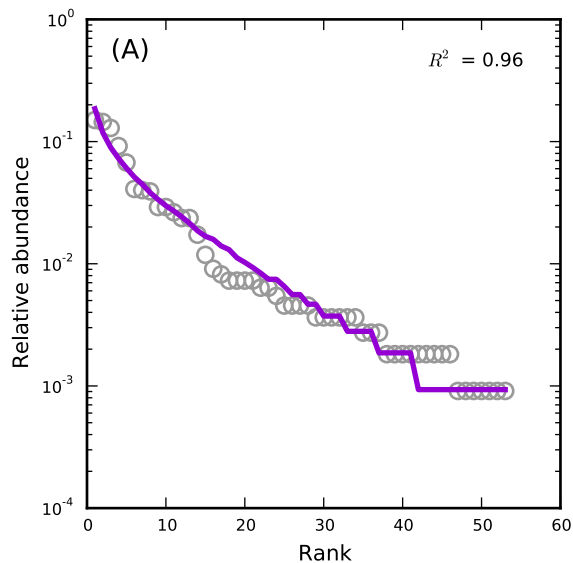
WesternGhats,BSP85



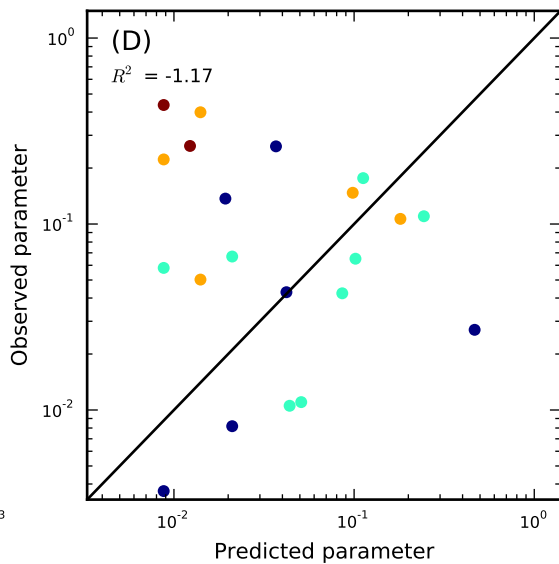
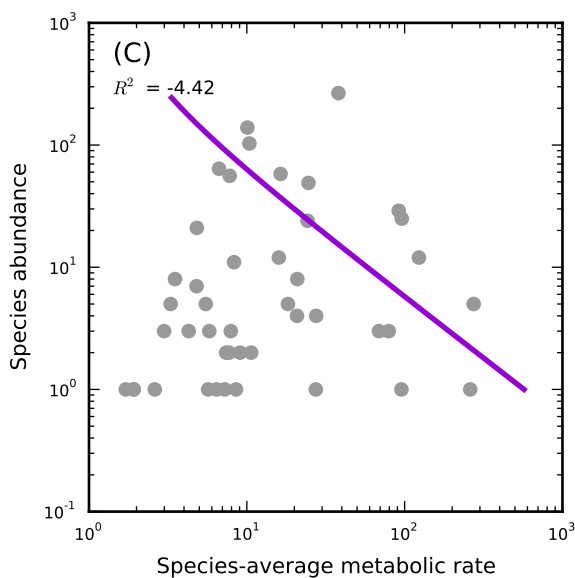
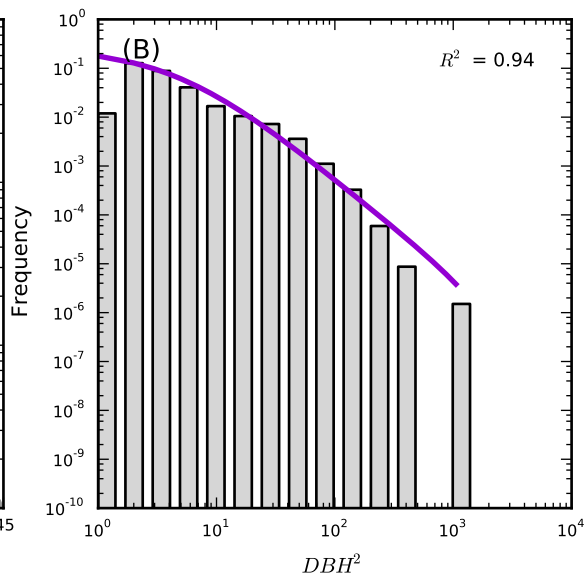
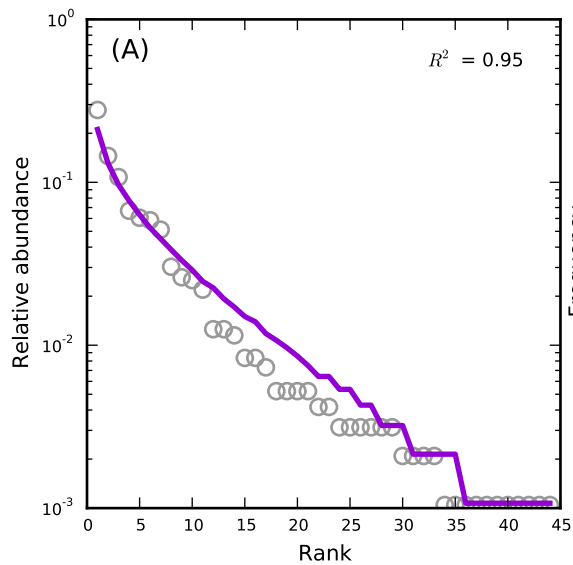
WesternGhats,BSP88



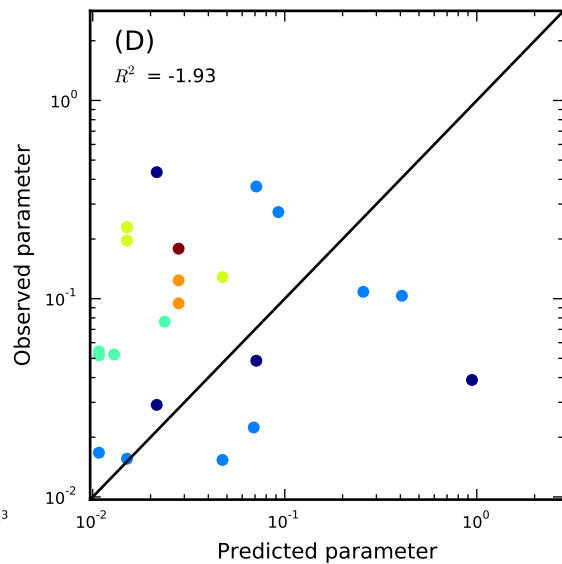
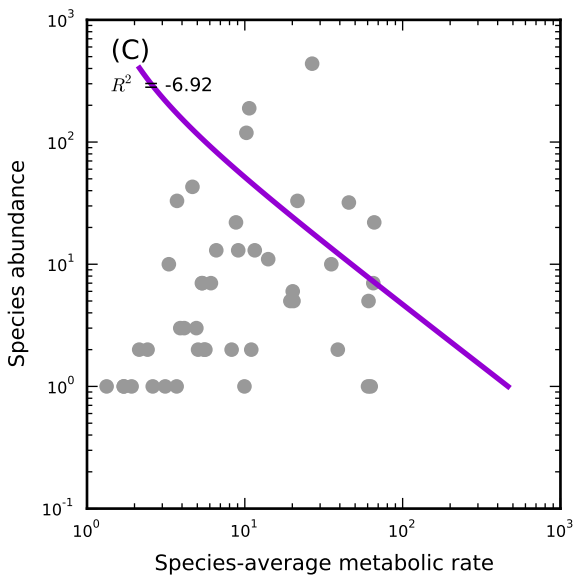
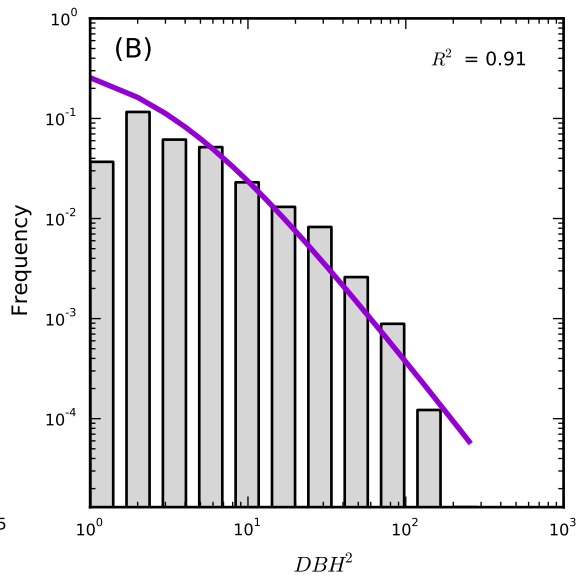
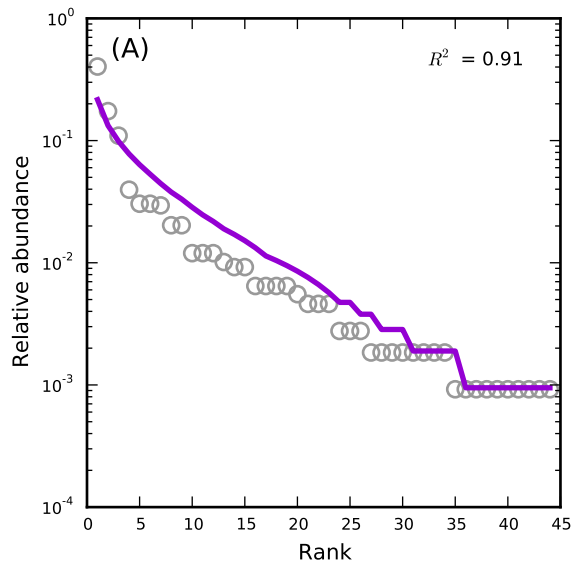
WesternGhats,BSP89



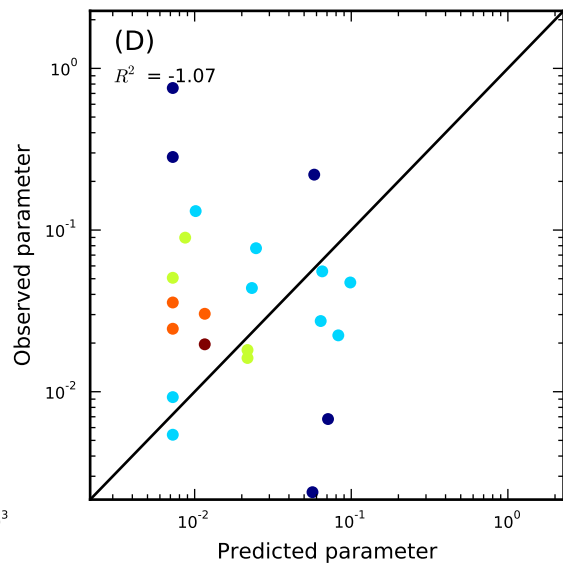
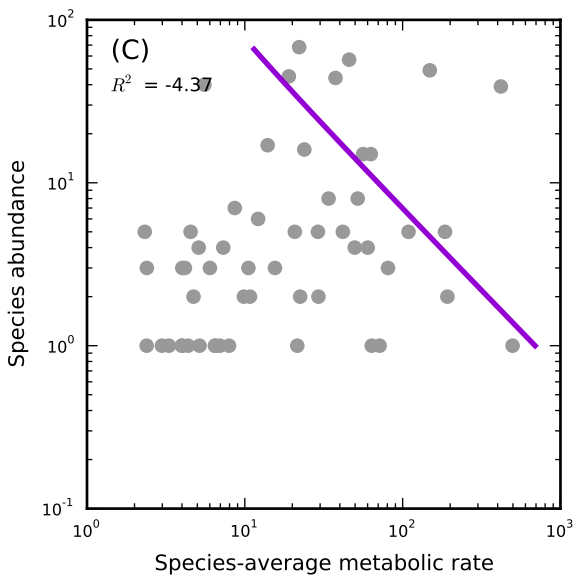
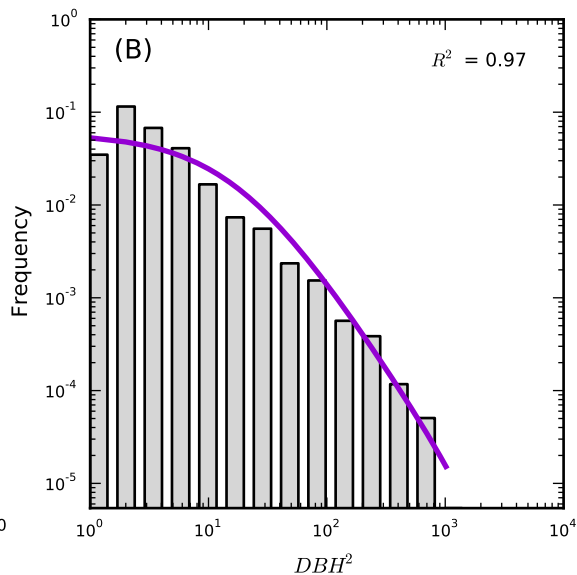
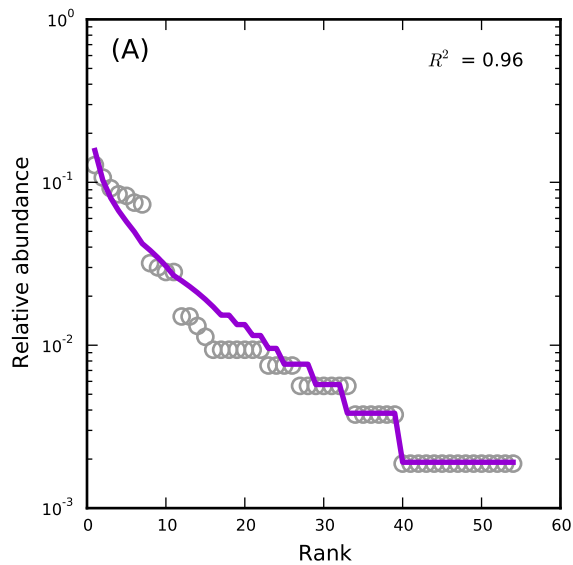
WesternGhats,BSP90



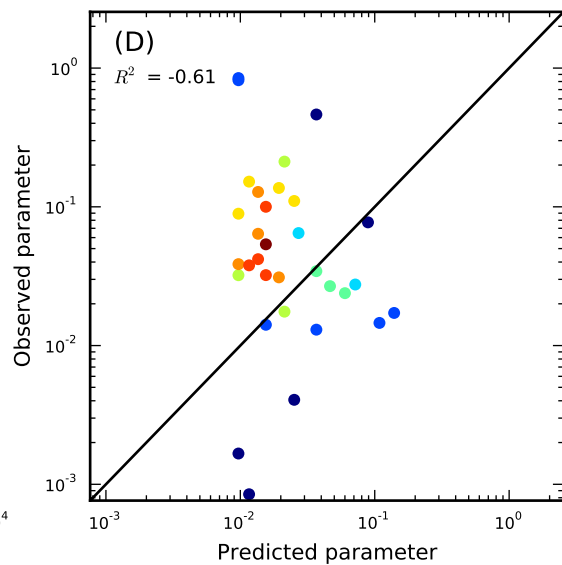
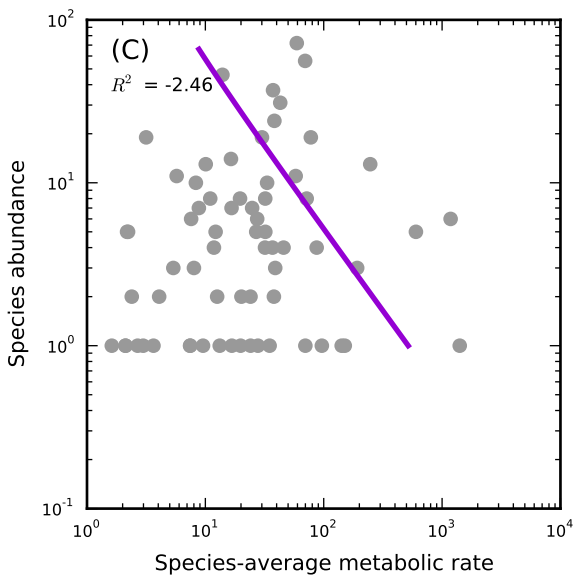
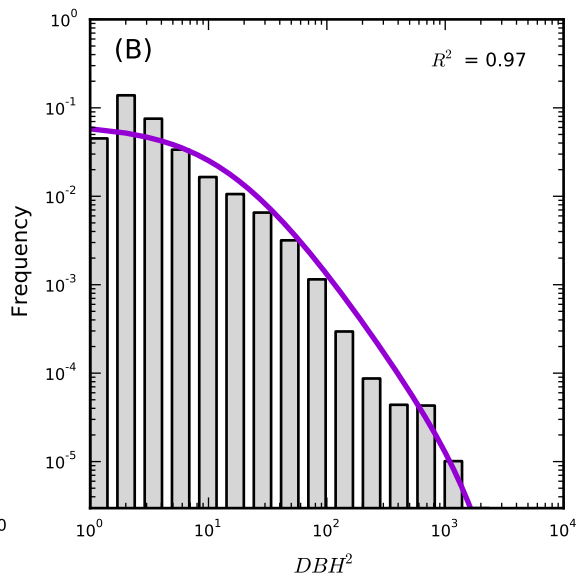
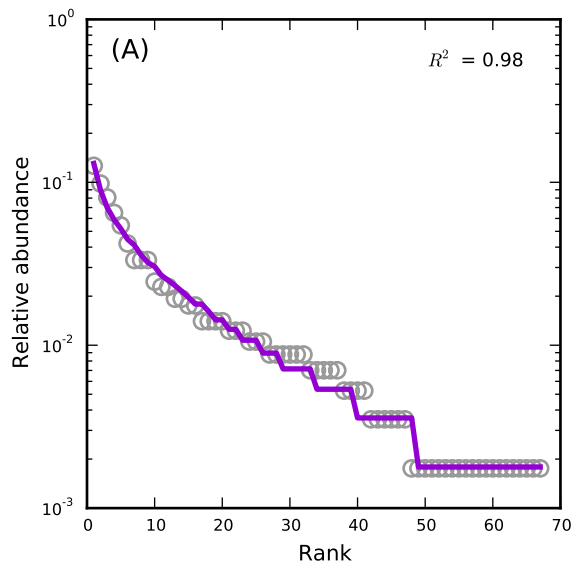
WesternGhats,BSP91



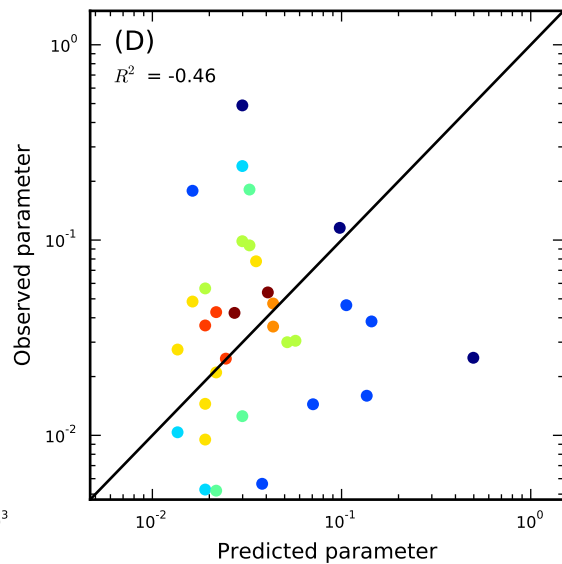
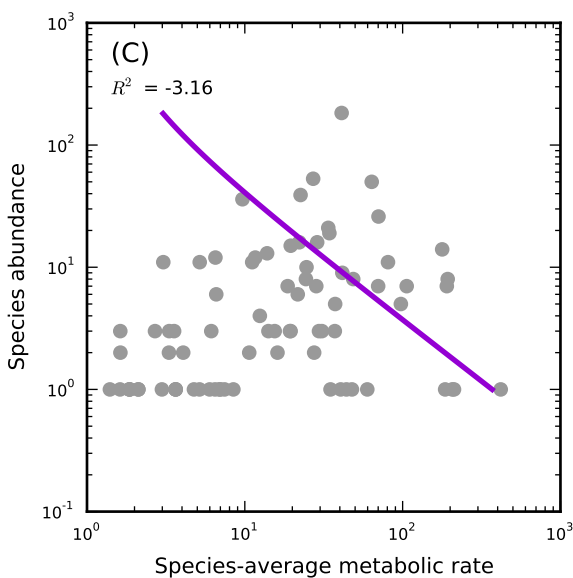
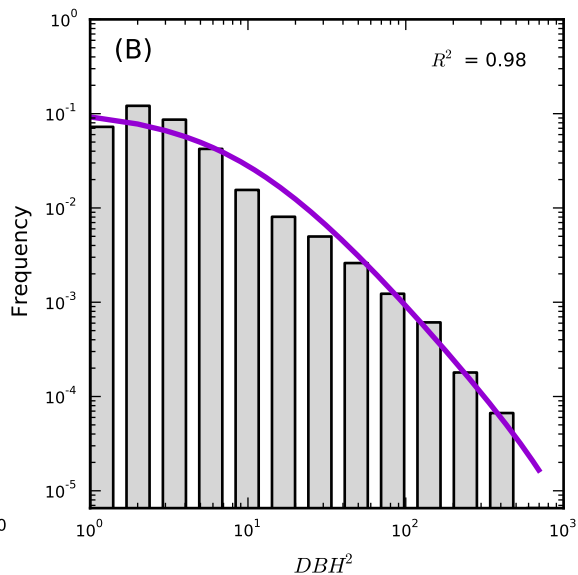
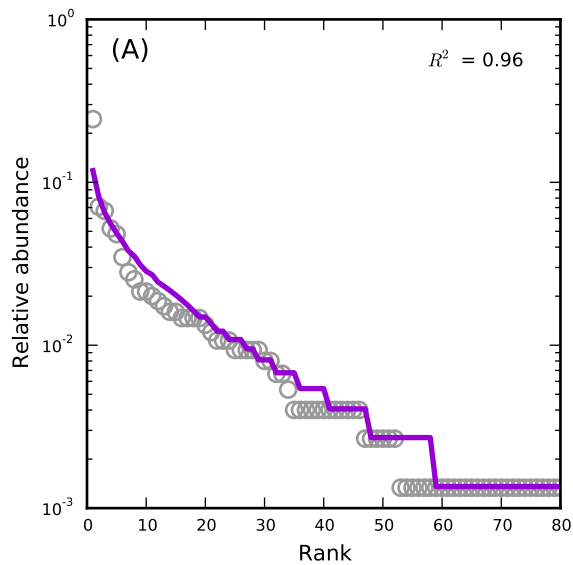
WesternGhats,BSP92



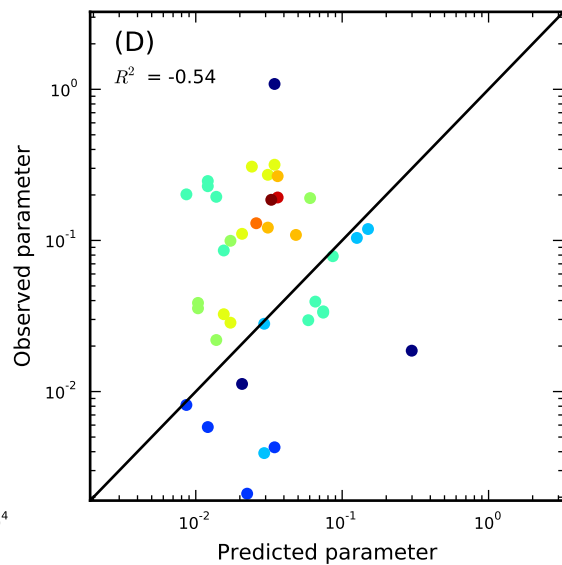
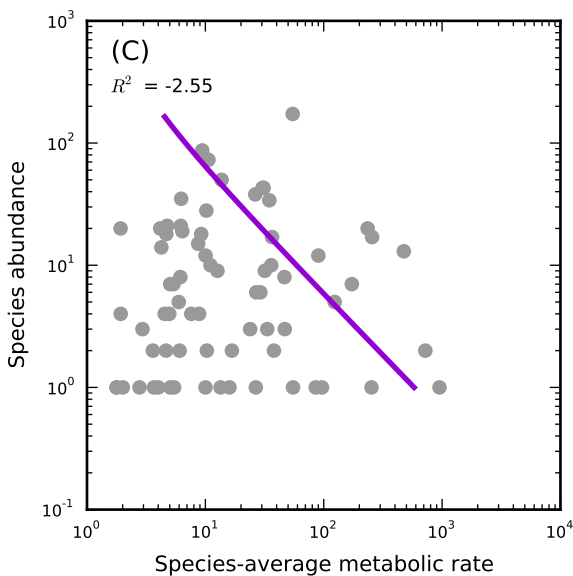
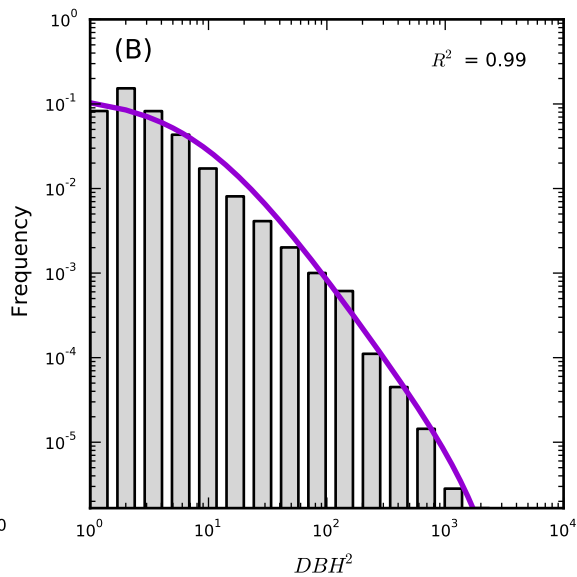
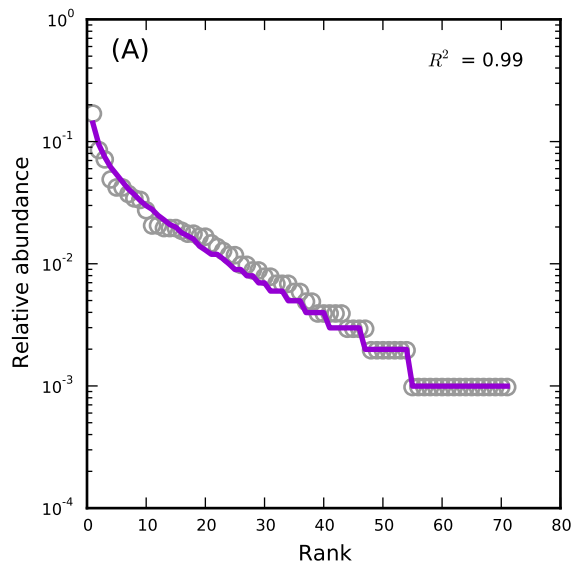
WesternGhats,BSP94



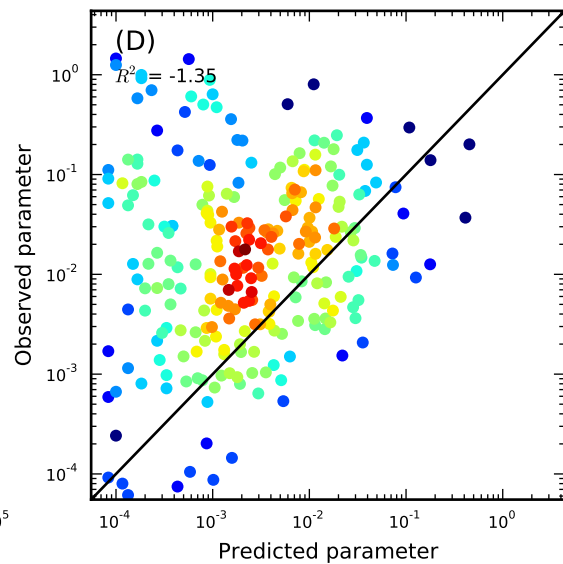
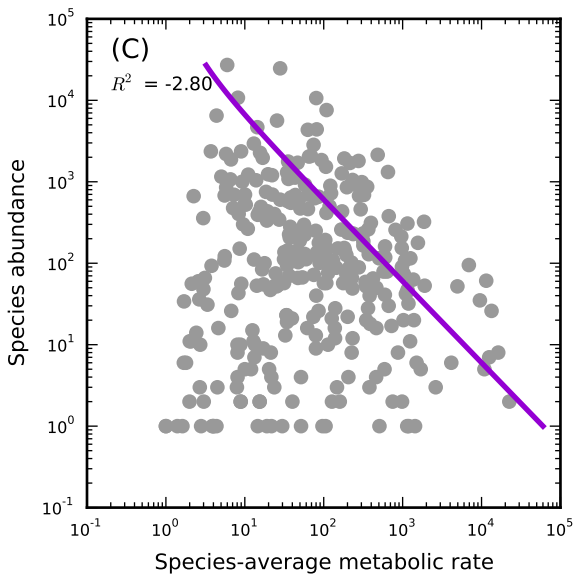
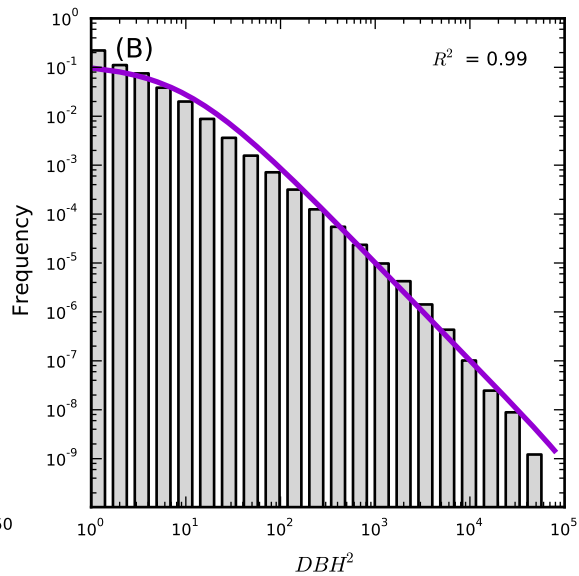
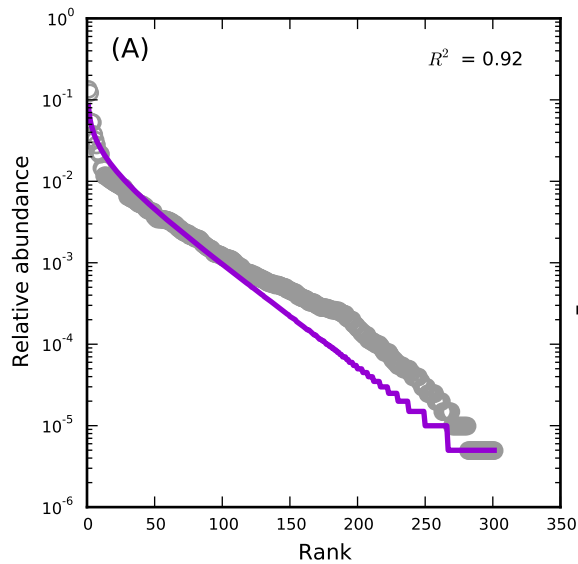
WesternGhats,BSP98



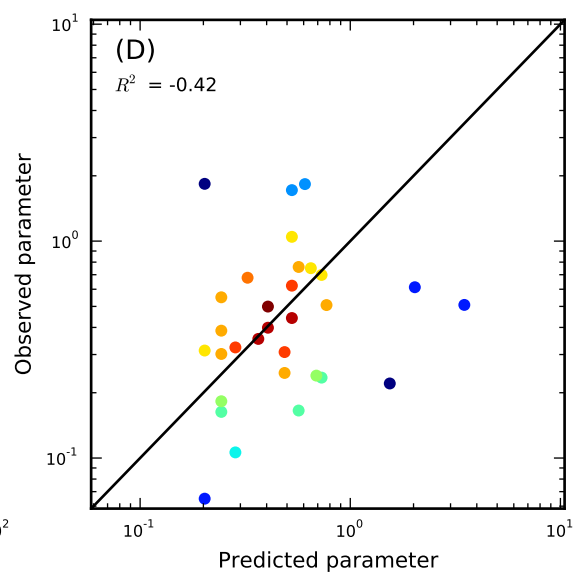
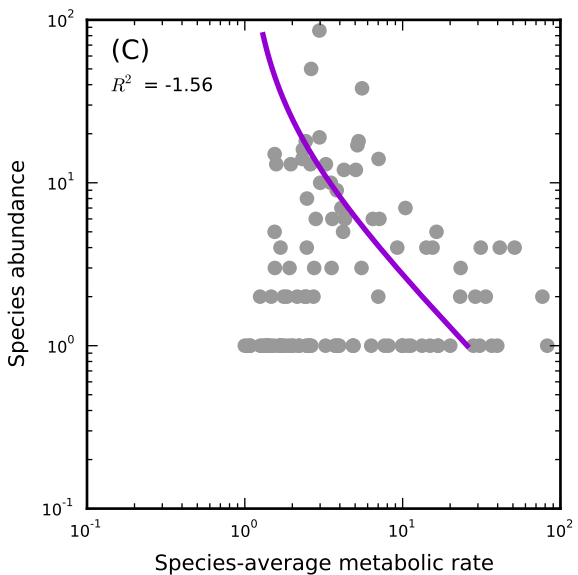
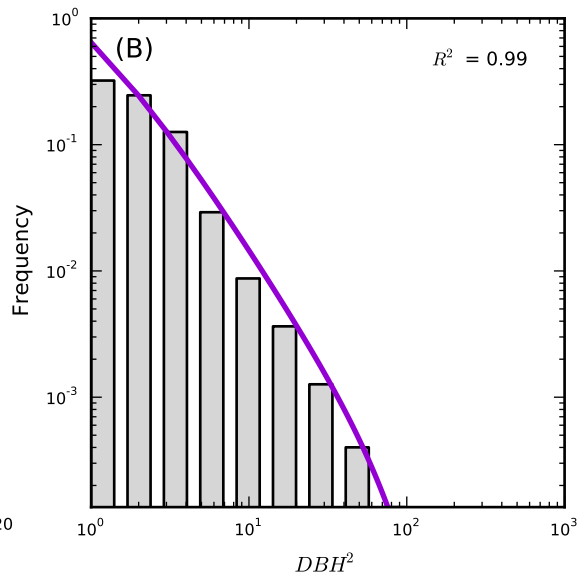
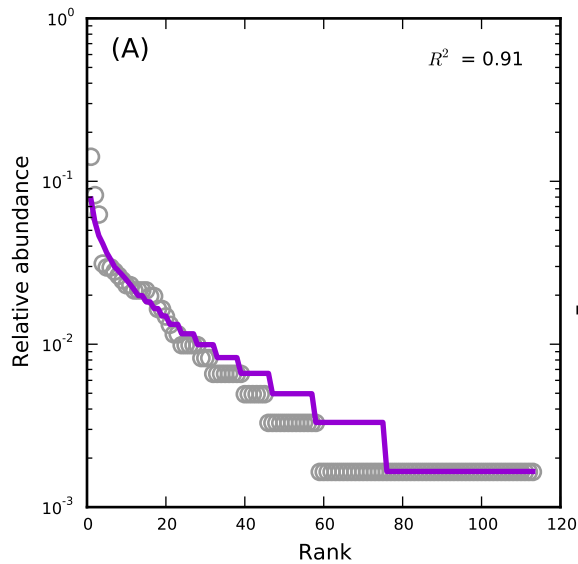
WesternGhats,BSP99



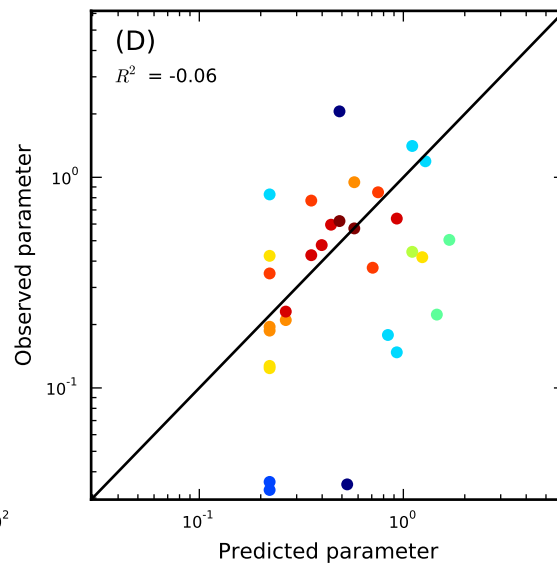
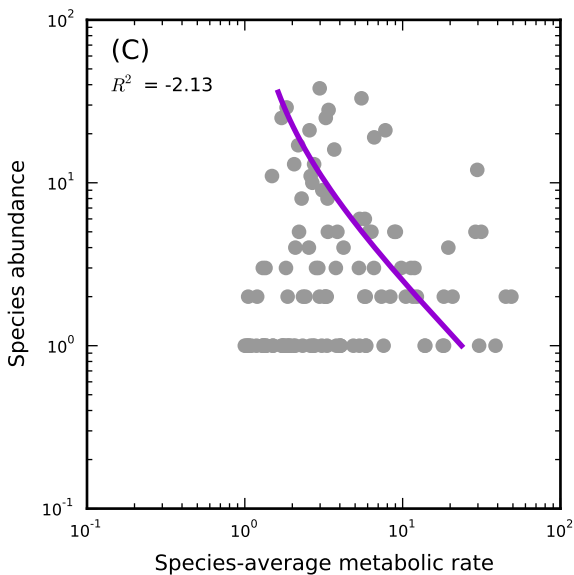
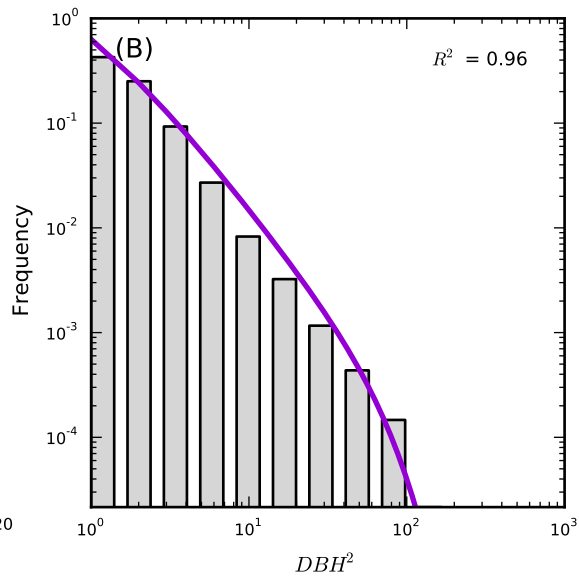
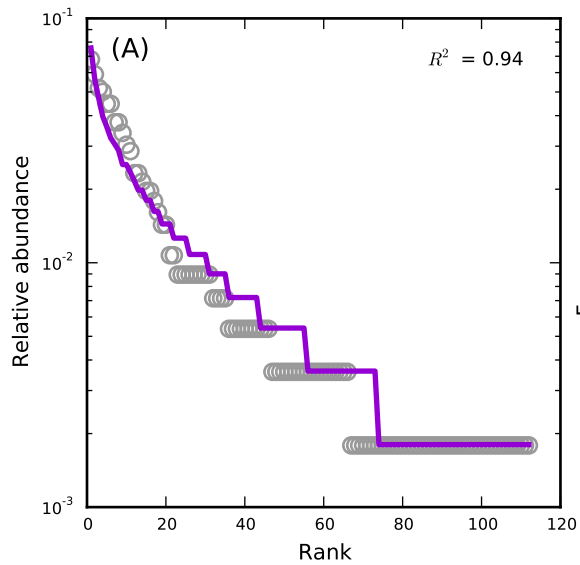
BCI, bci



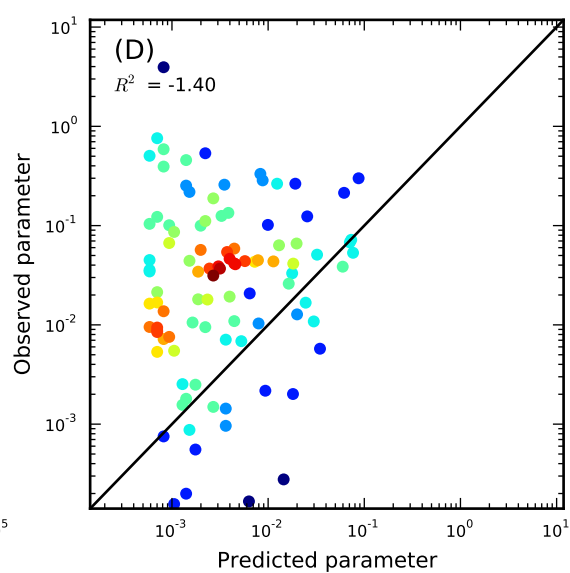
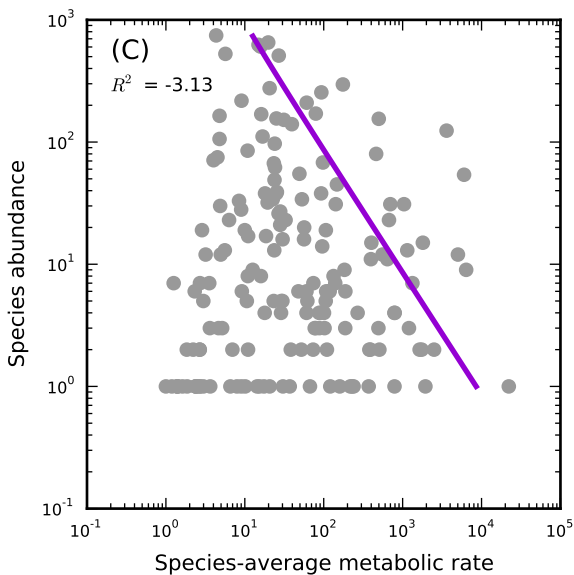
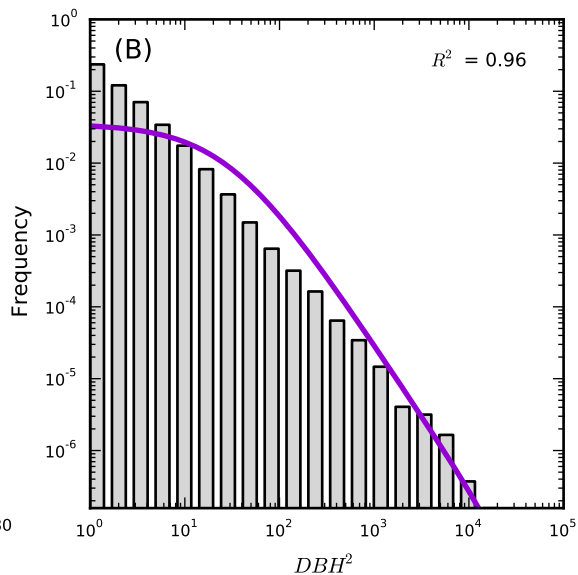
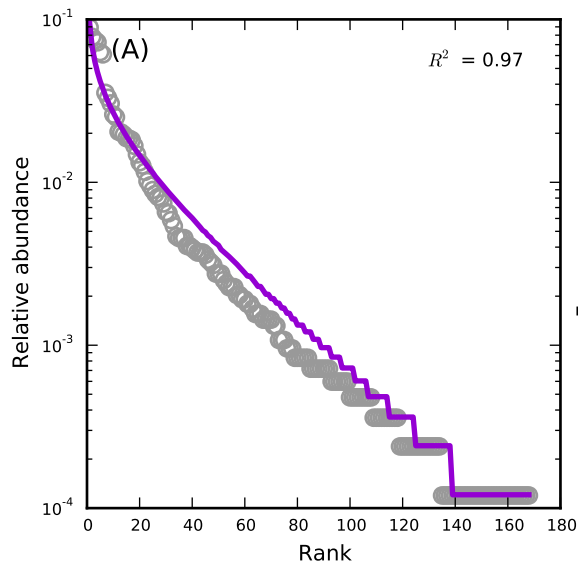
BVSF, BVPlot



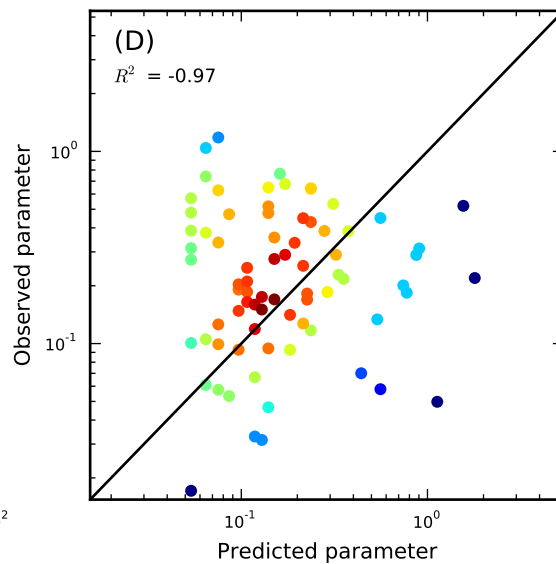
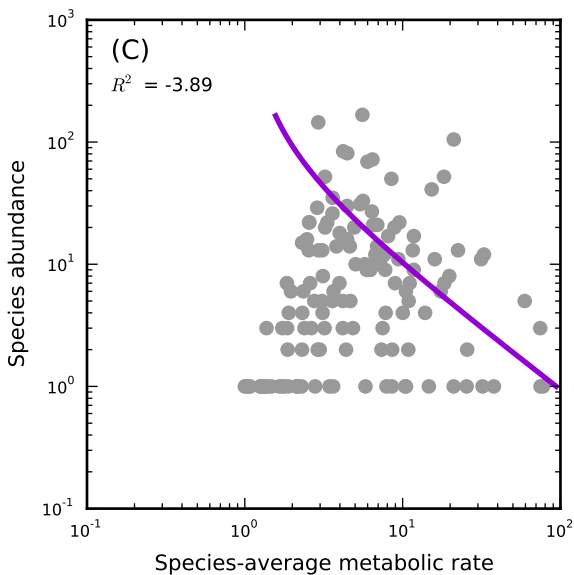
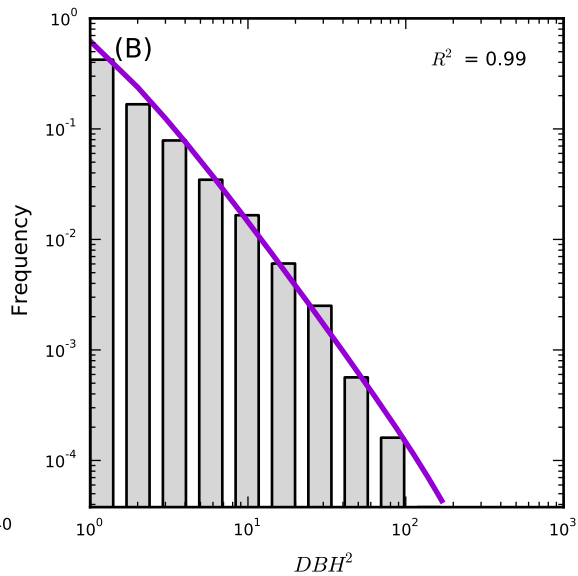
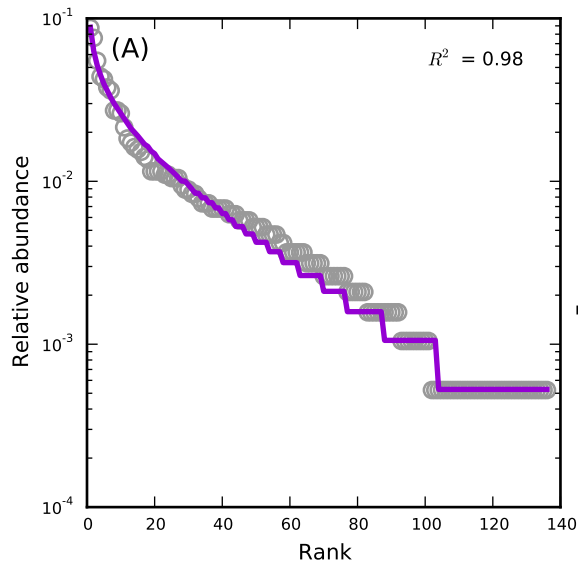
BVSF,SFPlot



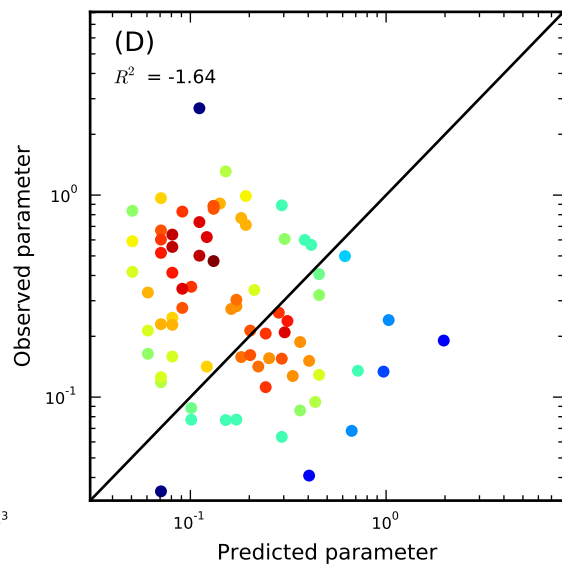
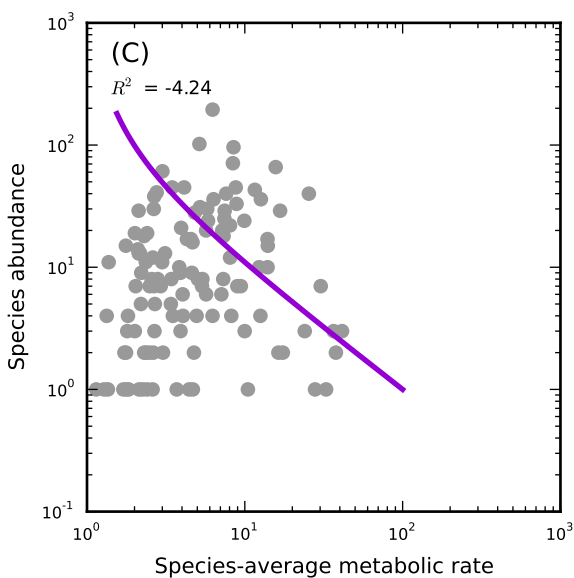
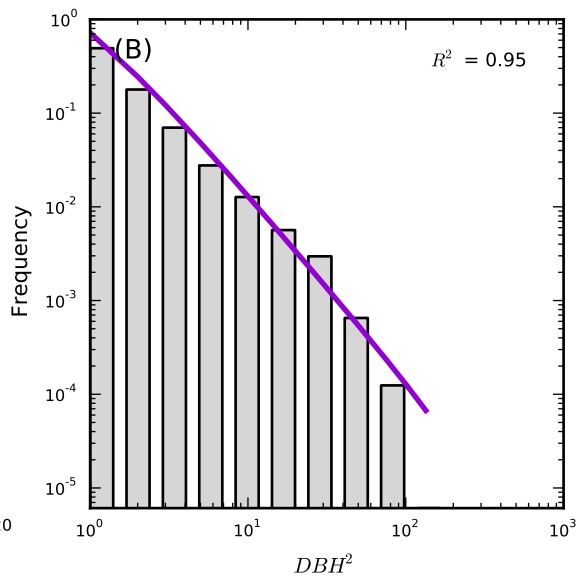
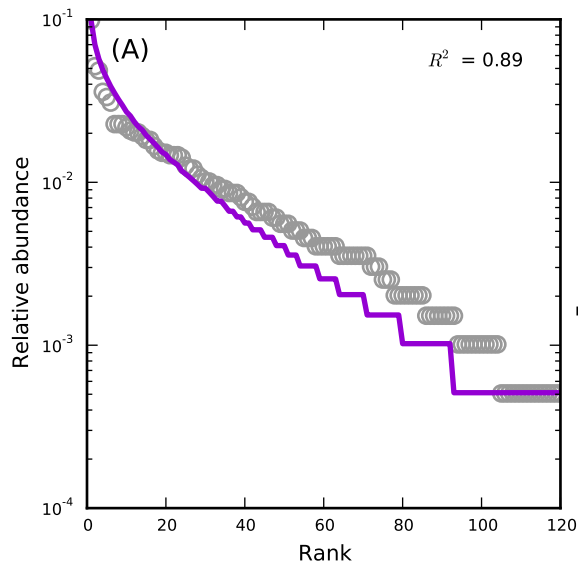
Cocoli,cocoli



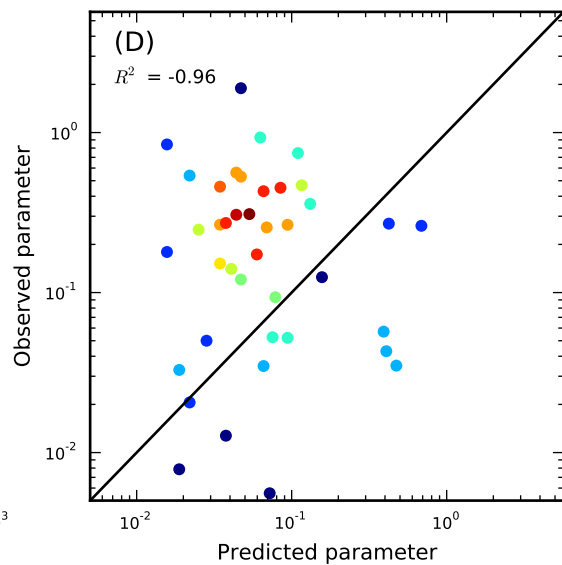
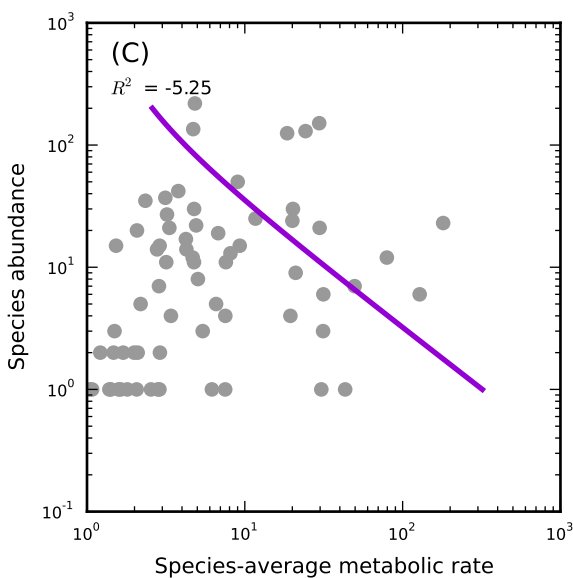
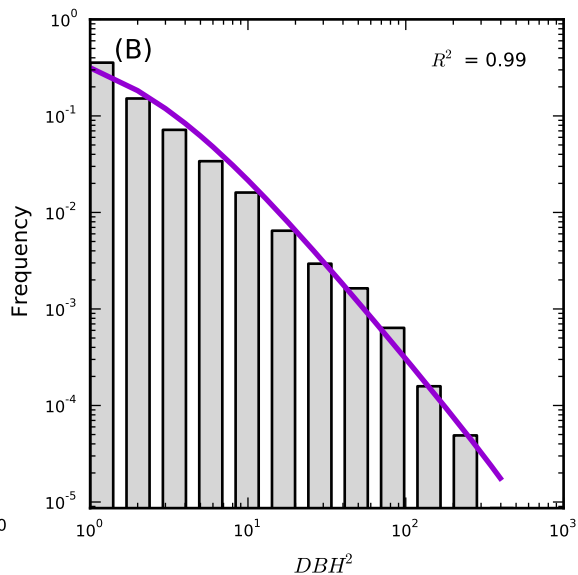
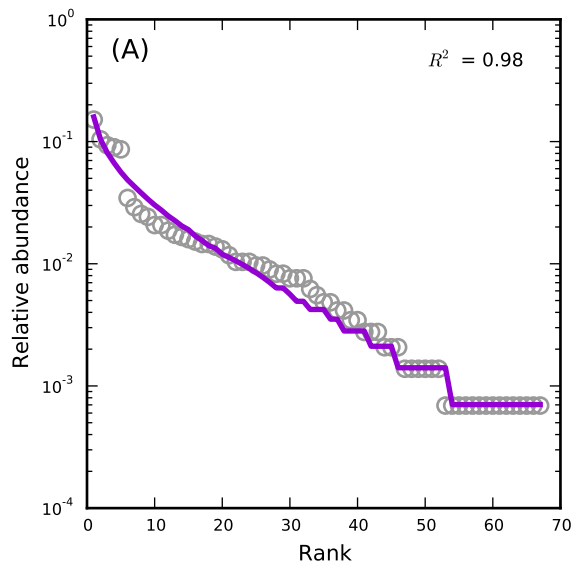
Lahei,heath1



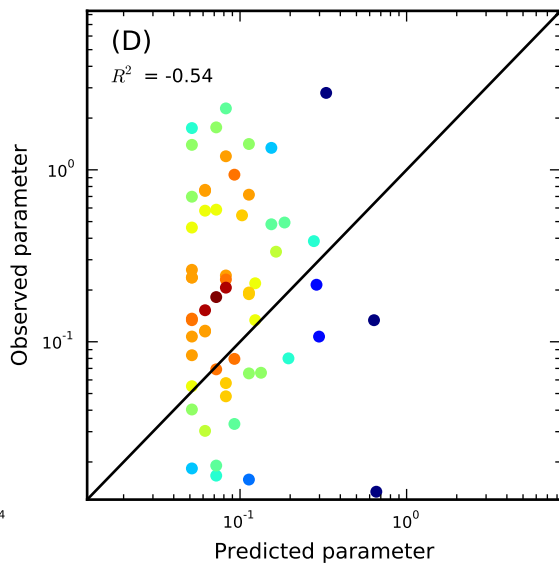
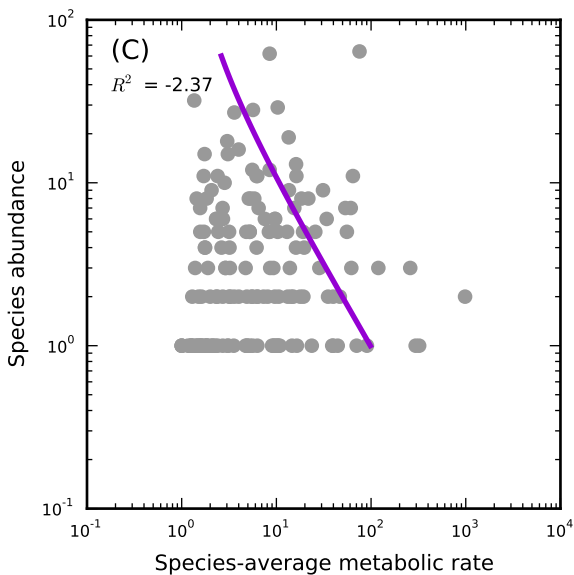
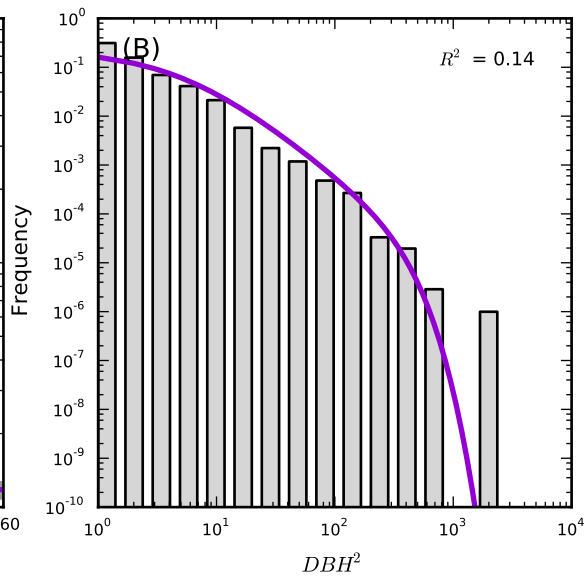
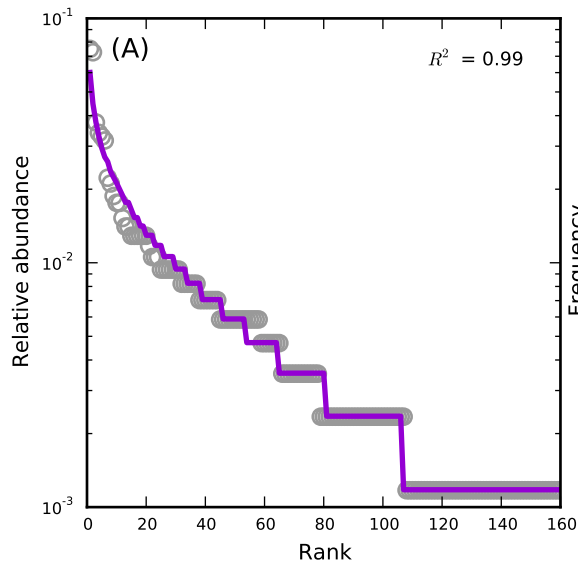
Lahei,heath2



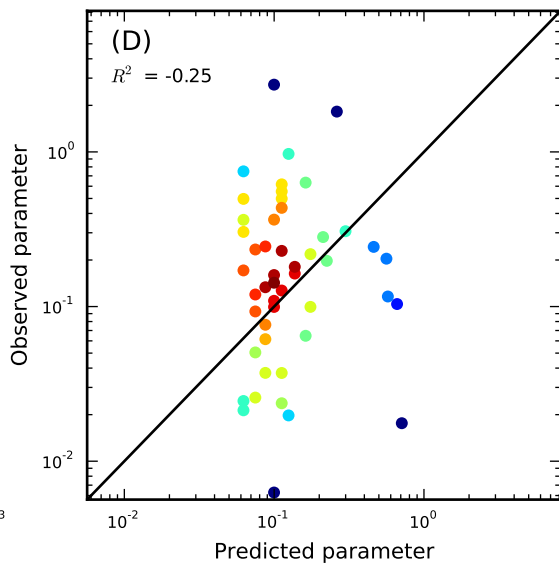
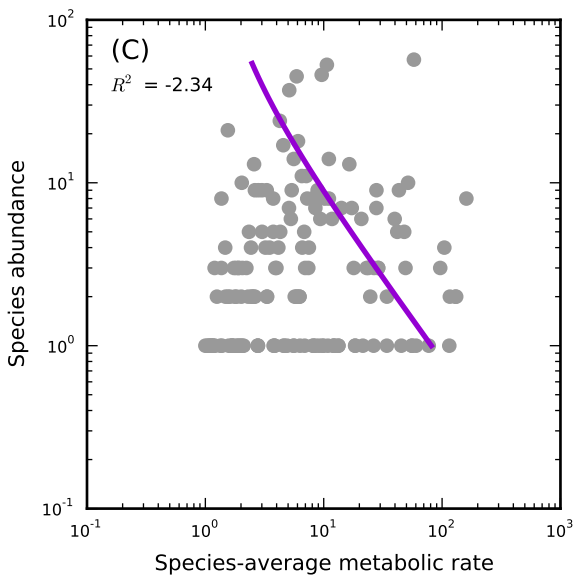
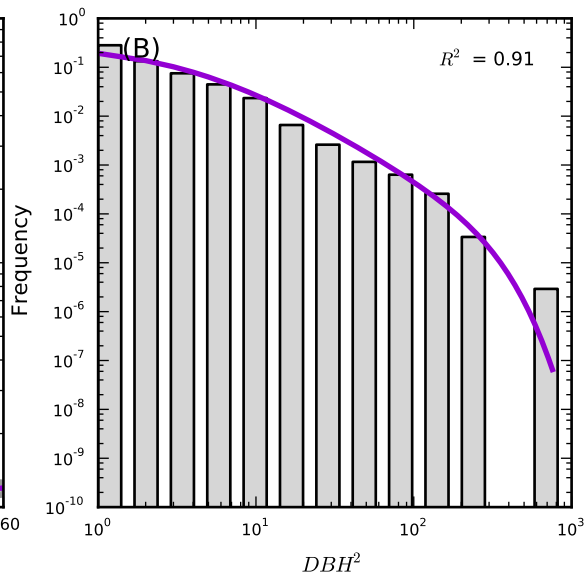
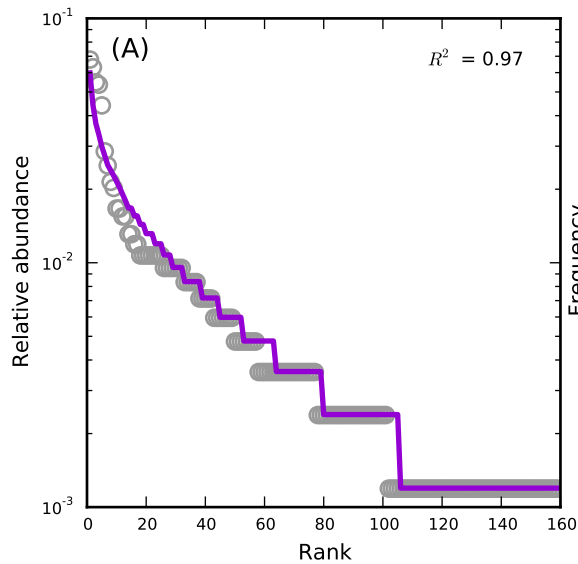
Lahei,peat



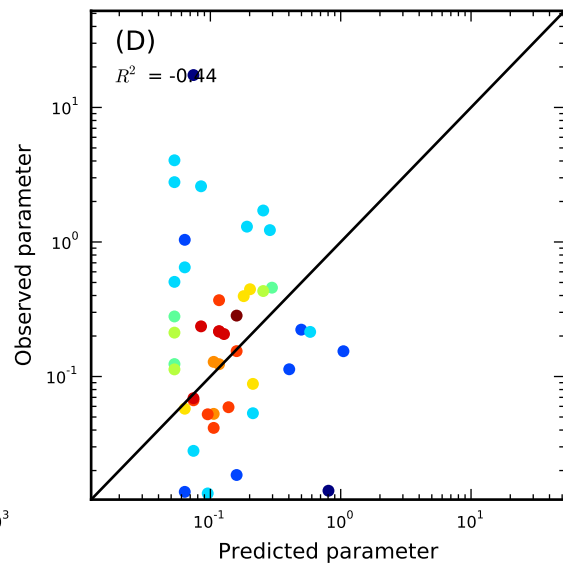
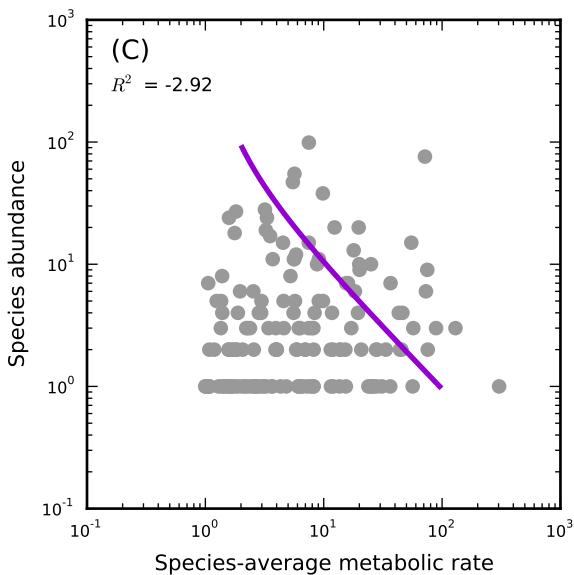
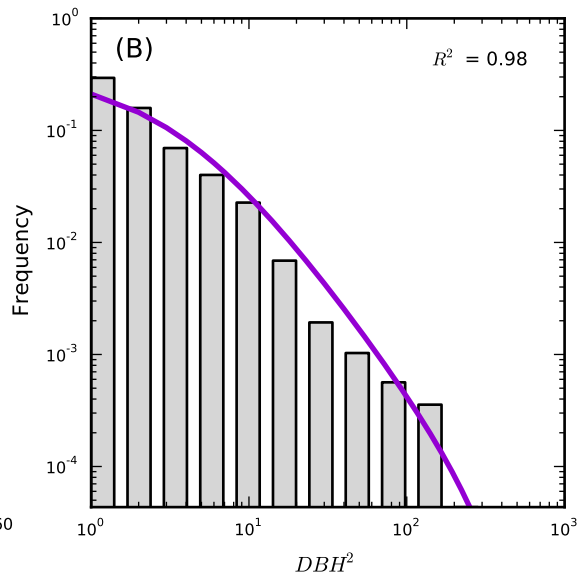
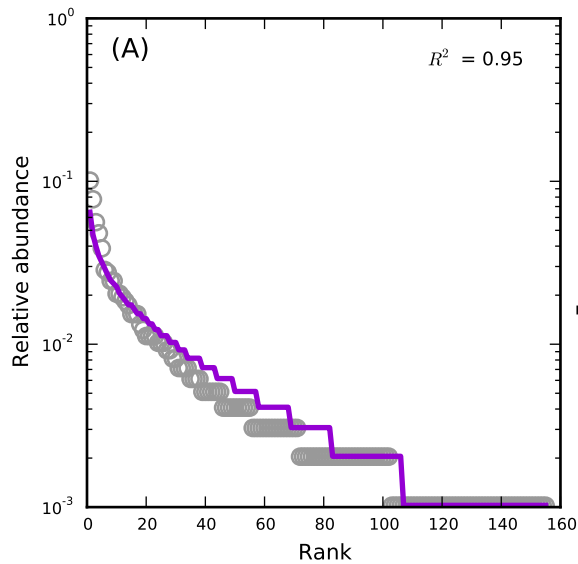
LaSelva,1



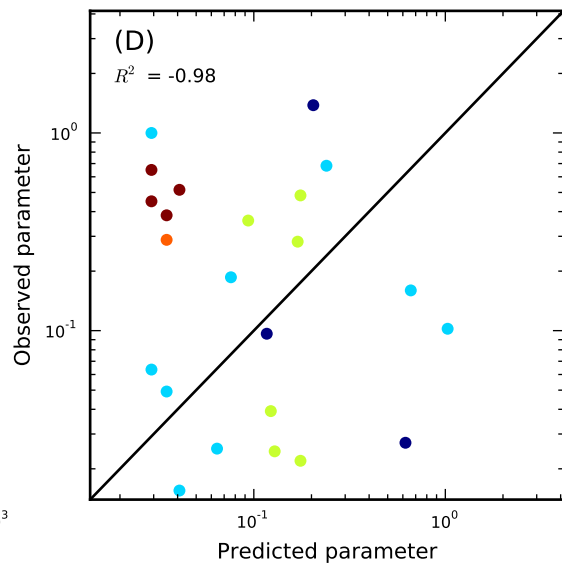
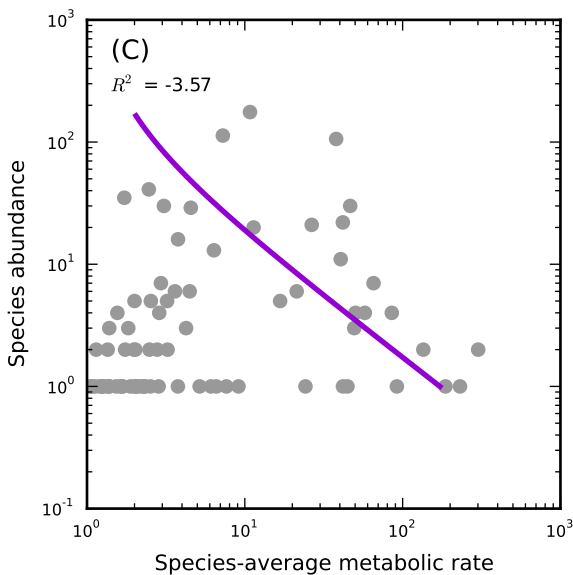
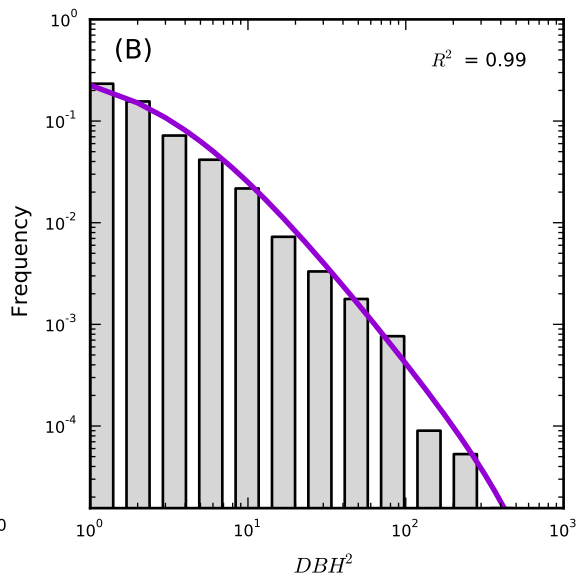
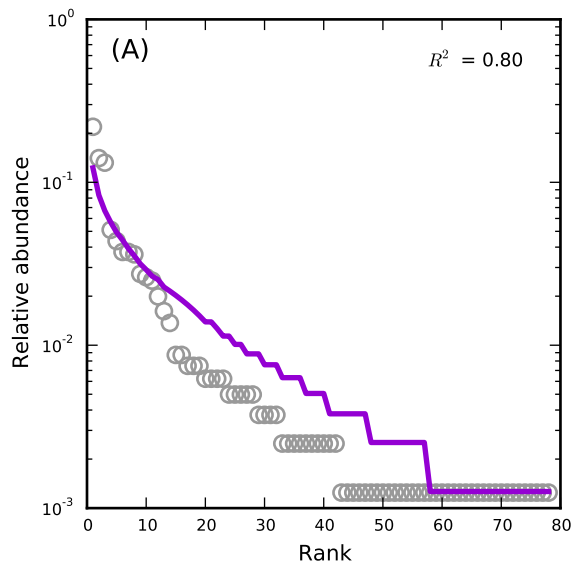
LaSelva,2



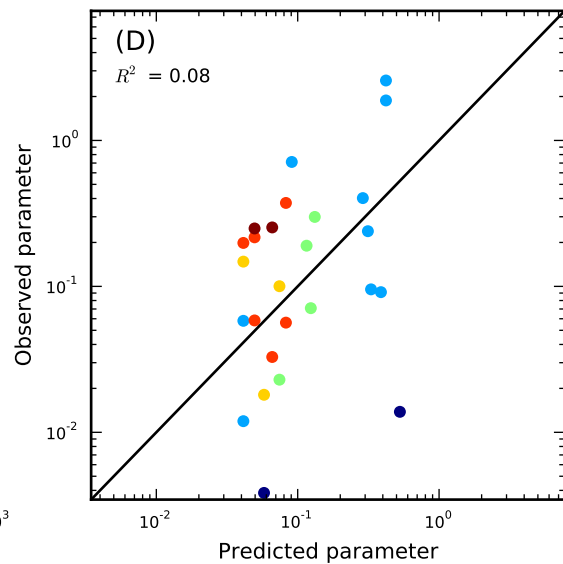
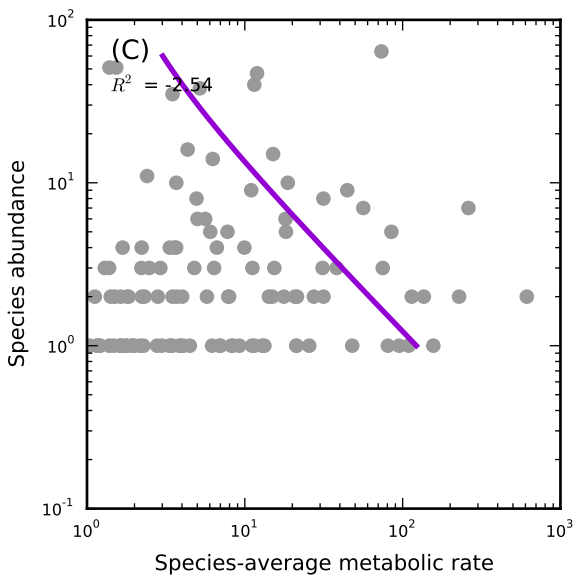
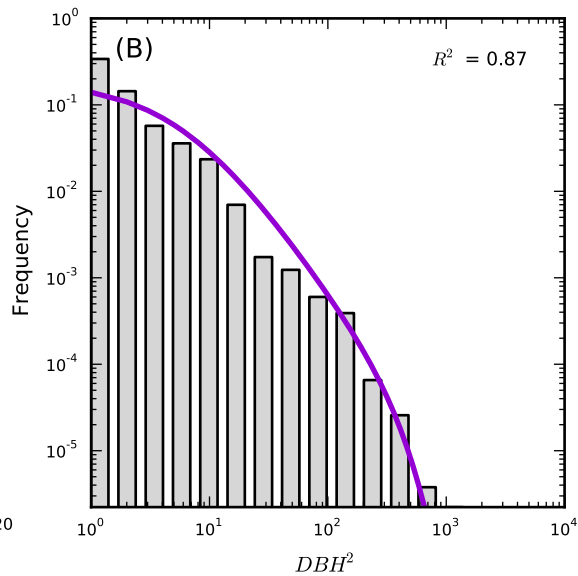
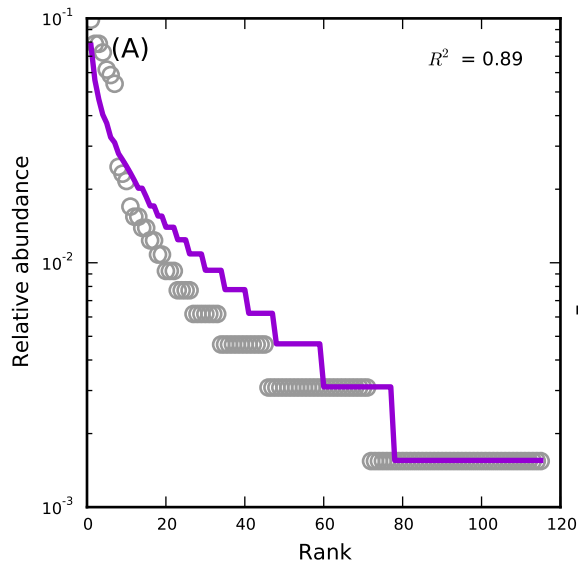
LaSelva,3



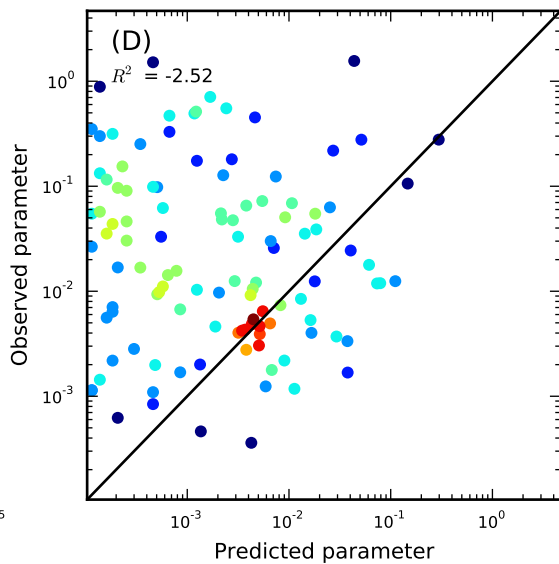
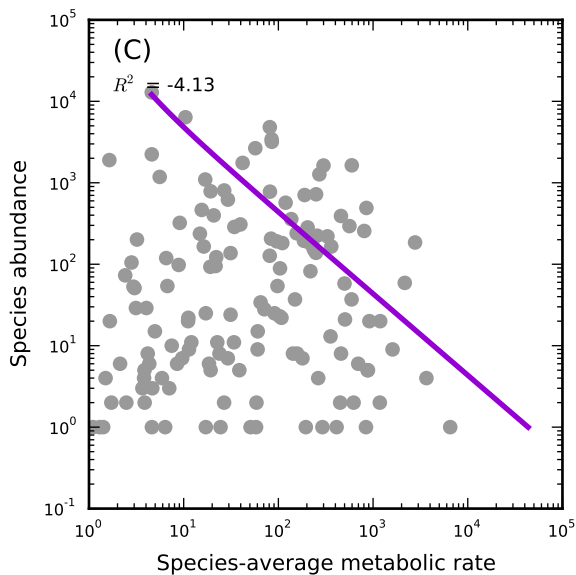
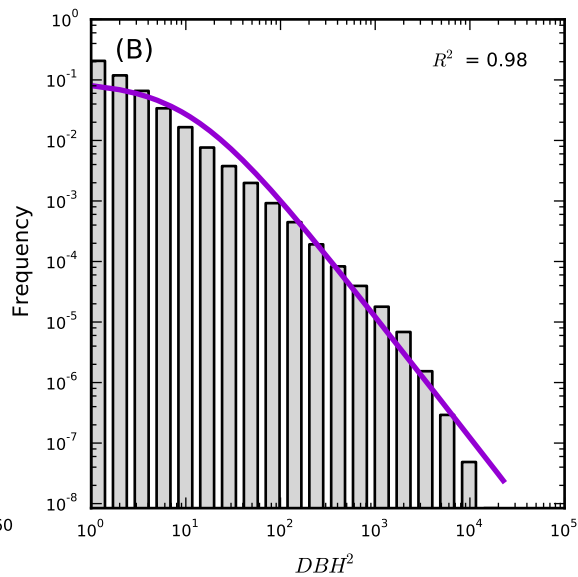
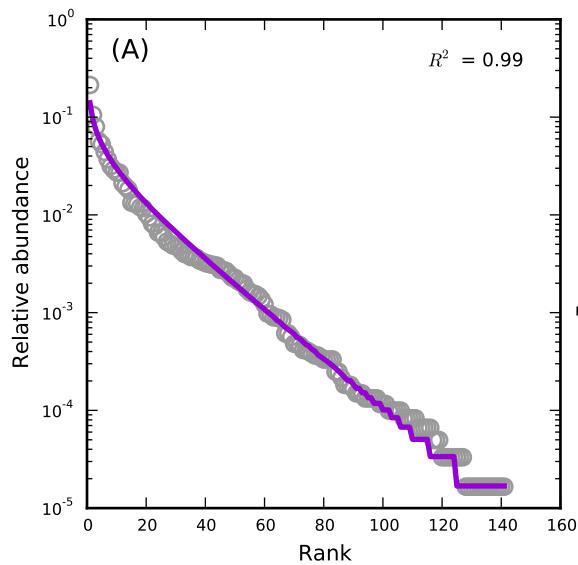
LaSelva,4



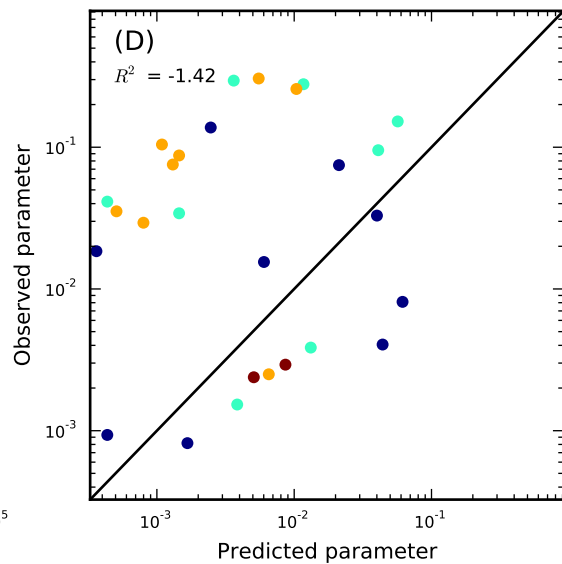
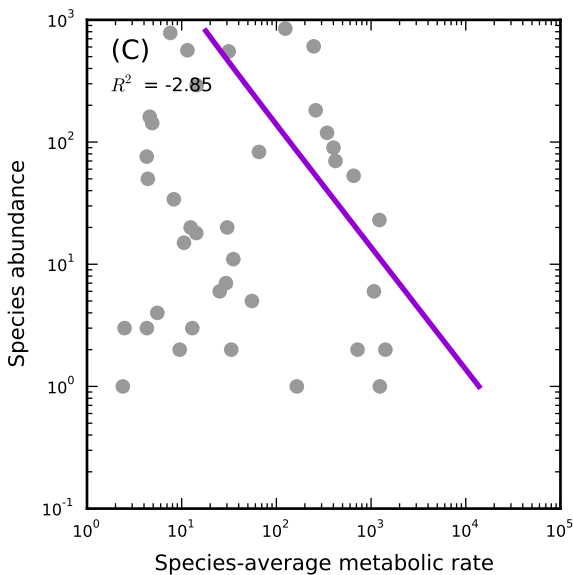
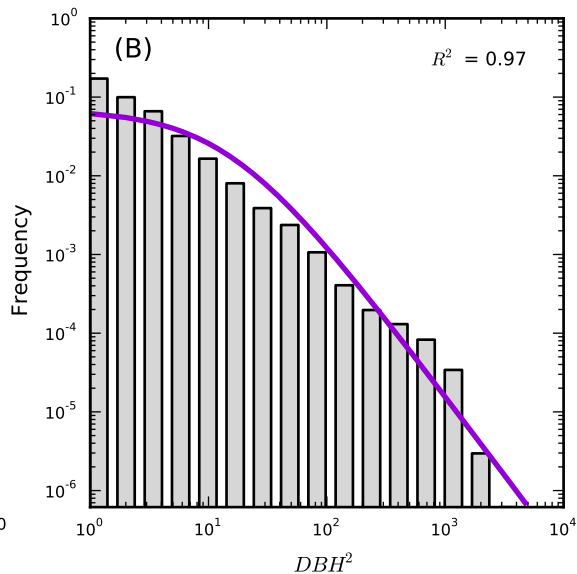
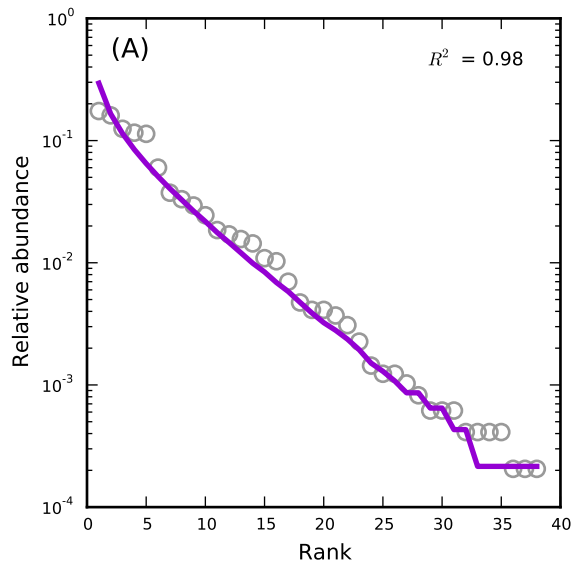
LaSelva,5



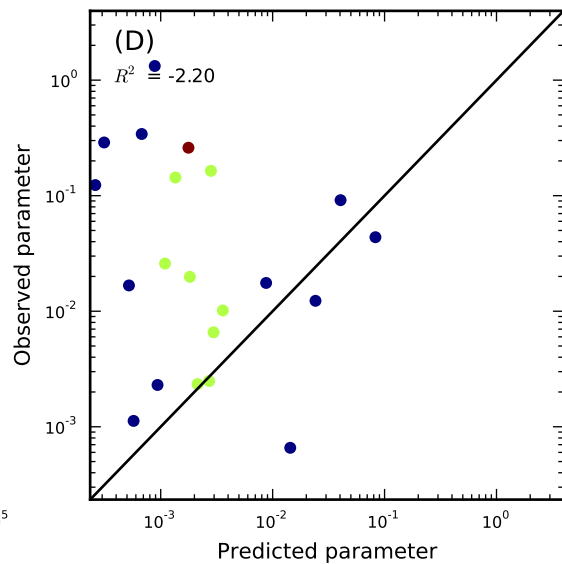
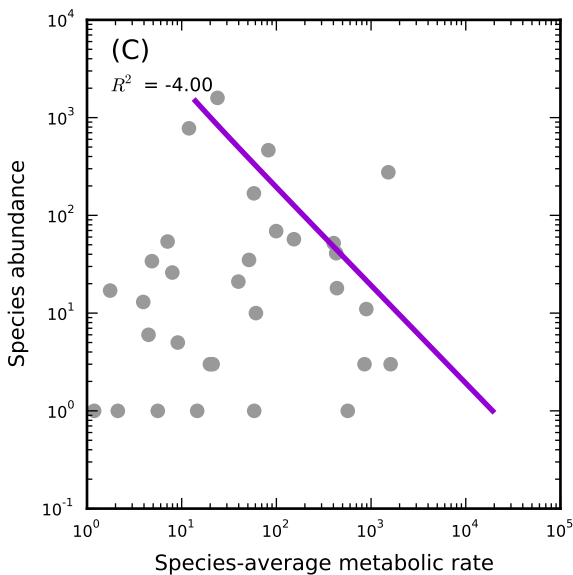
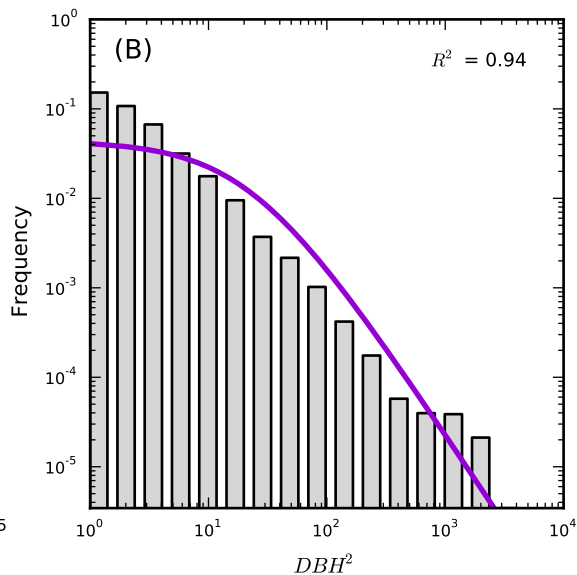
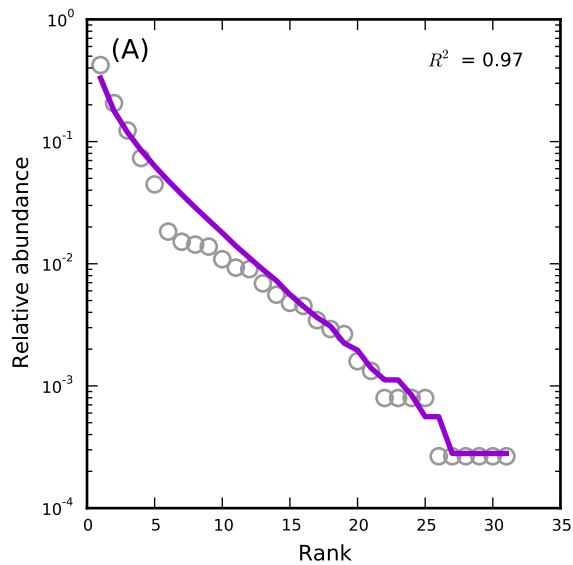
Luquillo, lfdp



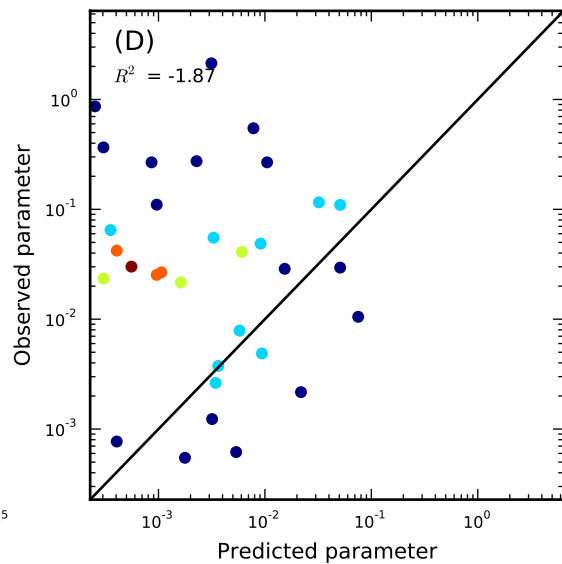
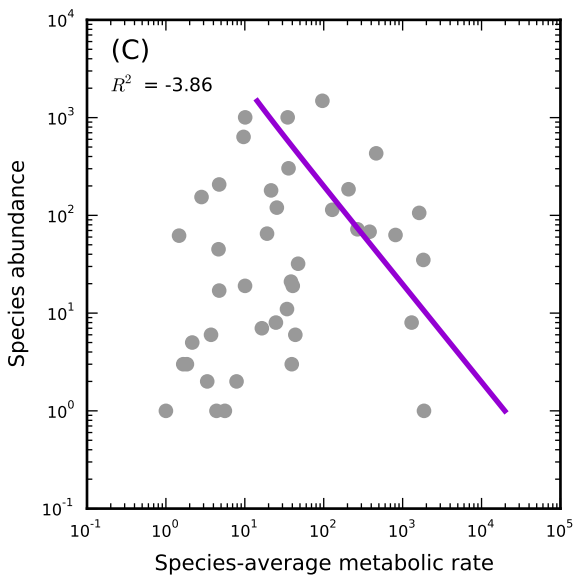
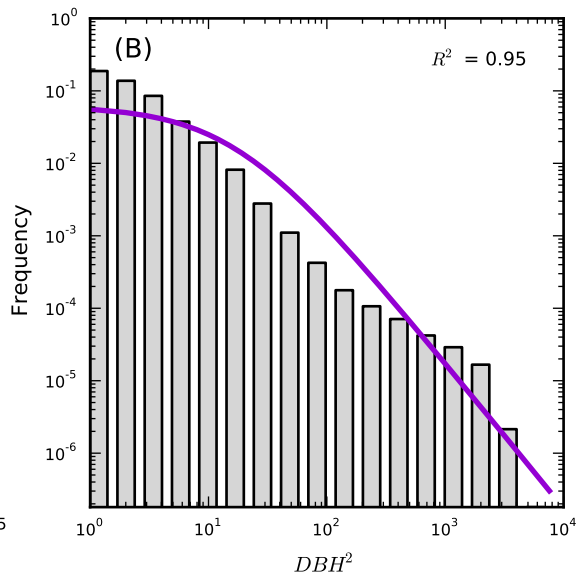
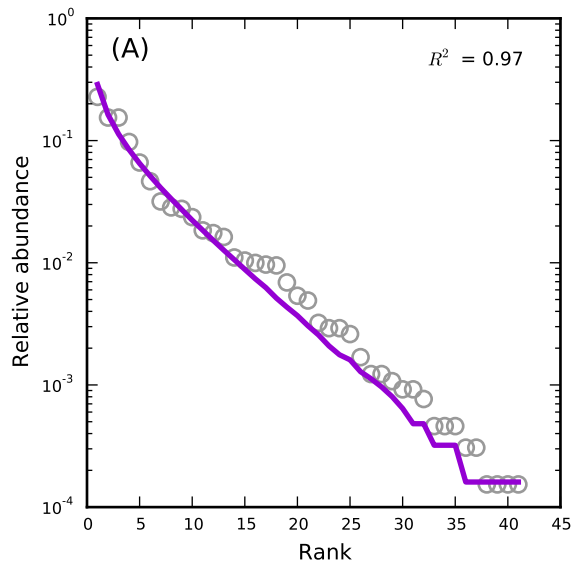
NC,12



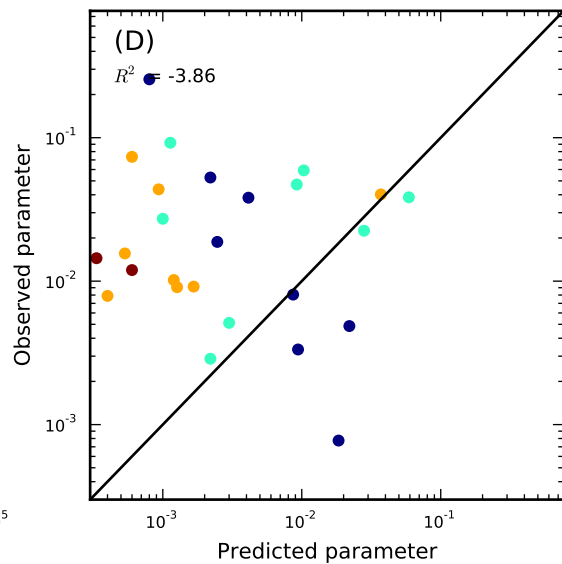
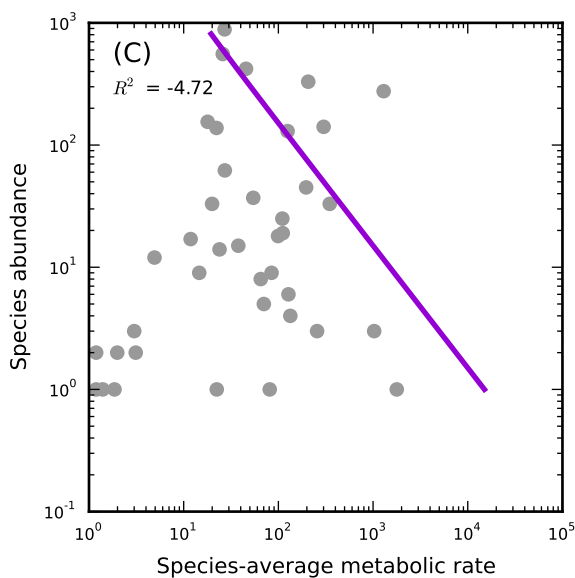
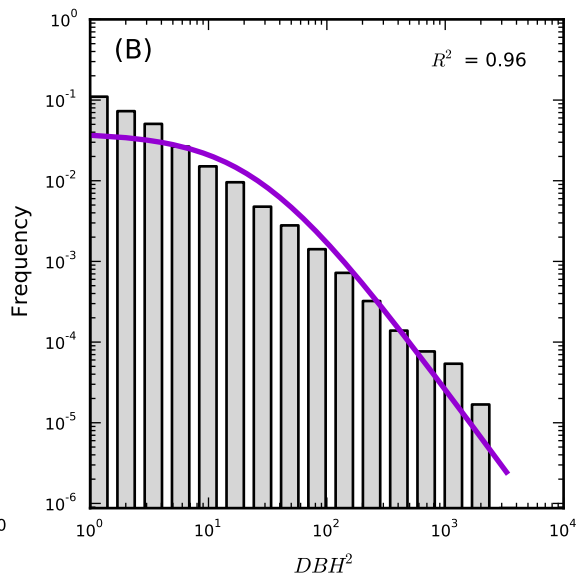
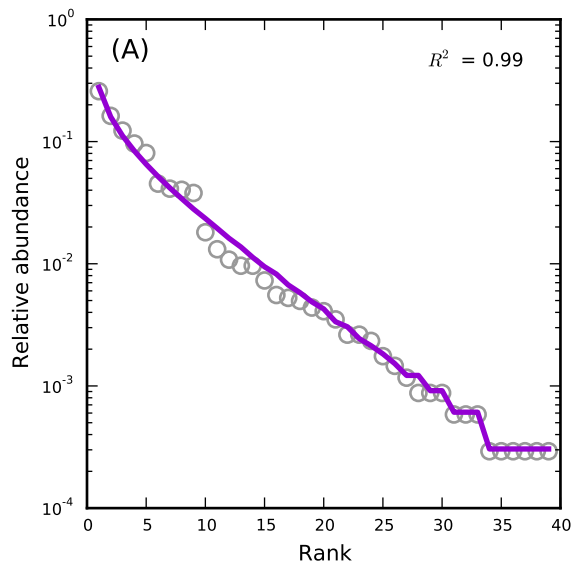
NC,13



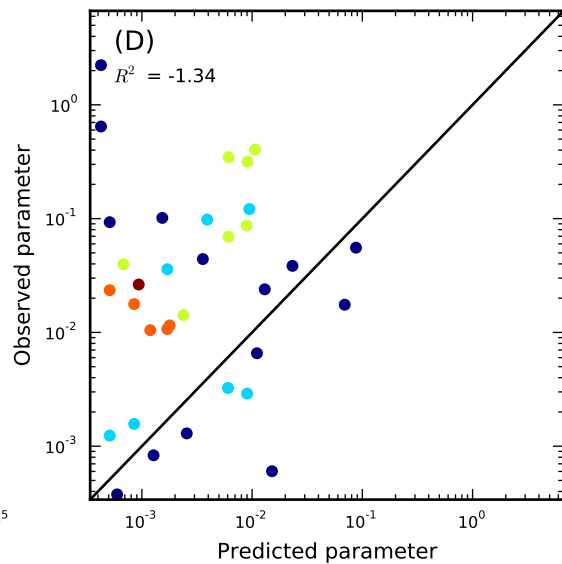
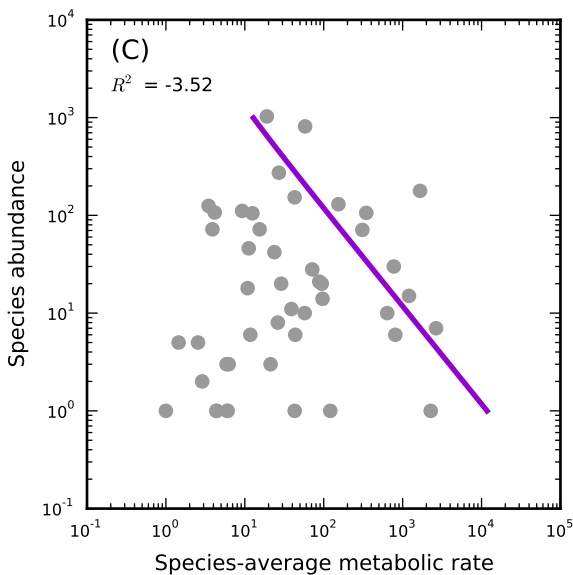
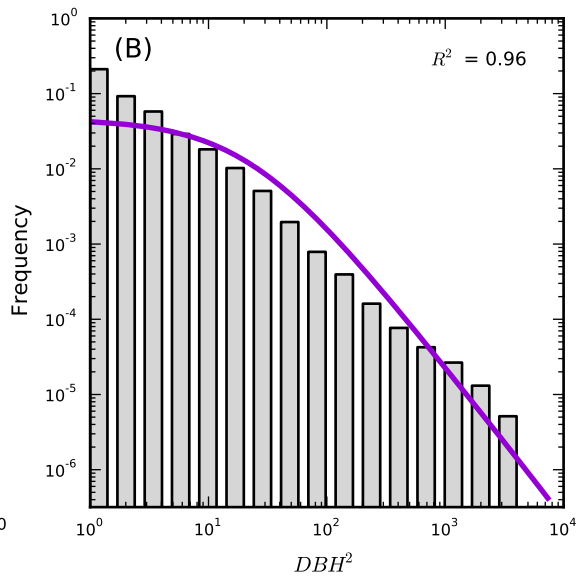
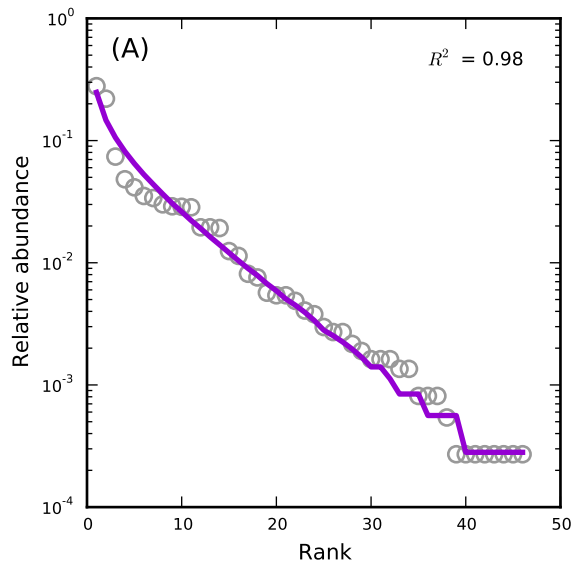
NC,14



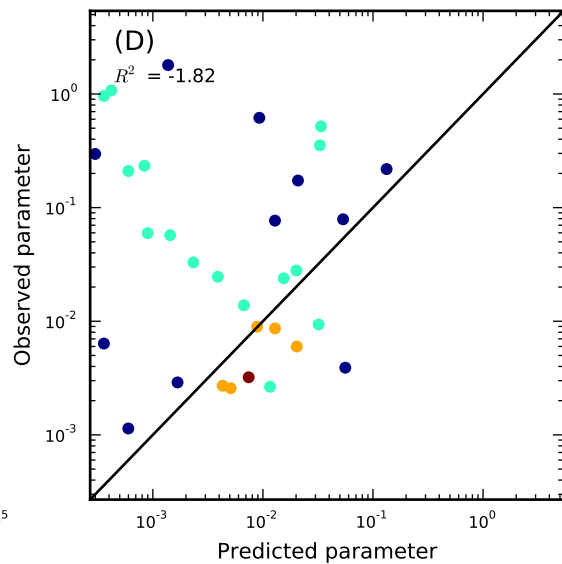
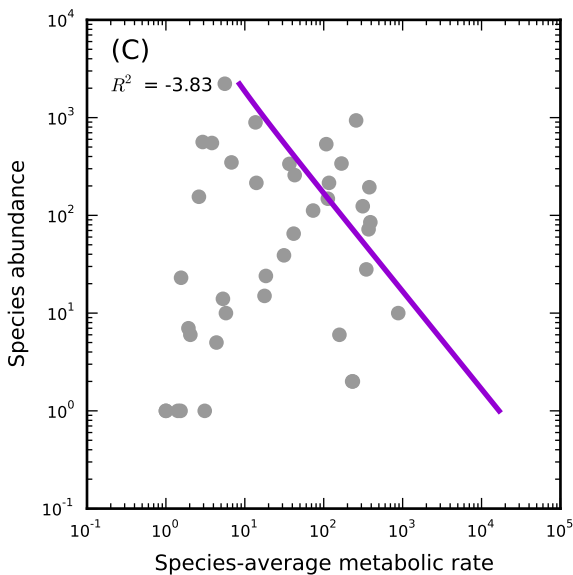
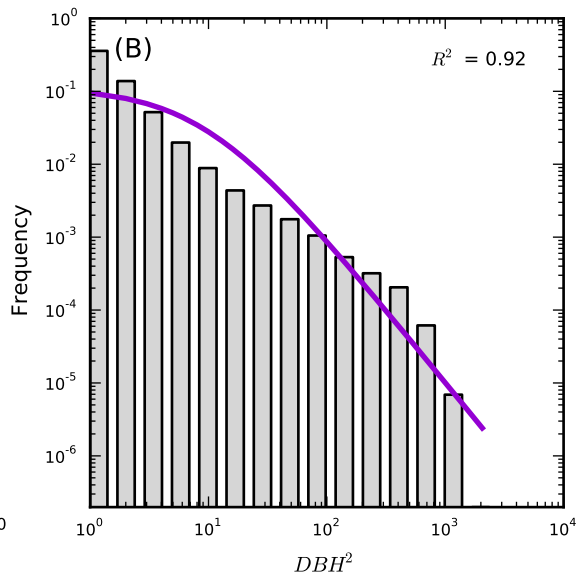
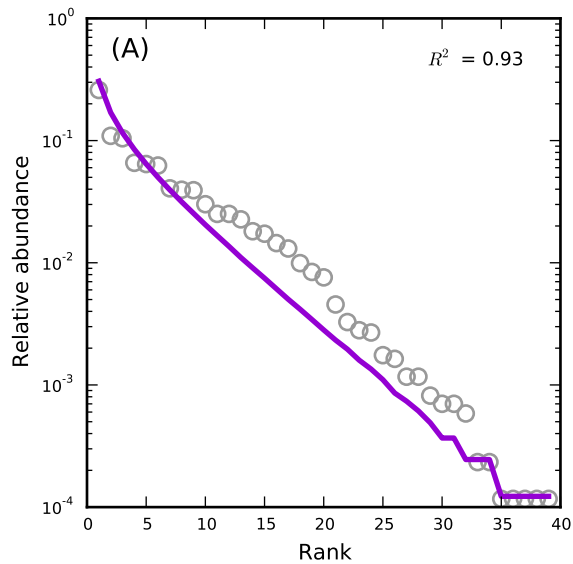
NC,4



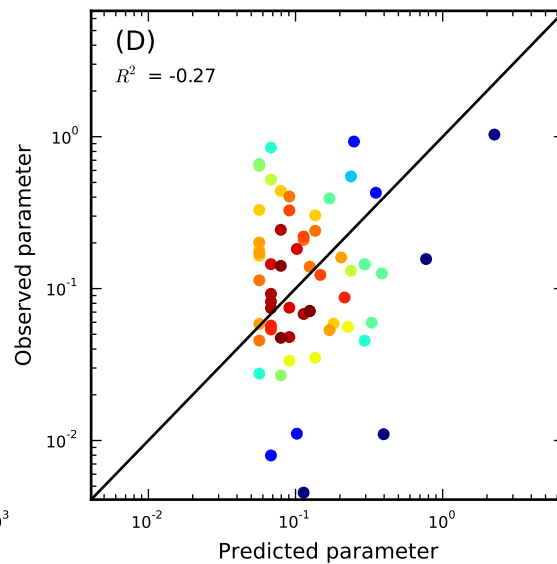
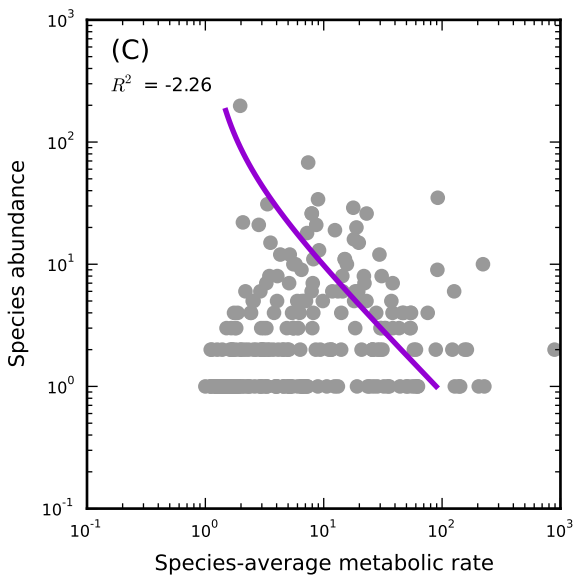
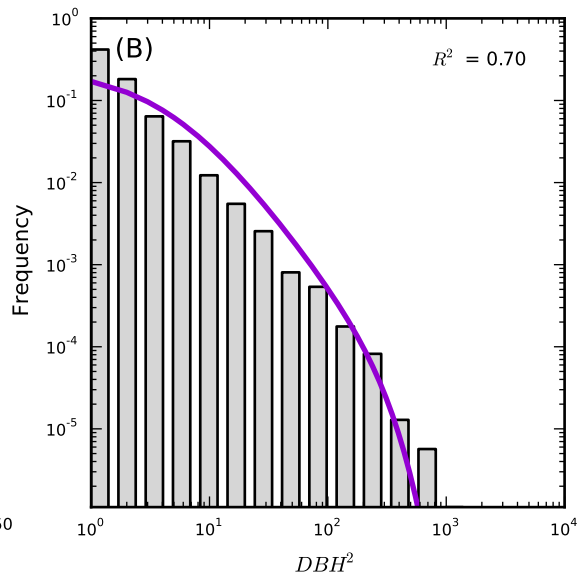
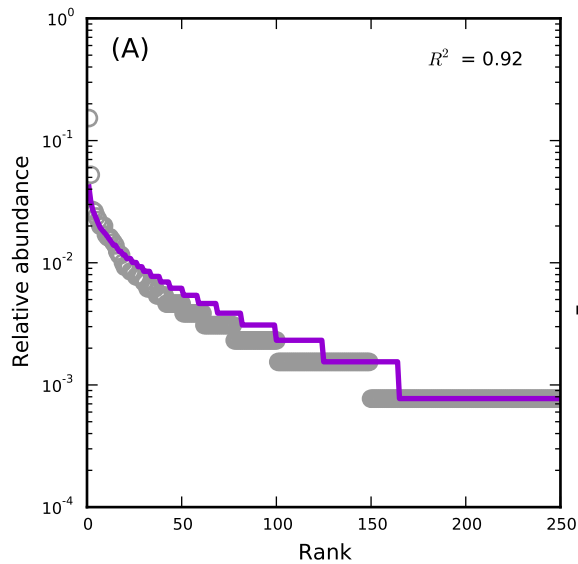
NC,93



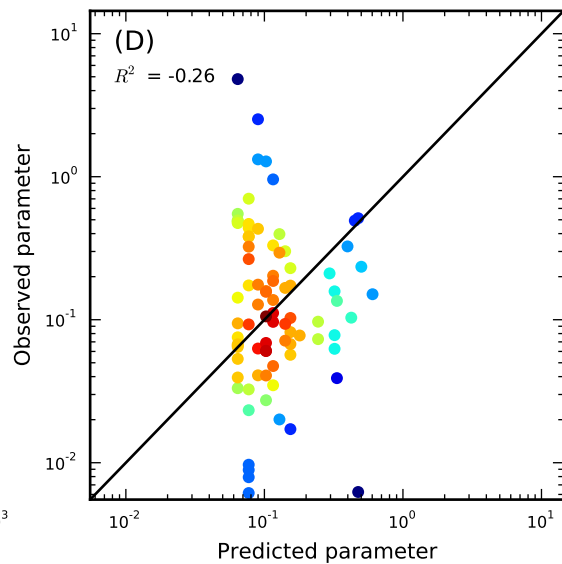
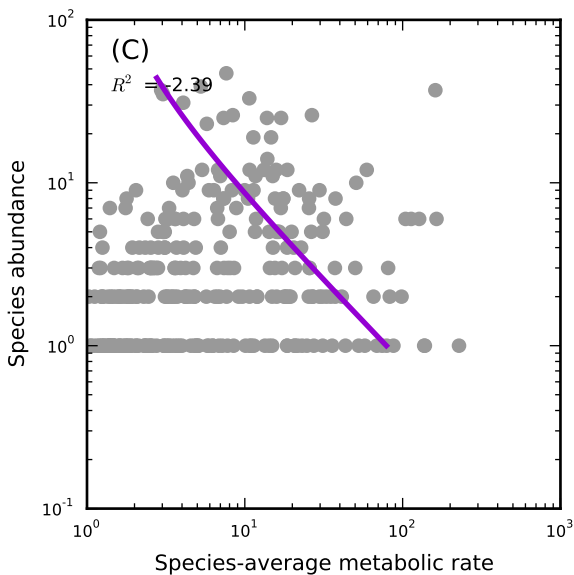
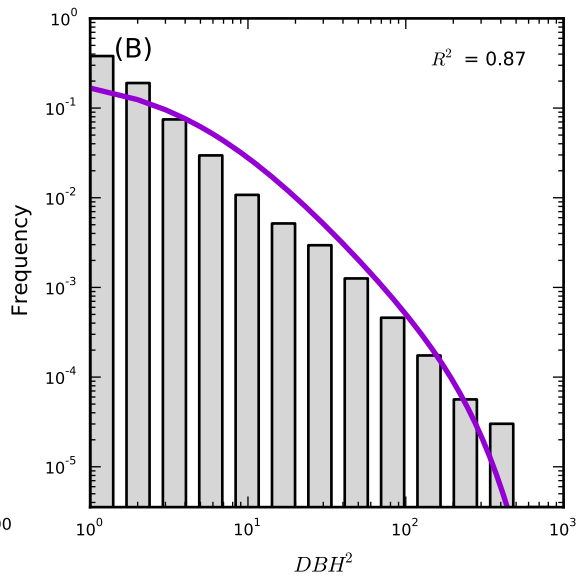
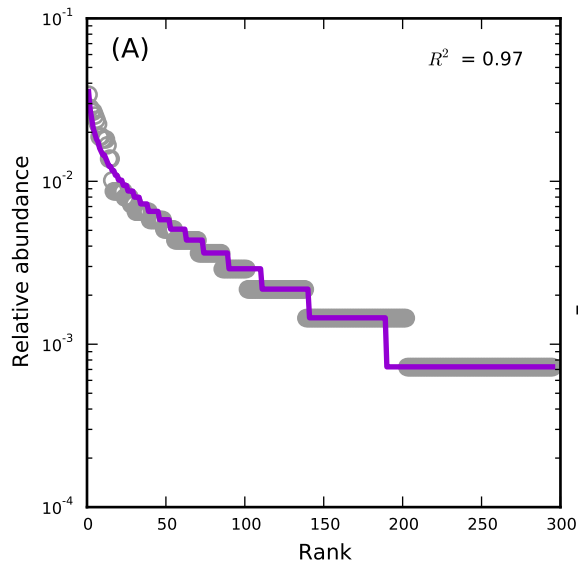
Oosting, Oosting



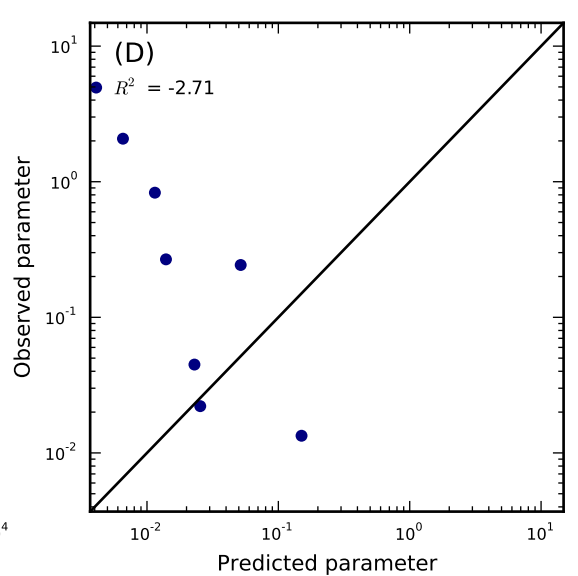
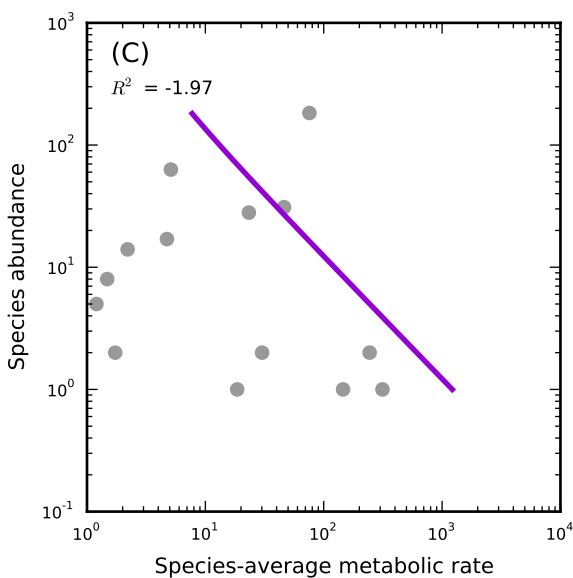
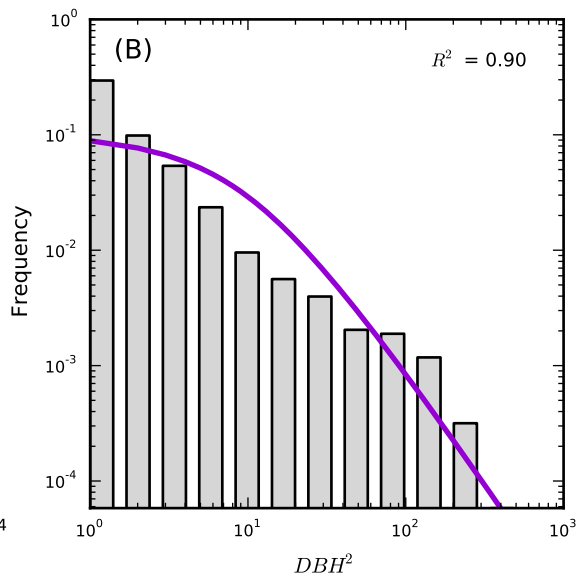
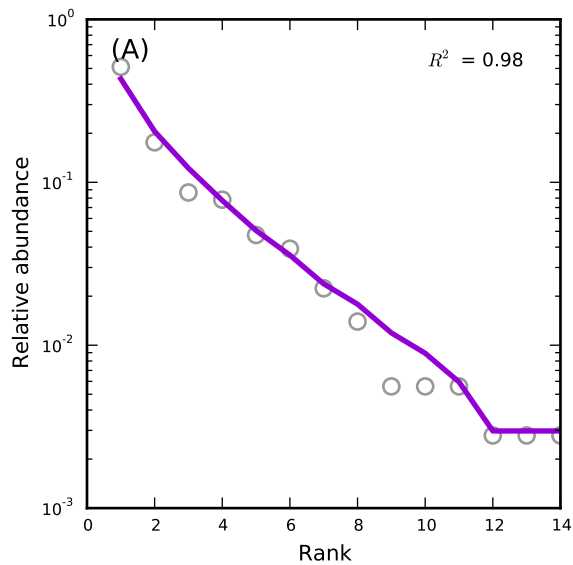
Serimbu, S-1



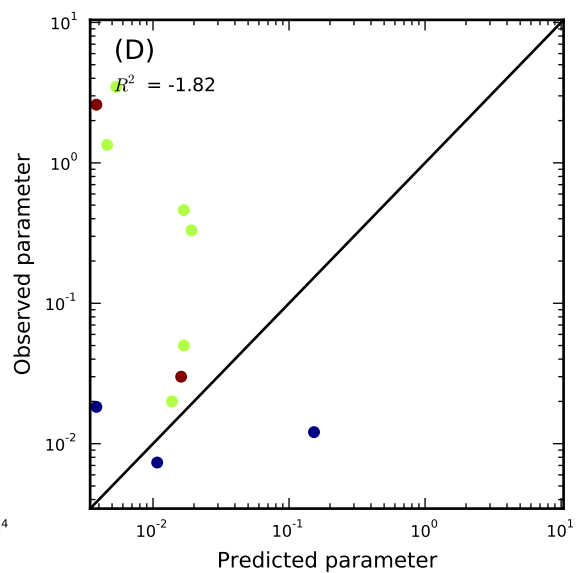
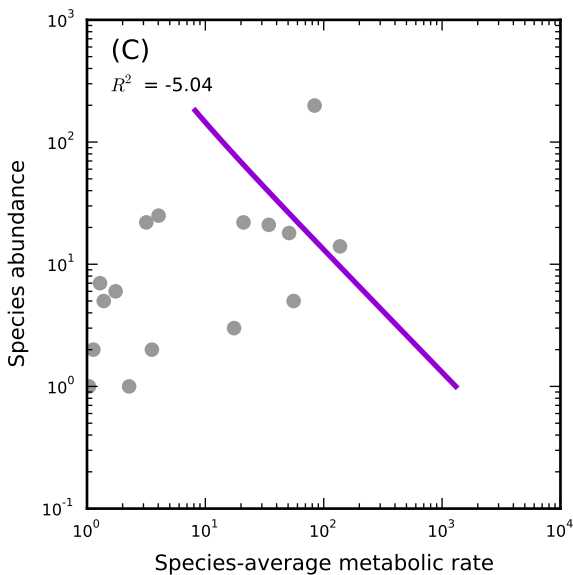
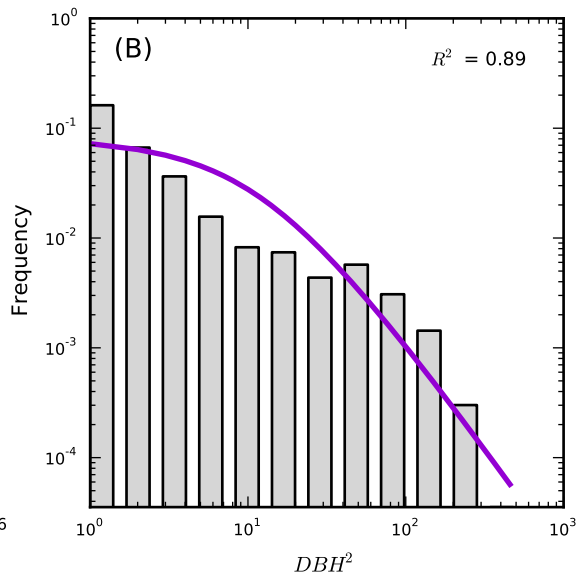
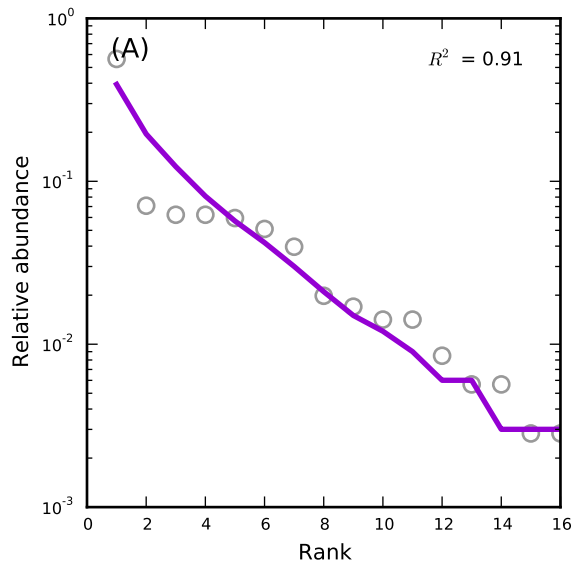
Serimbu, S-2



Shirakami, Akaishizawa



Shirakami, Kumagera



Sherman, sherman

